



Nordic nuclear safety research

NKS-483

ISBN 978-87-7893-579-3

Development and testing methods to locate lost
gamma-ray sources in ordinary environs
by mobile gamma spectrometry,
NKS-B REALMORC Report 2023

Christopher L. Rääf¹ (chair), Robert R. Finck¹ (co-chair)
Christian Bernhardsson¹ (organizer), Vikas Chand Baranwal⁴
Marius-Catalin Dinca¹, Jon Drefvelin⁵
Marie- Andrée Dumais⁴, Per Otto Hetland⁵
Gísli Jónsson³, Naya Sophie Rye Jørgensen²
Simon Karlsson⁶, Marie Lundgaard Davidsdóttir²
Bredo Møller⁵, Charlotta Nilsson¹
Frode Ofstad⁴, Josefine Palmcrantz⁶
Henrik Öberg³

¹ Medical Radiation Physics, ITM, Lund University, Sweden

² Danish Emergency Management Agency; Denmark

³ Geislavarnir ríkisins, Iceland

⁴ Geological Survey of Norway, Norway

⁵ Norwegian Radiation and Nuclear Safety Authority Norway

⁶ Swedish Radiation Safety Authority, Sweden

February 2024

Abstract

The REALMORC 2023 report describes the Excel applications Source Distance and Activity Calculator (SODAC) and Source Shielding Calculator (SSC) to determine distance, shielding and activity of identified Cs-137 sources in lost source searching using mobile gamma-ray spectrometry. The report furthermore outlines a frequency analysis routine intended to enhance the advancement of detecting lost gamma-ray sources. The development proceeds towards detecting sources that may produce weak signals in a mobile gamma spectromete due to their distance and shielding. Standard deviations of the pulse height distribution (gamma spectrum) are utilised to indicate the presence of a radiation source instead of using fixed alarm levels for the count rate. REALMORC 2023 includes joint field experiments in mobile gamma spectrometric search of shielded Cs-137 point sources in actual environmental conditions. Six Nordic teams participated, and the report documents their results from the search experiment using the teams' proprietary analysis software to detect orphan sources.

Key words

Mobile gamma spectrometry, orphan sources, source search, shielding, MORC, radiation accidents, Compton scattering

NKS-483
ISBN 978-87-7893-579-3
Electronic report, February 2024
NKS Secretariat
P.O. Box 49
DK - 4000 Roskilde, Denmark
Phone +45 4677 4041
www.nks.org
e-mail nks@nks.org

Development and testing methods to locate lost gamma-ray sources in ordinary environs by mobile gamma spectrometry

NKS-B REALMORC Report 2023
Contract: AFT/B(23)3
January 31, 2024

Christopher L. Rääf¹ (chair), Robert R. Finck¹ (co-chair), Christian Bernhardsson¹ (organizer), Vikas Chand Baranwal⁴, Marius-Catalin Dinca¹, Jon Drefvelin⁵, Marie-Andrée Dumais⁴, Per Otto Hetland⁵, Gísli Jónsson³, Naya Sophie Rye Jørgensen², Simon Karlsson⁶, Marie Lundgaard Davidsdóttir², Bredo Møller⁵, Charlotta Nilsson¹, Frode Ofstad⁴, Josefine Palmcrantz⁶, Henrik Öberg³

¹ Lund University, Sweden, Medical Radiation Physics, ITM Beredskabsstyrelsen

² Danish Emergency Management Agency; Denmark, (DEMA)

³ Geislavarnir ríkisins, Icelandic Radiation Safety Authority, Iceland, (GR)

⁴ Norges geologiske undersøkelse, Geological Survey of Norway, Norway (NGU)

⁵ Direktoratet for strålevern og atomsikkerhet, Norwegian Radiation and Nuclear Safety Authority, Norway, (DSA)

⁶ Strålsäkerhetsmyndigheten, Swedish Radiation Safety Authority, Sweden, (SSM)

Stakeholder organization and contact

Säteilyturvakeskus, Strålsäkerhetscentralen, Radiation and Nuclear Safety Authority (STUK), Finland [Petri Smolander]

Abstract

The REALMORC 2023 report describes the Excel applications Source Distance and Activity Calculator (SODAC) and Source Shielding Calculator (SSC) to determine distance, shielding and activity of identified ^{137}Cs sources in lost source searching using mobile gamma-ray spectrometry. The report furthermore outlines a frequency analysis routine intended to enhance the advancement of detecting lost gamma-ray sources. The development proceeds towards detecting sources that may produce weak signals in a mobile gamma spectrometer due to their distance and shielding. Standard deviations of the pulse height distribution (gamma spectrum) are utilised to indicate the presence of a radiation source instead of using fixed alarm levels for the count rate. REALMORC 2023 includes joint field experiments in mobile gamma spectrometric search of shielded ^{137}Cs point sources in actual environmental conditions. Six Nordic teams participated, and the report documents their results from the search experiment using the teams' proprietary analysis software to detect orphan sources.

Contents

Abstract.....	2
Summary.....	7
1. Introduction.....	9
2. Theory and examples.....	10
2.1 Source distance, shielding and activity determination of point-shaped gamma-ray sources measured by mobile gamma spectrometry	10
2.1.1 Road-source distance determination	10
2.1.2 Shield thickness determination.....	12
2.1.3 Source activity determination.....	14
2.2 Using the standard deviation distribution to identify the existence of local gamma-ray sources.....	14
2.2.1 Poisson distribution of the number of counts per channel	14
2.2.2 Poisson distributed standard deviation of counts per channel.....	14
2.2.3 Mean value of counts per channel	15
2.2.4 Standard deviation in the mean number of counts per channel.....	15
2.2.5 Standard deviation difference distribution	16
2.2.6 Standard deviation indication quotient, SDIQ.....	17
2.2.7 Standard deviation units (SDU).....	18
2.2.8 Example of standard deviation units (SDU) and deviation display.....	18
2.2.9 Meaning and importance of the SDIQ and the SDU	19
2.3 Frequency analysis methods to identify lost gamma-ray sources by mobile gamma spectrometry	19
2.3.1 Frequency analysis of the SDU to increase the sensitivity to identify lost sources	20
2.3.2 Example of identifying a ¹³⁷ Cs point source by frequency analysis.....	20
2.3.2.1 The experimental data	20
2.3.2.2 Calculating the deviation in standard deviation units, SDU.....	21
2.3.2.3 Finding a source peak signal by the second derivate of SDU	23
2.3.2.4 Finding the location of a source by the third derivate of SDU	23
3. Method of source distance, shielding and activity determination.....	25
3.1 The Source Distance and Activity Calculator (SODAC).	25
3.1.1 First SODAC version, 2022	25
3.1.2 Second SODAC version, 2023	25
3.2 The Source Shielding Calculator - SSC.....	26
3.2.1 First SSC version, 2022.....	26
3.2.2 Second SSC version, 2023	27
4. Equipment and experiment	28
4.1 Aim of the REALMORC 2023 experiments.....	28
4.2 Teams and measuring equipment.....	28
4.3 “Safe area” measurements along a road with shielded sources	29

4.3.1 Mobile measurements, Tuesday October, 10	30
4.3.2 Semi-stationary measurements, Thursday October, 12	31
4.4. “Real-world” source search experiment	31
4.4.1 Source search along the road loop Bravo.....	32
4.4.2 Source search along the road loop Charlie.....	32
4.4.3 Source search along the road loop Delta.....	35
5. Results and discussion	37
5.1 “Safe area” measurements along a road with shielded sources	37
5.2 “Real-world” source search experiment	37
6. Conclusion	40
6.1 Suggested frequency analysis methods to identify lost gamma-ray sources by mobile gamma spectrometry.....	40
6.2 The search experiments.....	40
References.....	42
Acknowledgement.....	44
Disclaimer.....	44
Appendix A1 Results from team DEMA, Danish Emergency Management Agency– nuclear division, Denmark.....	45
A1.1 Measuring equipment.....	45
A1.2 Software	45
A1.3 Results	46
A1.4 Conclusion.....	47
Appendix A2 Results from team Norway – Norwegian Radiation and Nuclear Safety Authority (DSA).....	48
A2.1 Measuring equipment.....	48
A2.2 Software	49
A2.3 Results	49
A2.4 Conclusion.....	50
Appendix A3 Results from team GR, the Icelandic Radiation Safety Authority, Iceland	51
A3.1 Measuring equipment.....	51
A3.2 Software	52
A3.3 Results	52
A3.3.1 Road loop Bravo measurements	53
A3.3.2 Road loop Delta measurements	53

A3.3.3 Road loop Charlie measurements	54
A3.3.4 Results discussion	55
A3.4 Conclusion.....	55
Appendix A4 Results from the team LU, Lund University, Medical Radiation Physics, Sweden.....	56
A4.1 Measuring equipment.....	56
A4.1.1 Vehicle and detectors	56
A4.1.2 The region of interest (ROI) setting	58
A4.2 Software	58
A4.3 Results	58
A4.3.1 Road loop Charlie	59
A4.3.2 Road loop Delta	62
A4.4 Conclusion.....	66
Appendix A5 Results from team NGU, Geological Survey of Norway, Norway	67
A5.1 Measuring equipment.....	67
A5.2 Software	67
A5.3 Results	69
A5.3.1 Road loop Bravo measurements	69
A5.3.2 Road loop Charlie measurements	70
A5.3.3 Road loop Delta measurements	72
A5.4 Conclusion.....	75
A5.5 Reference.....	75
Appendix A6 Results from team SSM, Swedish Radiation Safety Authority, Sweden	76
A6.1 Measuring equipment.....	76
A6.2 Software	76
A6.3 Results	77
A6.3.1 Road loop Bravo measurements	77
A6.3.2 Road loop Charlie measurements	77
A6.3.3 Road loop Delta measurements	77
A6.4 Conclusion.....	77
Appendix B1 Instructions and time schedules for teams during the Tuesday, October 10, mobile data monitoring experiments.	78
Tuesday Time Schedule.....	79
Appendix B2 Instructions and time schedules for teams during the Wednesday, October 11, search experiments.	80
REALMORC experiment Rules	81

If you cannot follow the time schedule, the following applies:	81
Reporting during the day	81
Mission for team DEMA	82
Mission for team DSA.....	83
Mission for team GR	84
Mission for team LU	85
Mission for team NGU	86
Mission for team SSM.....	87
Appendix B3 Instructions and time schedules for teams during the Thursday, October 12, semi-stationary monitoring experiments.	88
Thursday Time Schedule	89
Appendix C Recommended ROI regions for gamma spectrometers and teams.....	90
C1. Generic ROI.....	90
C2. DEMA	91
C3. DSA.....	91
C4. IRSA/GR	91
C5. LU, Lund University	92
C6. NGU	93
C7. SSM.....	93
Appendix D1 Conversion of measured gamma spectra to MGS.CSV files.....	95
Appendix D2 Conversion of measured MGS.CSV to ROI.CSV files	96

Summary

Loss of radioactive material out of the authorities' control (MORC) can occur through accidents, theft, sabotage or acts of war against facilities where radiation sources exist. It is necessary to locate and secure lost radiation sources to avoid harm to people who could be exposed to the radiation unknowingly. In particular, acts of war, such as the bombing of process industries, can destroy the protection of radiation sources, and sources may become hidden and mixed with debris from bomb ruins. Hazards such as mines, unexploded ordnance and booby traps could be around and make it necessary to assess the dangerousness of a radiation source from a distance. The assessment incorporates determining the location of the radiation source and its shielding and activity.

The method of determining a gamma ray source's location, shielding and activity with mobile gamma spectrometry has been developed in Nordic cooperation with financial support from NKS in the projects SHIELDMORC 2019-2020 and COMBMORC 2021-2022, in which the radiation safety authorities of all Nordic countries participated. In 2023, the NKS project REALMORC further developed the Excel-based Source Distance and Activity Calculator (SODAC) and Source Shield Calculator (SSC). SODAC can now consider a detector's angular efficiency variation, essential when mobile gamma spectrometry teams use horizontally oriented 4 L NaI(Tl) detectors.

Searching for lost radiation sources over large areas could bring monotonous observational work, especially when detecting weak signals from shielded radiation sources or sources at a great distance. Automatic detection methods make the work easier. The present report describes methods to automatically detect point radiation sources in a varying natural radiation background. The detection method involves analysing and identifying changes in the standard deviation of the measurement data in combination with numerical filtering to identify weak anomalies that may indicate a lost radiation source in the environment. The report provides the theory for this and an example of analysis. The intention is to develop the methods for operational use in 2024.

Nordic teams have, until 2022, developed and tested methods for mobile gamma spectrometric search of radiation sources in environments with relatively constant natural background radiation levels. However, this is not an entirely realistic situation. Varying background levels along a measurement path always occur, increasing the difficulty in analysing and identifying weak signals from hidden sources.

During REALMORC 2023, conducted between 10-12 October 2023, Nordic mobile gamma spectrometry teams performed a first joint experiment, searching for six setups of shielded ^{137}Cs point sources in a realistic environment with varying backgrounds. Each team covered 137 km of road, with over two hours of collection time for mobile spectrometry or about 8,000 one-second measurements. The sources had been placed with shielding so that the probability of detecting them with mobile gamma spectrometry was near the theoretical detection limits. The teams used their proprietary software for the analysis. Altogether, the teams detected 61% of the sources and observed possible source signals in another 11% of cases. Some teams observed anomaly signals at locations where there were no ^{137}Cs sources. The

detection result was better than the calculated 50% obtained from the theoretical maximum detection distance model from the NKS-project AUTOMORC 2018, which uses preset alarm levels. The teams had better results because they did all the analyses manually. After all, the measurements only covered a few hours of time, allowing extra hours for post-processing the data during the exercise.

The teams found the search experiments helpful in testing their ability to locate hidden radiation sources. However, the complete analysis of whether an area can be declared free of radiation sources over a given activity requires more in-depth measurement data analysis than achievable at runtime. The teams also pointed to the need for more accurate post-analysis through a "reach-back" capability, where specialists can do computer processing and evaluation.

With the analysis methods outlined in the report for the calculation of standard deviation combined with numerical filtering, it should be possible to detect hidden gamma-ray sources at least as sure as with the labour-intensive manual analysis. However, as planned in the activities of REALMORC 2024, it remains to be proven.

1. Introduction

Radioactive sources lost from the authorities' control can cause severe radiation injury to people unknowingly exposed to the radiation. (UNSCEAR 2011). Loss of radiation sources can occur through accidents, theft, sabotage or acts of war where, for example, industrial radiation sources can become buried in bomb ruins. Lost sources must be located and secured. Stolen and hidden or war-damaged radiation sources buried under rubble could be heavily shielded, significantly attenuating the radiation. Such sources can be challenging to detect from a distance. In addition, the area where a source may exist could be inaccessible or dangerous to enter. Having methods and the ability to identify shielded radiation sources at a distance, which produce weak signals in a detector, is essential for the safety of personnel and the public.

All Nordic countries have units for mobile gamma spectrometry organized by the respective country's radiation safety authority. Since 2016, these mobile groups have participated in research programs funded by the Nordic Nuclear Safety Research (NKS) to develop and test methods for mobile gamma spectrometric search of lost gamma-ray sources (Finck et al. 2019). The programs have combined theoretical method development with well-controlled experiments within secured areas. Program activities have developed a calculation procedure to determine the maximum detection distance for gamma-ray point sources (Finck et al. 2022; Rääf et al. 2019) and methods for the determination of distance, shield thickness and activity for hidden ^{137}Cs sources (Bukartas et al. 2019, 2021, 2022; Rääf et al. 2020, 2021, 2023a, 2023b). The mobile gamma spectrometry teams conducted these practical experiments in areas with a near-constant natural background. However, a well-controlled background is unrealistic in a real-world search scenario. Program activities have, therefore, extended in 2023 to encompass search methods in difficult-to-detect situations with varying natural background radiation levels.

The REALMORC 2023 project aimed to continue the development of methods for mobile detection of lost gamma-ray sources that produce weak signals in detectors. The project included experiments with the search for ^{137}Cs sources in a realistic environment with varying background levels and a more complex shielding and irradiation environment than heretofore. The work intended to provide a basis for further improvement of methods for sustained mobile search of lost radiation sources.

2. Theory and examples

This chapter describes the theory for computing the distance, shielding and activity of gamma-ray point sources from mobile gamma spectrometric data. There is also a description and some examples of how standard deviation and frequency analysis of spectral data can enhance the capability of mobile gamma spectrometry teams to detect radiation sources that give weak signals in the detector.

2.1 Source distance, shielding and activity determination of point-shaped gamma-ray sources measured by mobile gamma spectrometry

The distance, shielding and activity of gamma-ray point sources computed from mobile gamma spectrometry data have been described in NKS reports (Finck et al. 2019; Rääf et al. 2020, 2021, 2023a, 2023b). The following is an overview of the theory.

2.1.1 Road-source distance determination

The primary photon fluence rate $\dot{\phi}$ of energy E in the air at a distance R from a point source with activity A and branching ratio b for emitting photons of energy E can be expressed by the "point kernel" equation:

$$\dot{\phi}(R, A) = \frac{Ab e^{-(\mu_a/\rho_a)\rho_a R}}{4\pi R^2} \quad (1)$$

where (μ_a/ρ_a) is the mass attenuation coefficient of air at photon energy E , and ρ_a is the air density.

Suppose the nearest (perpendicular) distance between the point source and a straight road passing the source is x metre. The mobile gamma spectrometry vehicle travels along the road $-\infty < y < +\infty$, where $y = 0$ is at the point of the nearest source-road distance x , then the primary fluence rate along the road can be expressed as:

$$\dot{\phi}(x, y, A) = \frac{Ab e^{-(\mu_a/\rho_a)\rho_a\sqrt{x^2 + y^2}}}{4\pi(x^2 + y^2)} \quad (2)$$

Eqn (2) is a positive symmetric function along the y -axis with its symmetry axis and maximum at $y = 0$. The function's denominator will be predominant for a source located within a few tens of meters from the road, forming a Lorentzian function with its amplitude depending on the source distance, generally called the "inverse square law". At source distances beyond about a hundred metres and more, the attenuation of the gamma rays in air dominates the photon fluence reduction described by the exponential term in the numerator. The Lorentzian function obtains exponentially decreasing tails as the absolute value of the distance y along the road increases.

For a point source with a slab shield placed in front of the source, perpendicular to the source-detector direction, an additional exponential term to account for the photon attenuation in the shield must be included, Eqn 2 becoming:

$$\dot{\phi}(x, y, A) = \frac{Ab e^{-(\mu_a/\rho_a)\rho_a\sqrt{x^2 + y^2}} e^{-(\mu_s/\rho_s)\rho_s z_s \sec\theta}}{4\pi(x^2 + y^2)} \quad (3)$$

where (μ_s/ρ_s) is the shield mass attenuation coefficient, ρ_s is the density of the shield material, and z_s is the linear thickness of the shield, assumed to be much smaller than x . The term $\rho_s z_s$ is the shield mass thickness. The term $\sec \theta = 1/\cos \theta$ represents the

penetration angle of primary photons of energy E through the shield in the direction of the measurement point (x,y) . Eqn 3 should be multiplied by further exponential terms representing each shielding layer if additional materials are present.

Figure 1 shows the Lorentzian-shaped functions with exponential tails for the primary photon fluence from an unshielded and a shielded ^{137}Cs source 50 and 100 meters from the straight road where the measurement vehicle passes. The half-width of the photon fluence function increases as the distance between the source and the road increases. A shielded source results in a steeper decrease in the photon fluence rate as the distance $|y|$ along the road path away from the source increases.

In a gamma spectrometer, the primary photon fluence rate for gamma energy E produces a Gaussian-shaped count rate distribution \dot{N} in an energy range centred around the expected value E , which has a Gaussian shape. For a photon detector, the count rate is always less than the number of photons per unit time $\dot{\phi}a$ reaching the detector, where a is the projected area of the detector perpendicular to the direction of the photon fluence rate. The ratio $\varepsilon = \dot{N}/\dot{\phi}$ where $\varepsilon < a$ is defined as the *effective detector area* (also called the detector field efficiency). The effective detector area corresponds to the surface area of an ideal total absorption detector where all incident primary photons are registered in the full energy peak. One can determine the effective detector area by measuring the count rate for a well-known primary photon fluence rate and computing their ratio. Defining a reference direction for the primary photon fluence rate is practical. For a mobile gamma spectrometer, the reference direction is generally chosen on the vehicle's right side perpendicular to the direction of travel. Then, the reference direction becomes the same as the shortest direction to a point source on the right side of the road when passing the source.

The relationship between the detector count rate and the primary photon fluence rate at any location along a straight road passing the source is:

$$\dot{N} = \dot{\phi} \varepsilon_0 (\varepsilon_\theta / \varepsilon_0) \tag{4}$$

where ε_0 is the effective detector area (m^2) at photon energy E for photons incident in the reference direction, $\theta = 0$, and the ratio $(\varepsilon_\theta / \varepsilon_0)$ is the relative angular effective detector area, a dimensionless quantity. The angle θ is a function of the location (x, y) .

Combining Eqn 3 and 4 gives the count rate $\dot{N}(y)$ along the road coordinate y as a function of the road-source distance x :

$$\dot{N}(y) = \frac{\varepsilon_0 (\varepsilon_\theta / \varepsilon_0) A b e^{-(\mu_a / \rho_a) \rho_a \sqrt{x^2 + y^2}} e^{-(\mu_s / \rho_s) \rho_s z_s \sec \theta}}{4\pi (x^2 + y^2)} \tag{5}$$

By measuring the count rate at different locations y along the road and fitting Eqn 5 to measured data points, the source distance x can be determined from the best fit. The Excel™ routine SODAC (described in section 3.1) solves the distance x from measured data.

The shield mass thickness $\rho_s z_s$ must be known to solve Eqn 5 for the distance x . The mass thickness can be determined by measuring the ratio of count rates from scattered to primary radiation in the location $(x, y = 0)$, as described in Section 2.1.2 below. The shield mass attenuation coefficient (μ_s / ρ_s) depends on photon energy but is nearly

constant for atomic numbers between 3 and 25, of which commonly occurring building materials are composed. Thus, knowing the exact composition of the shielding material is unnecessary as long as the shielding can be assumed to be building material (wood, clay, concrete, gypsum). However, if the shielding material is of high atomic number (lead, uranium), the method in Section 2.2 of determining shield thickness does not apply.

A significant problem is if the relative angular effective detector area (the detector's relative angular efficiency), $(\varepsilon_\theta / \varepsilon_o)$, for primary photons from the source strongly depends on the angle of incidence θ , depending on the source distance x . This dependence is the case with horizontally oriented 4 L NaI(Tl) detectors where the angular efficiency varies with the angle of incidence θ (Räaf et al., 2023). The angular dependence complicates the solution of the distance x in Eqn 5. However, an iterative procedure in fitting Eqn 5 to the measurement data may provide a solution if the statistical uncertainty in the sampled measurement data is low.

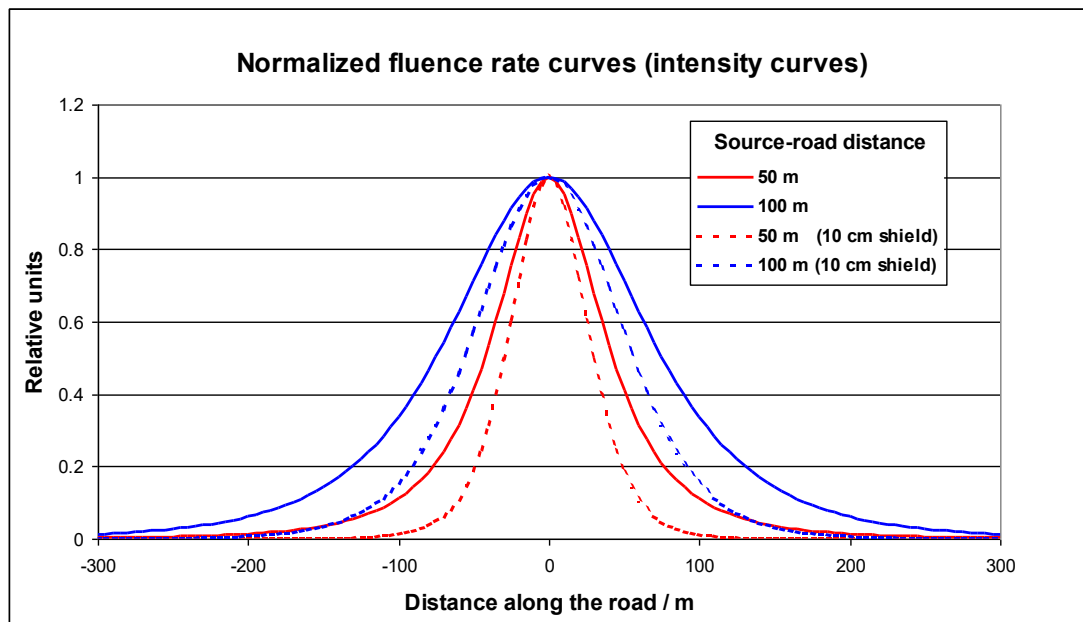


Fig 1. Normalized fluence rate curves from a ^{137}Cs point source at 50 m (red line) and 100 m (blue line) from the measurement route. Solid lines are valid for an unshielded source. Dotted lines are valid for a source with a 10 cm thick concrete slab shield in front of the source. The shielding produces steeper exponential tails in the Lorentzian-shaped fluence rate curves.

2.1.2 Shield thickness determination

Shielding material around a gamma-ray source reduces the primary (unscattered) photon fluence, thus shortening the distance at which the source can be detected when using the full energy peak count rate. However, a shielded source also gives rise to Compton scattered photons from the shield material. The Compton scattered photons in turn give rise to recordings over an extended part of the gamma spectrometer's energy range below the primary photon energy. These lower energy records can contribute to detecting a shielded source and determining the shield thickness provided that the shielded material consists of elements with atomic numbers between

3 and 25, for which the Compton effect is the dominant interaction for gamma radiation from radioactive substances.

Nordic teams have measured the ratio of count rates for Compton scattered photons to primary photons emitted from shielded ^{137}Cs point sources as a function of the shield thickness with shields containing common building materials. (Räaf et al, 2021, 2023). Three energy regions (regions-of-interest, ROI) were defined for the Compton scattered radiation (ROI A: 77-239 keV, ROI B: 245-407 keV, and ROI C: 413-575 keV) and three energy regions for registrations from the primary photons (ROI PL: 589-659 keV, ROI PR: 665-743 keV, and ROI P 589-743 keV). The energy ranges varied slightly between teams' gamma spectrometers because of different conversion gains.

The background-subtracted count rate ratios are:

$$q_i = \frac{\dot{N}_{i,compton} - \dot{N}_{i,Comptonbackground}}{\dot{N}_{i,primary} - \dot{N}_{i,primarybackground}} \quad (6)$$

where q_i , $i = 1, 3$ denotes the three count rate ratios ROI A/P, ROI B/P, and ROI C/P.

An exponential function can approximate the count rates:

$$q_i = a_i e^{b_i \rho_s z_s} \quad (7)$$

where ρ_s is the shield density, z_s is the shield linear thickness, $\rho_s z_s$ is the shield mass thickness and a_i and b_i are coefficients. (Räaf et al., 2023).

Table 1 provides values of the coefficients a_i and b_i as an average for six 4 L NaI(Tl) detectors used by the Nordic teams. Using the tabulated coefficients and the measured count rate ratios returns the mass thickness of the shield:

$$\rho_s z_s = \frac{\ln(q_i / a_i)}{b_i} \quad (8)$$

Eqn 8 provides three solutions of $\rho_s z_s$, one for each of the three count rate ratios ROI A/P, ROI B/P, and ROI C/P. The solutions should give approximately the same value for the shield mass thickness. If the values deviate significantly, the result is uncertain. The Excel routine SSC (described in section 3.2) calculates the shield mass thickness $\rho_s z_s$ from measured data.

Table 1. Coefficients a_i and b_i in the exponential model for determining shield mass thickness using Eqn 8. The values are valid for measurements with a 4 L NaI(Tl) detector using ^{137}Cs point sources. ROI energy regions are A: 77-239 keV, B: 245-407 keV, C: 413-575 keV, and P: 589-743 keV. The uncertainty in the coefficients is a 3% standard error of the mean.

ROI ratio model	a_i	b_i (m^2/kg)
$i = 1$, ROI A/P	1.63	0.00393
$i = 2$, ROI B/P	0.842	0.00318
$i = 3$, ROI C/P	0.571	0.00218

2.1.3 Source activity determination

When the road-source distance x and the shield mass thickness $\rho_s z_s$ have been determined, then the source activity A can be calculated from a net (background subtracted) count rate measurement, $\dot{N}(y) = \dot{N}_\theta$, where $\theta = \arctan(y/x)$ at any chosen location y along the straight road passing the source using the relation from Eqn 5:

$$A = \frac{\dot{N}(y) 4\pi (x^2 + y^2)}{\varepsilon_o (\varepsilon_\theta / \varepsilon_o) b e^{-(\mu_a / \rho_a) \rho_a \sqrt{x^2 + y^2}} e^{-(\mu_s / \rho_s) \rho_s z_s \sec\theta}} \quad (9)$$

The angle θ is the angle between the shortest road-source distance x and the direction from the source to the detector location (x, y) along the road. If the detector directly opposes the source, then $\theta = 0$, $y = 0$, and Eqn 9 is simplified:

$$A = \frac{\dot{N}(0) 4\pi x^2}{\varepsilon_o b e^{-(\mu_a / \rho_a) \rho_a x} e^{-(\mu_s / \rho_s) \rho_s z_s}} \quad (10)$$

The ExcelTM routine SODAC calculates the source activity from measured count rate data and a chosen assumption of the shield thickness.

2.2 Using the standard deviation distribution to identify the existence of local gamma-ray sources at post-processing assessment

It is well known that photon registrations in a detector placed in a stationary gamma-ray field obey Poisson's statistical law of probability, for which the variance and standard deviation in a pulse height distribution depend solely on the total count per channel. However, if the detector moves relative to the gamma sources, a variable space and time component adds to the variance and standard deviation. Analysing the influence of this component in post-processing of data can reveal the presence of unknown gamma-ray sources as shown in the following.

2.2.1 Poisson distribution of the number of counts per channel

Poisson's law can be written as:

$$P(X = k) = \frac{\lambda^k e^{-\lambda}}{k!} \quad (11)$$

where $P(X = k)$ is the probability of getting $X = k$ number of registrations (counts) in an energy range (in a channel) in the detector and λ is the expected number of counts obtained during the acquisition time. The expected value λ can also be expressed as the mean (average) counts if the experiment is repeated many times, i.e. the total acquisition time is sufficiently long.

2.2.2 Poisson distributed standard deviation of counts per channel

The expected positive value λ_j in counts per channel equals the variance in the variable X . The standard deviation is the square root of the variance, so the standard deviation of the Poisson distribution can be expressed as:

$$\sigma_{p,j} = \sqrt{\lambda_j} \quad (12)$$

Thus, for an unchanged geometry between the source and the detector, the standard deviation in the number of counts per channel and acquisition time equals the square root of the mean counts per channel.

2.2.3 Mean value of counts per channel

The sum counts channel-by-channel of M pulse height distributions recorded by a mobile gamma spectrometer along a travel path is a sum distribution:

$$s_j = \sum_{i=1}^M n_{i,j} \quad (13)$$

where $n_{i,j}$ is the number of counts in the j :th channel for the i :th pulse height distribution (gamma spectrum).

The distribution of mean counts per channel is:

$$\mu_j = \frac{1}{M} \sum_{i=1}^M n_{i,j} \quad (14)$$

The mean distribution μ_j is proportional to the sum distribution s_j because $1/M$ is a scalar. Thus, the shape of the sum s_j and the mean distribution μ_j is the same, but the amplitude is different. Fig 2 shows an example of a sum pulse height distribution s_j recorded in an area with ^{60}Co and ^{131}I point sources arranged 20 - 100 m from the road. However, there is no sign of the sources in the sum distribution (spectrum) because the natural radionuclides are predominant. Fig 3 shows the mean distribution μ_j of the same data (blue crosses).

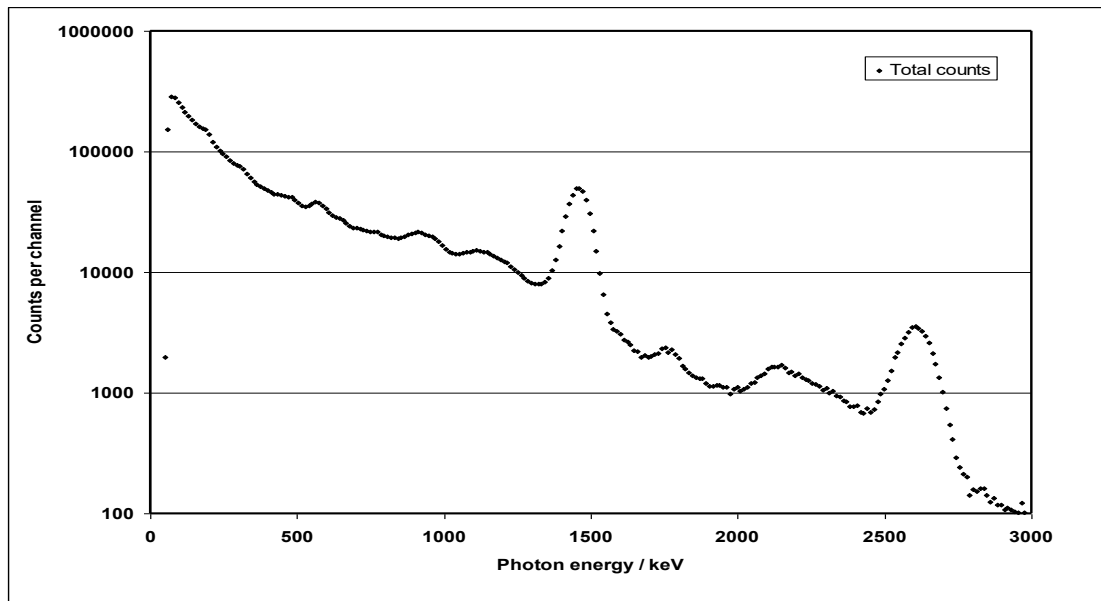


Fig 2. Sum distribution s_j of 2066 pulse height distributions (gamma spectra), each with acquisition time 2 s, recorded with a mobile 4 L NaI(Tl) detector along a 27 km route with ^{60}Co and ^{131}I point sources placed at 20 - 100 m from the road. There is no sign of registrations from the point sources in the sum distribution; only the natural background is visible.

2.2.4 Standard deviation in the mean number of counts per channel

The standard deviation of the mean number of counts μ_j in the j :th channel calculated according to the definition is:

$$\sigma_{s,j} = \sqrt{\frac{1}{M} \sum_{i=1}^M (n_{i,j} - \mu_j)^2} \quad (15)$$

The standard deviation distribution $\sigma_{s,j}$ (Fig 3, red triangles) also shows the shape of a gamma spectrum, as expected since the number of counts per channel $n_{i,j}$ is in the

numerator of Eqn 15. However, full energy peaks from the ^{60}Co and ^{131}I sources also appear in the standard deviation distribution (standard deviation spectrum). These peaks are not visible in the sum or mean value distribution.

The influence from ^{60}Co and ^{131}I point sources on the standard deviation distribution is because these radionuclides only appear in a few measurements where their contribution to the counts in the gamma spectrometer significantly affects the standard deviation at their full energy peak(s) and at lower energies because of the scattered radiation also produced.

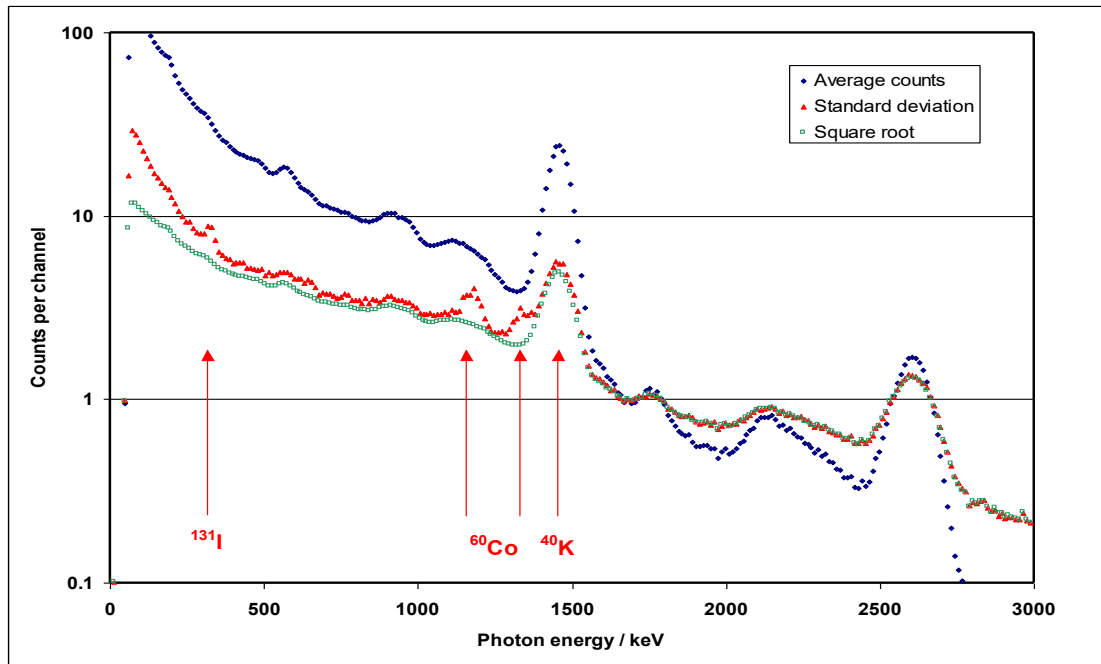


Fig 3. Mean (average) distribution μ_j of 2066 pulse height distributions, each with acquisition time 2 s, recorded with a mobile 4 L NaI(Tl) detector (blue crosses), standard deviation distribution $\sigma_{s,j}$ (red triangles), and the square root of the mean distribution $\sigma_{p,j}$ (green quadrates). The presence of ^{131}I and ^{60}Co in the recorded pulse height distributions is not visible in the average and square root distributions. However, the standard deviation distribution shows the full energy peaks from ^{131}I (364 keV) and ^{60}Co (1173 and 1332 keV). In addition, an increased standard deviation in the full energy peak of ^{40}K indicates that this natural radionuclide varies in concentration along the measurement route. In contrast, the variation in the natural thorium and uranium series radionuclides is low along the route.

2.2.5 Standard deviation difference distribution

The difference between the standard deviation distributions $\sigma_{s,j}$ calculated according to the definition and the square root distribution $\sigma_{p,j}$ calculated according to the Poisson distribution is:

$$\sigma_{d,j} = \sigma_{s,j} - \sigma_{p,j} \tag{16}$$

The standard deviation difference distribution $\sigma_{d,j}$ shows positive values if the radionuclides along the measurement route vary in concentration, which is the case if there is a point source along the route or significant variations in the naturally occurring radionuclides. The distribution of $\sigma_{d,j}$ over photon energies appears as a gamma spectrum. Fig 4 shows an example where the full energy peaks from ^{131}I at

364 keV and ^{60}Co at 1173 and 1332 keV are visible, indicating that the mobile gamma spectrometer has passed locations with these radionuclides. A ^{40}K peak at 1461 keV indicates that the potassium content along the measurement route varies.

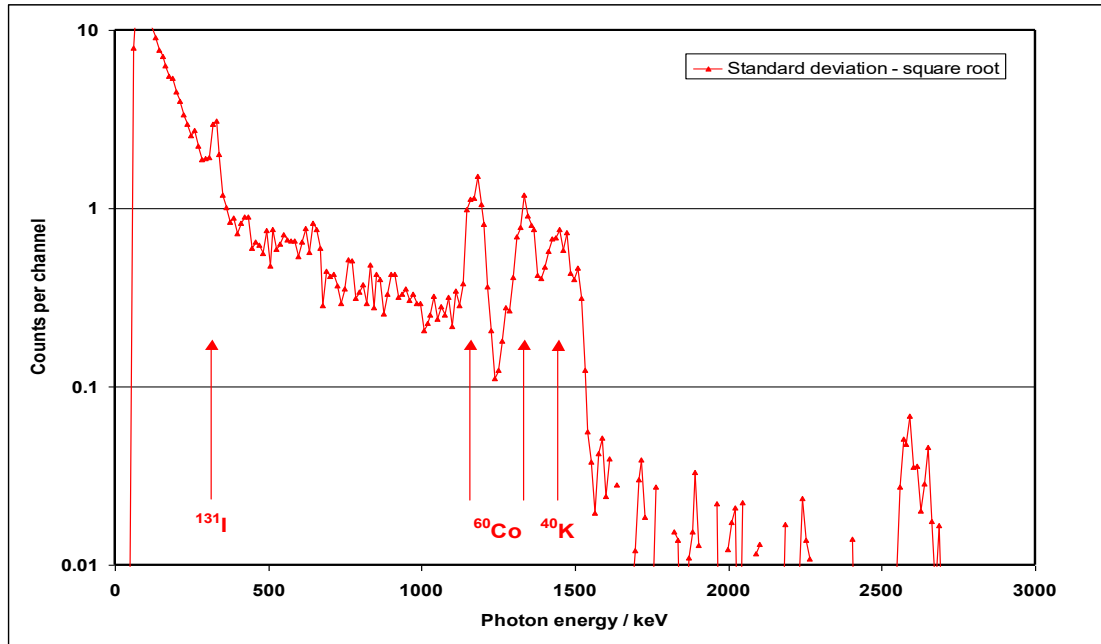


Fig 4. Difference between the standard deviation distribution $\sigma_{s,j}$ and the square root of the mean $\sigma_{p,j} = \sqrt{\mu_j}$. The difference, resembling full energy peaks for ^{131}I , ^{60}Co , and ^{40}K , indicates a larger variation in channel count rate than would be obtained for a constant radiation background following the law of Poisson distribution, thus indicating local variations in the radionuclide content along the measurement route.

2.2.6 Standard deviation indication quotient, SDIQ

The two ways of calculating standard deviation for the number of counts in an energy range during a specific acquisition time, the standard deviations σ_s according to its definition (Eqn 15) and σ_p if count data follows the Poisson distribution (Eqn 12), provide the same result if the source geometry is constant during a measurement series. The ratio between the two ways to calculate standard deviation is:

$$\eta_j = \frac{\sigma_{s,j}}{\sigma_{p,j}} = \frac{\sqrt{\frac{1}{N} \sum_{i=1}^N (n_{i,j} - \mu_j)^2}}{\sqrt{\mu_j}} \quad (17)$$

Here, the ratio distribution η_j is named the *standard deviation indication quotient* (SDIQ). For gamma spectrometric measurement series performed in a constant radiation field, the η_j distribution approaches unity when acquisition times increase.

In mobile measurements, the source-detector geometry is not constant. However, if the natural background radiation field along the measurement route is relatively constant, the SDIQ distribution will be close to unity over the photon energy range.

Should a local gamma-ray source produce registrations in the moving detector when it passes the source, the standard deviation $\sigma_{s,j}$ calculated according to Eqn 15 will increase. The Poisson standard deviation $\sigma_{p,j}$ calculated according to Eqn 12 will also

increase, but not as much because it originates from the average of all measurements made in the series and not only those near the source. The SDIQ distribution η_j becomes larger than unity for the energies (channels) affected. The increased SQIQ is, thus, a sign of a radiation source that does not follow Poisson's law of a constant radiation field at the detector, i.e. a local gamma-ray source has affected the measurements (the gamma spectra) along the road.

2.2.7 Standard deviation units (SDU)

Another way to show the deviation of the measured data from an average value of the background is to calculate the deviation for each channel count (or ROI count) and each acquired pulse height distribution (gamma spectrum) in units of standard deviation, $u_{i,j}$:

$$u_{i,j} = \frac{n_{i,j} - \mu_j}{\sigma_{p,j}} \quad (18)$$

where $n_{i,j}$ is the acquired counts in channel j (or ROI j), and μ_j is the average counts in channel j of a set of measurements. The function $u_{i,j}$ is called *standard deviation units* (SDU). For gamma spectrometric measurements performed in a constant radiation field, the SDU value u_i usually varies between -1 and 1 due to the stochastic variations inherent in the Poisson law. In contrast, some more notable variations always happen now and then. These variations can be seen as Poisson distributed noise.

The concept of using SDU, according to Eqn 18, was applied as a *deviation display* method for visualising data in mobile gamma-ray spectrometry (Kock et al., 2010), but the designation SDU was not used at that time.

2.2.8 Example of standard deviation units (SDU) and deviation display

Fig 5 shows gamma spectrometric measurement data in standard deviation units (SDU) as a colour scale (a deviation display) along part of the road in the Demoex 2006 exercise (Finck et al., 2008). Values for SDU between -1 and 1 have been coloured different shades of blue. These variations are due to statistical count fluctuations and can be regarded as noise in the measurement data. Values significantly above three have been given the colour scale green-yellow-white for increasing levels. They indicate the presence of radiation sources that affect the pulse height distribution recorded for a limited geographical area and time while the gamma spectrometry vehicle passes by the source. Fig 5 shows the impact from ^{60}Co for about 4 s and ^{131}I for about 16 s.

Note that the SDU for count rate values near the background level is assigned a blue colour regardless of the absolute value of the background counts per channel in the gamma spectrometer. Although in absolute value, there is a spectrum from uranium, thorium and potassium distributed over the gamma spectrometer's energy range (channels), the entire spectrum gets values near zero and a blue colour. This colour is maintained as long as the background is nearly constant, i.e. only statistical noise (the probability of recording photons according to Poisson's law) affects the display.

When the mobile gamma spectrometry vehicle passes a local radiation source, the radiation field "seen" by the detector changes and Poisson's law of registered counts does not apply to those changes. The standard deviation in the measurement data

increases, and the SDU becomes significantly greater than 0. The green-yellow-white colour scale in the deviation display visualizes the change.

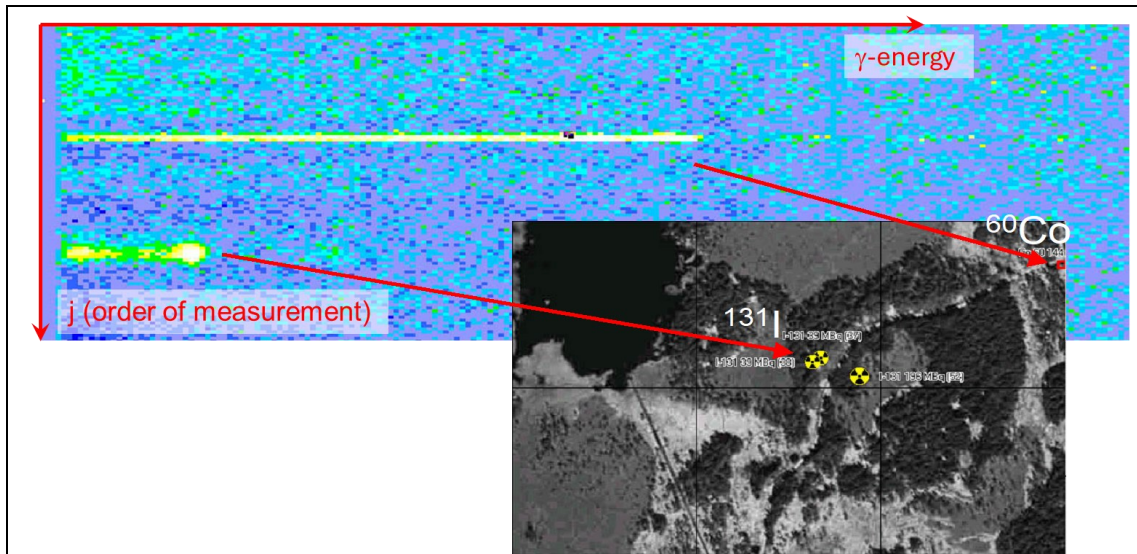


Fig 5. Colour diagram (deviation display) of gamma energy (x -axis) for measured data expressed in standard deviation units (SDU) for individual mobile measurements (y -axis) obtained in the Demoex 2006 mobile gamma-ray spectrometric survey in a military exercise area. Light blue represents SDU in the range -1 to 1, which means that no significant change has occurred in the spectrum for the current measurement. The green-yellow-white colour represents increases in the SDU. The increased SDU appears for ^{60}Co in two measurements (4 s) and ^{131}I in eight measurements (16 s). The vehicle speed varied between 20 and 40 km/h.

2.2.9 Meaning and importance of the SDIQ and the SDU

In practice, the standard deviation indication quotient, SDIQ, and the standard deviation units, SDU, can be likened to a "motion detector" for changes in gamma-ray fields. As long as the measuring vehicle passes through a constant or near-constant radiation field, the SDIQ becomes close to 1, and the SDU ranges from -1 to 1. If the detector moves through a changing radiation field when driving past a local radiation source, the "motion detector" responds with increasing values. This method provides better sensitivity for detecting hidden radiation sources than only using alarm levels set on counts or count rates. The SDU suppresses signals from slow variations in the natural background and highlights transient variations in the radiation field from local sources.

2.3 Frequency analysis methods to identify lost gamma-ray sources by mobile gamma spectrometry

The "classic" method of detecting a lost gamma-ray source with mobile (or airborne) gamma-ray spectrometry is to set an alarm level on the count rate in the energy range(s) where the sought gamma-ray source(s) have their primary gamma energy. The method is a straightforward way to signal the presence of a source if it is of high activity and near the path (or flight line) where the gamma spectrometer passes. However, if the source's signal (the count rate) is low relative to the count rate from the natural background radiation, detecting the source can be significantly more challenging. The weak signal may be due to the source being shielded or located at a distance from the path of the gamma spectrometer. Here, an alarm based on an increase in the count rate does not work well because the increase may be slight and

obscured in the natural background variations. Lowering the alarm level to increase the sensitivity can cause an unacceptable rise in the rate of false positives. Instead, such a situation can be better identified through frequency analysis, where the specific signs of the signal from a local gamma-ray source can be filtered out and amplified. Simultaneously a slower-varying background signal is suppressed.

2.3.1 Frequency analysis of the SDU to increase the sensitivity to identify lost sources

In mobile gamma spectrometry, the measurement data consists of a series of counts in an energy range as a function of time or the distance travelled. Typical is one-second acquisition time series corresponding to 17 m path distance intervals at 60 km/h. The measurement data can vary with different "wavelengths" (frequencies along the path). The fastest variations from one measurement to another can be regarded as noise whose amplitude variation is Poisson distributed. Superimposed on the noise are more coherent deviations due to environmental variations in uranium, thorium and potassium content. These variations have a "wavelength" in the order of the average path length of the gamma radiation in the air for the gamma energies emitted from the naturally occurring radionuclides (about 100 m). Shorter "wavelength" variations are due to local, more substantial increases in photon fluence from natural radionuclides. It can, for example, occur when passing through a viaduct with uranium-containing concrete ballast. A short "wavelength" could also be due to the short-term change in photon fluence from a lost radiation source registered by the moving detector when it passes the source. One way to separate a local radiation signal from the natural background variations is to filter and analyse the "wavelengths" or frequency variations along the path. The mathematics for this is well known from frequency analyses in other contexts. The following shows an example of an application that identifies the signal from a point source over a background variation.

2.3.2 Example of identifying a ^{137}Cs point source by frequency analysis

2.3.2.1 The experimental data

Fig 6 shows measurement data in ROI B, ROI C (Compton scattered radiation), and ROI P (primary radiation) collected during the NKS COMBMORC 2021 experiments in Barsebäck by the Danish Emergency Management Agency with a 4 L NaI(Tl) spectrometer when passing a weak ^{137}Cs point source, difficult to detect by the usual "alarm method". The data were taken from two passes along a 1 km road and interpolated to 5 m distance units. The vehicle speed was 50 km/h.

The signal from the ^{137}Cs source indicates a slight increase at location 125 (625 m along the road) in the energy region of primary photons (ROI P) and a slightly more significant increase for the signal from Compton scattered radiation (ROI B and ROI C). However, the increase is not so significant that it would trigger an alarm. Variations in the natural background radiation can be greater than the signal from the ^{137}Cs source at the current distance. An alarm based on the number of counts per acquisition time would have given many false alarms if set so low that it would react on the ^{137}Cs source.

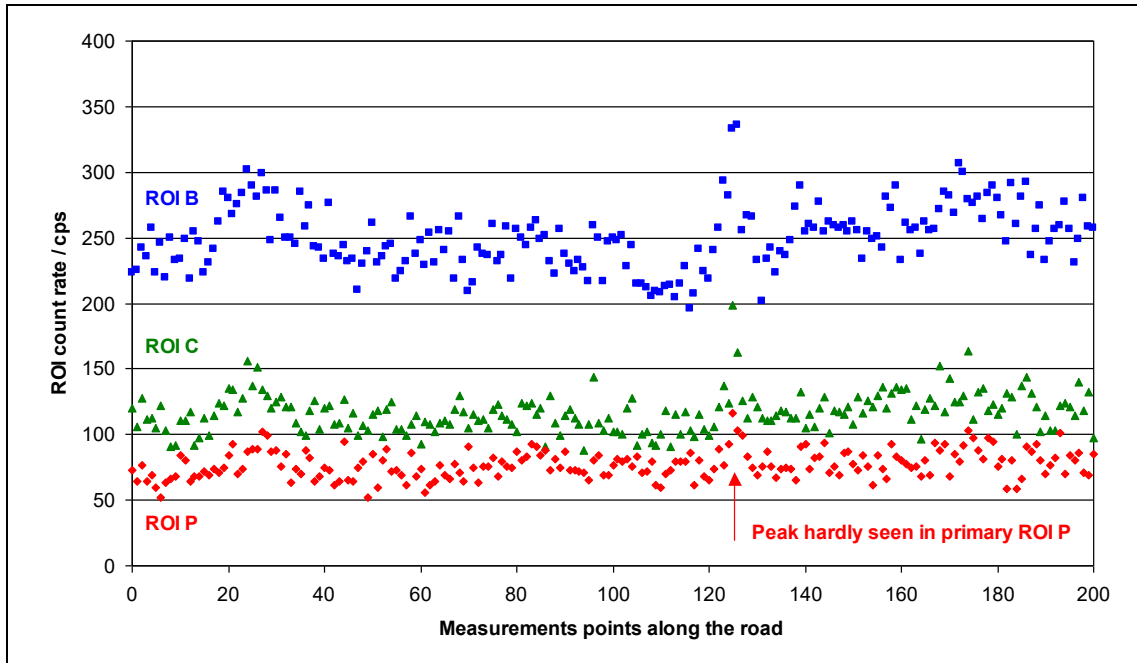


Fig 6. The Danish Emergency Management Agency (DEMA) collected mobile gamma spectrometry data using a 4 L NaI(Tl) spectrometer during NKS COMBMORC 2021. A 600 MBq ^{137}Cs point source was located 45 m from the road at measurement point 125 (625 m along the road). A 13 cm concrete wall shielded the source. The spectral energy range 245 - 407 keV was defined as ROI B, 413 - 575 keV as ROI C (Compton scattered radiation) and 581 - 743 keV as ROI P (primary radiation). Measured data are from two passes along the 1 km road and interpolated to 5 m distance units. The vehicle speed was 50 km/h.

2.3.2.2 Calculating the deviation in standard deviation units, SDU

The first processing calculates the SDU $u_{i,j}$ where i denotes a single measurement and j denotes the ROI. The result is shown in Fig 7. Noise with variations between -1 and 1 is dominates the picture, but higher values, 3 to 6, are found in three places. Two of these, at location 25 (125 m) and 170 (850 m) of the sequence, appear to have longer "wavelengths" than the third at location 125 (625 m), which gives the highest signal. The "short-wave" (high-frequency) noise along the road is due to statistical variations in counts per acquisition time following the Poisson distribution. A smoothing (filtering) algorithm reduced the noise. The multiplication coefficients 1, 5, 15, 30, 45, 51, 45, 30, 15, 5, 1 divided by the sum of the coefficients 243 were chosen as filter. The result after filtering is shown in Fig 8.

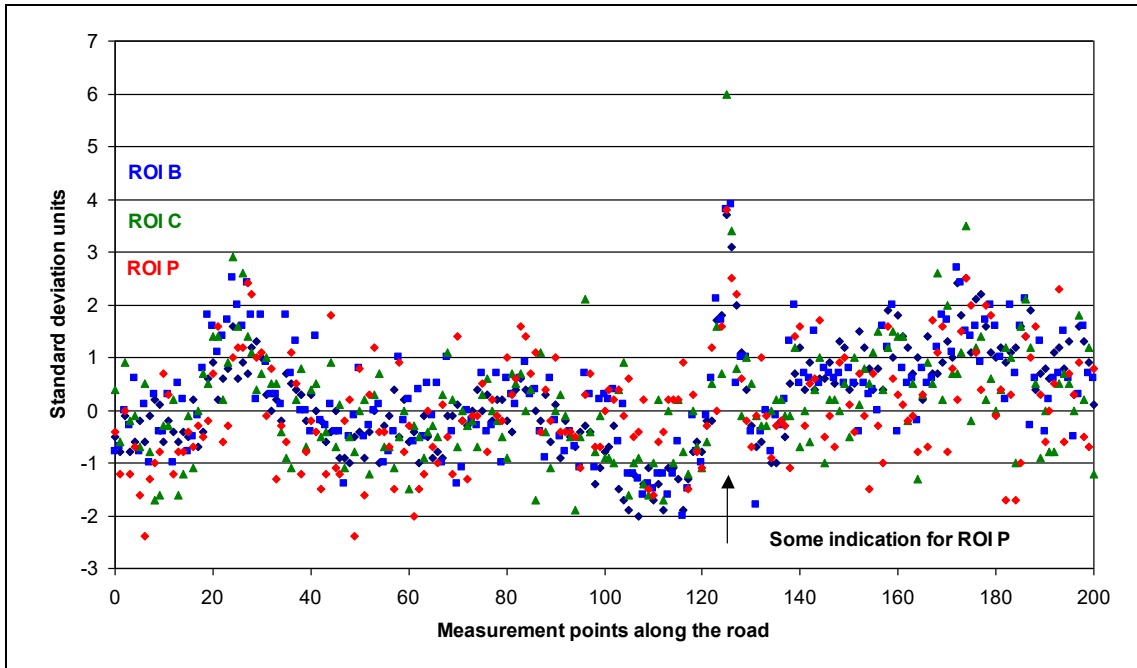


Fig 7. Calculated standard deviation units (SDU) on data from the DEMA mobile gamma spectrometric measurements shown in Fig 6.

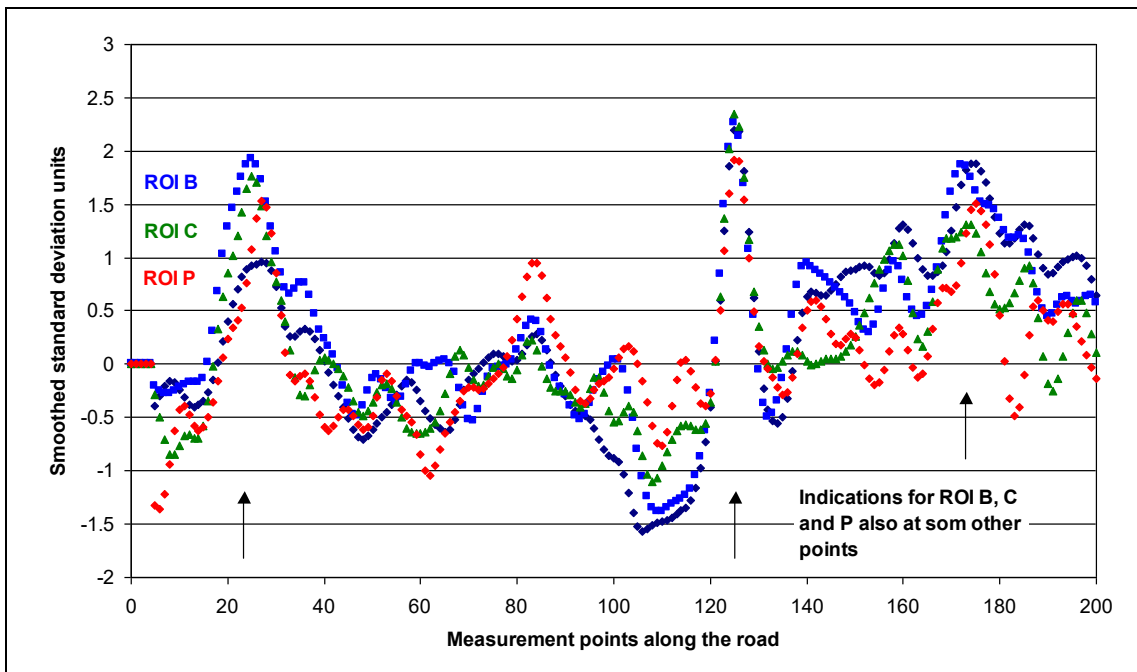


Fig 8. Smoothed SDU for the DEMA mobile gamma spectrometric measurements shown in Fig 6, filtering out the statistical Poisson distributed noise from the data shown in Fig 7. Smoothing coefficients were 1, 5, 15, 30, 45, 51, 45, 30, 15, 5, 1. Possible peaks (source locations) are indicated at point 25 (125 m along the road), point 125 (625 m) and 170 (850 m). Data in the three ROIs B, C, and P, are in phase at point 125 (625 m).

ROIs B, C and P variations are pretty "wild". Only in location 125 (625 m) are the variations of ROIs A, C and P in phase. *Signals in phase indicate a possibility that the scattered radiation registered in ROI A and B is related to the signal in ROI P, i.e. the primary energy of a ^{137}Cs source.*

Further evidence for a possible radiation source can be obtained by studying the shape of the maxima and minima in SDU. It is done through the derivatives of SDU.

2.3.2.3 Finding a source peak signal by the second derivatve of SDU

The derivative of a function is a measure of the function's rate of change. Fig 9 shows the second derivative of the SDU for the DEMA mobile gamma spectrometric measurement. At point 125 (625 m along the road), the second derivative is negative, indicating a peak in the original data and a possible radiation source. Moreover, the second derivatives of SDU in ROI B, C and P are in phase at this location, which tells that the rate of change in the scattered and primary part of the gamma spectrum for a ^{137}Cs source is related, which further supports the hypothesis and that a ^{137}Cs point source is located in the indicated point.

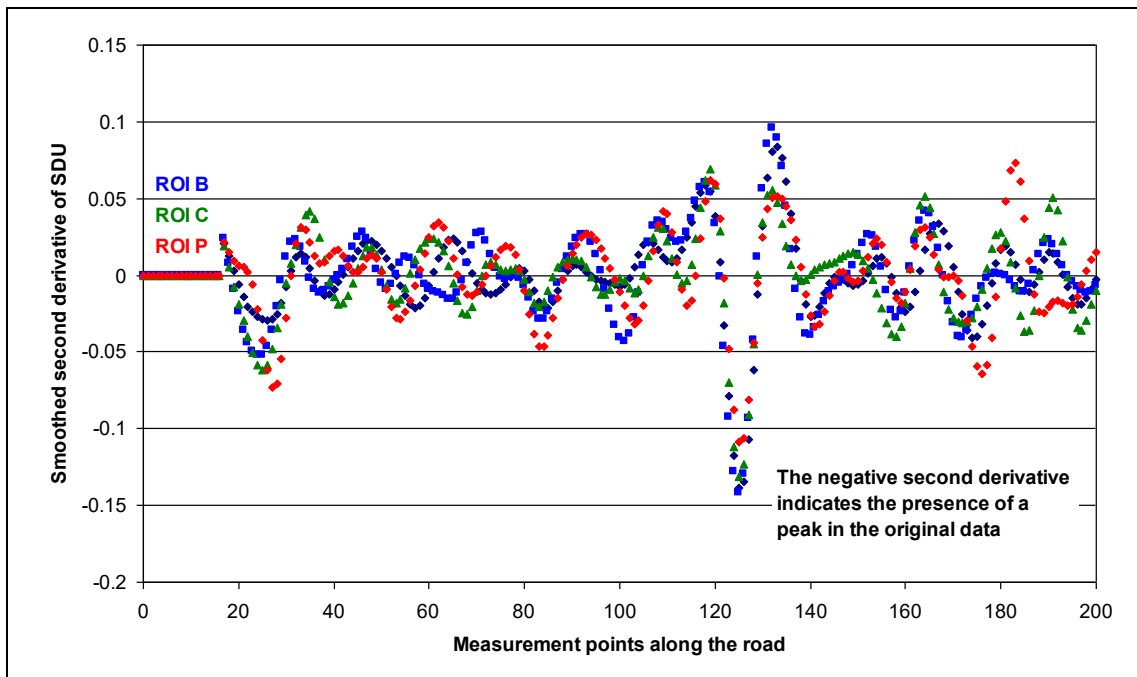


Fig 9. The second derivative of the SDIQ for the DEMA mobile gamma spectrometric measurements indicates the presence of a source at point 125 (625 m) by its negative value. Data in ROI B, C and P are in phase at this location, while data along other parts of the road are not, which supports the hypothesis that a ^{137}Cs point source is located in the indicated point.

2.3.2.4 Finding the location of a source by the third derivatve of SDU

The third derivative shows the changes in the second derivative. The location of the radiation source along the path is where the second derivative shows a minimum value. There, the third derivative is zero. Fig 9 shows how the third derivative goes from positive over zero to negative, almost like a straight line. Where the third derivative crosses the abscissa (path coordinate), the position of the source is indicated along the path coordinate, which is 650 m from the starting point.

The oscillations in the derivatives at other locations along the path where the data for ROIs A, B and P are out of phase are due to statistical fluctuations in the measurement data and do not imply any indication of a varied radiation field. It is purely the effect of statistical Poisson distributed noise.

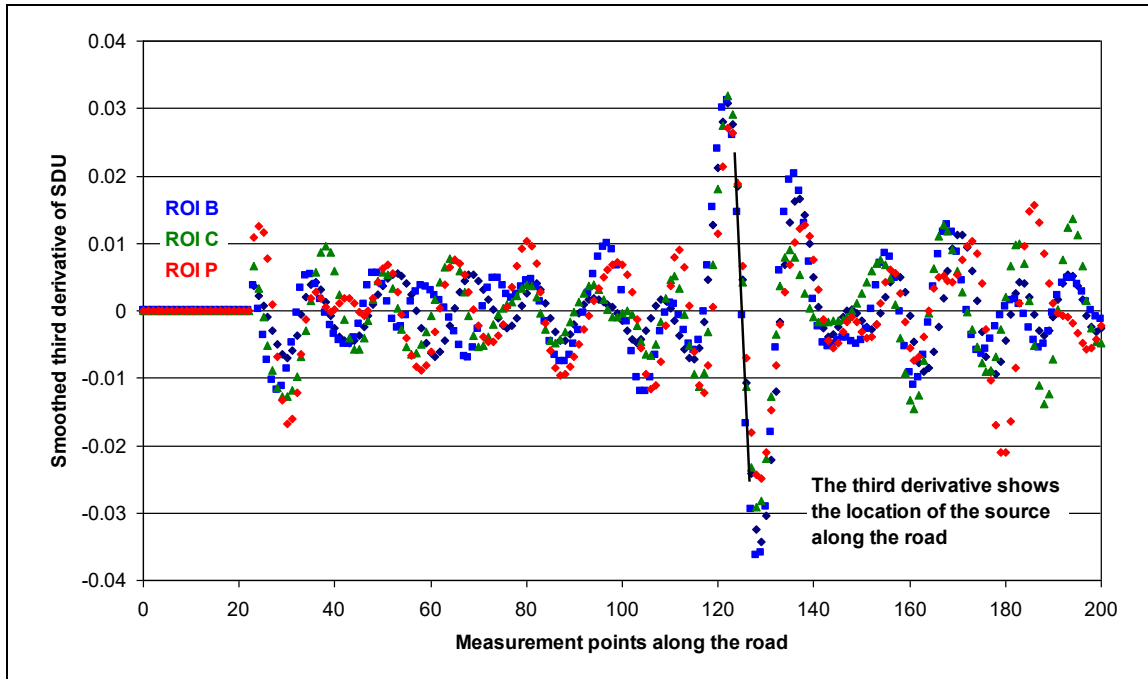


Fig 10. The third derivative of the SDU for the DEMA mobile gamma spectrometric measurements indicates the location of the ^{137}Cs point source along the road where the zero value of the third derivative crosses the abscissa.

3. Method of source distance, shielding and activity determination

The method development for determining a gamma ray source's location, shielding and activity with mobile gamma spectrometry started in the NKS-supported project SHIELDMORC 2019 - 2020 (Rääf et al., 2021, 2022) and continued in NKSCOMBMORC 2021 - 2022 (Rääf et al., 2023a, 2023b) by presenting the Excel applications Source Distance and Activity Calculator (SODAC) and Source Shield Calculator (SSC). In 2023, the methods were further developed. Short descriptions of the 2022 and 2023 versions are given below.

3.1 The Source Distance and Activity Calculator (SODAC).

3.1.1 First SODAC version, 2022

The fluence function for different source distances (Eqn 2 for unshielded sources and Eqn 3 for sources with a slab shield) was programmed in an Excel routine (SODAC) for road-source distances, x , from 5 to 150 m. The fluence function in steps of 5 m along the road, y , normalized to 1 at $y = 0$ (the maximum), was precalculated and stored in SODAC as a "knowledge library". SODAC was programmed for semi-stationary measurements, i.e. all gamma spectrometric measurements should be made stationary, and the measuring vehicle should move from one measuring point to another, encompassing the maximum count rate location at $y = 0$. The net (background-subtracted) count rate in the full-energy peak at stationary locations along a road is entered into the routine, which then searches for the fluence function curve that best fits the measured values. The best-fit function curve determines the source distance x . SODAC displays the function curve, the measured full energy peak count rate values and the obtained road-source distance in a graph.

For a NaI(Tl) detector, the background count rate must be known to calculate the source's full energy peak count rate correctly. A background should be measured in any area that represents the radiation environment along the road. In the COMB-MORC experiments, the background count rate was measured along the road when no source was deployed. In an actual situation, this is not possible, and the background count rate must be determined from background measurements far enough from the source. The uncertainty of a representative background measurement leads to additional uncertainty when determining the distance and activity of an unknown gamma-ray source.

When the distance to the source is known, the source's activity can be calculated with knowledge of the detector's count rate for primary photons using the effective detector area ε_0 (in the first SODAC version by using Eqn 5 without the angular efficiency correction $\varepsilon_0/\varepsilon_0$).

3.1.2 Second SODAC version, 2023

When the results from the distance determination to an unshielded ^{137}Cs source were compared with the actual distance, it was found that measurements with horizontally placed 4 L NaI(Tl) detectors consistently gave too short distances. The fluence function (Eqn 3) SODAC identified as having the best agreement with the measurement data showed a narrower half-width value than the distance-correct function. That resulted in a too-short source distance estimate and too-low calculated source activity. The reason for the underestimation is the oblong shape of a 4 L NaI(Tl) detector. This shape results in a lower effective detector area (detector

efficiency) for obliquely incident photons compared to photons incident perpendicular to the detector side area. In the NKS project AUTOMORC 2018, Lund University measured the relative angular efficiency $\varepsilon_{\theta}/\varepsilon_0$ of horizontally oriented 4 L NaI(Tl) detectors (Räaf et al., 2019). For a 40-degree incidence, the efficiency was 86 per cent of the maximum and 62 per cent for a 60-degree direction. In 2023, SODAC was updated with a routine that corrects the measurement data for a detector's varying angular efficiency (the $\varepsilon_{\theta}/\varepsilon_0$ function), using Eqn 5 to obtain the source distance from the best fit of count rate data $\dot{N}(y)$ along the road path y . Appendix K in the COMBMORC 2022 report (Räaf et al., 2022b) gives instructions for using SODAC in the 2023 version.

When all teams' results on distance determinations with the updated 2023 version of SODAC were made based on the 2022 measurements, the average value for distance determinations between 30 and 90 meters was -20 ± 3 per cent. The method thus still gave a systematic underestimation of the distance to the radiation source even though corrections for the varying angular efficiency of the detectors were made. Five out of six measurements were made against shielded radiation sources. The underestimated distance values may be because the correction in SODAC for shielded sources is not entirely adequate. The number of semi-stationary measurements was also few, which means that statistical uncertainties have a significant impact, especially at longer distances from the source where shielding of the source substantially reduces the primary photon fluence.

It is essential to carry out additional accurate measurements against shielded and unshielded sources to determine whether additional corrections need to be added in SODAC. The Nordic teams made such measurements in October 2023, described in Chapter 4. Evaluation of the measured data is scheduled for the coming REALMORC 2024 project.

3.2 The Source Shielding Calculator - SSC

3.2.1 First SSC version, 2022

The exponential model for determining mass thickness for a slab shield in front of a gamma-ray point source as a function of net count rate ratios ROI A/PL, A/P, B/PL, B/P, C/PL, C/P was programmed as an Excel™ application named the Source Shielding Calculator, SSC. The Nordic teams used the application in the NKS field experiments COMBMORC 2022 (Räaf et al., 2023b). The teams performed "calibration measurements" ^{137}Cs point sources placed behind nine different shields with thicknesses from 43 to 735 kg/m², consisting of wood and concrete. The net count rates in the six defined ROIs A, B, C, PL, PR and P for the background and the source geometries were stored in SSC as a "knowledge library", which also gave the coefficients of the exponential relationship (Eqn 7). The teams then tested the SSC method on shielded ^{137}Cs point sources placed at three distances (30, 60 and 90 m) with three different slab shield thicknesses ranging from the air-only to 310 kg/m². When all team measurement results were weighed together, the agreement between measured and actual shield thickness was 3 ± 10 per cent. However, the variation in results for individual measurements was significant, in some cases up to 50 per cent.

3.2.2 *Second SSC version, 2023*

Significant variations in calculated shield thickness for individual measurements and that there seemed to be some systematic deviation in the exponential model for specific shield thicknesses led to the idea of trying another model for the relationship between the count rate ratios ROI A/PR, A/P, B/PR, B/P, C/PR, C/P and the mass thickness of a shield. The model chosen was a logarithmic polynomial model where the count rate ratios were first logarithmized and then used as a variable in a five-degree polynomial. The second SSC routine was developed in the spring of 2023 to apply the polynomial model simultaneously with the exponential model to compare results. The polynomial coefficients were determined automatically in the SSC routine by least squares fitting. The NKS report for COMBMORC 2022 (Rääf et al., 2023b) describes the mathematics. Appendix J in the COMBMORC 2022 report gives instructions for using SSC in the 2023-year version.

When all the results from the polynomial model were weighed together, it showed a 6 ± 9 per cent too high value of the shield mass thickness compared to the actual value. There was no significant difference in results between the exponential and the polynomial models. Both models gave correct results on average within the statistical margin of error. For the polynomial model, it is essential to observe the validity limits in the shield mass thickness, as it is strictly adapted to apply within the "calibration" limits. The polynomial model oscillates uncontrollably outside limits, while the exponential model does not. The exponential model applies even slightly outside its "calibration" limits.

The conclusion from the comparison between the exponential model and the five-degree logarithmic polynomial model is that they give equivalent results and uncertainty. However, because the polynomial model is more complex and can lead to significant errors if applied outside its range of validity, it is not recommended. The exponential model is more stable and appears to give reasonably accurate results.

4. Equipment and experiment

The Nordic mobile gamma spectrometry teams conducted a joint field experiment with the mobile search for ^{137}Cs point sources in ordinary environs in southern Sweden in October 2023. Teams performed controlled experiments to test methods to locate hidden ^{137}Cs point sources in “near real” situations and to determine the distance, shielding and activity of the same radiation geometries as in the search experiment. The teams used their ordinary measuring equipment and software to analyse the measurement results. They stored and reported all raw data in an agreed standard format (the comma-separated MGS format). The intention is to conduct additional analysis on measured data in 2024 according to the theory described in Chapter 2 of this report.

4.1 Aim of the REALMORC 2023 experiments

The experiments aimed to obtain a practical measurement basis to investigate whether the previously developed routines SODAC and SSC for determining a ^{137}Cs source’s distance, shielding and activity with mobile gamma spectrometry can be used in a “real-world” environment. Since the SODAC and SSC routines are based on a series of semi-stationary (still-standing) measurements along the road where a radiation source is suspected, and this procedure would constitute a traffic hazard if carried out in an actual situation without the assistance of the police, the experiments were divided into two parts:

1. “Safe area” experiments where the mobile teams made recurrent measurements along a road with the same source geometries as in the “real-world” search experiment.
2. “Real-world” source search experiment.

4.2 Teams and measuring equipment

Six mobile gamma spectrometry teams participated in the joint “near reality” search experiments on October 10 - 12, 2023, around Barsebäck in southern Sweden. The teams were from the Danish Emergency Management Agency (DEMA), Norwegian Radiation and Nuclear Safety Authority (DSA), Geislavarnir ríkisins, Iceland (GR), Medical Radiation Physics, ITM, Lund University, Sweden (LU), Geological Survey of Norway (NGU), and the Swedish Radiation Safety Authority (SSM).

Table 2 summarises the detectors, multi-channel analysers and proprietary software used by the teams. Each team describes their equipment and software in Appendices A1 - A6.

Table 2. Teams, detectors, MCAs, and software used in the REALMORC 2023 experiment.

Team	DEMA	DSA	GR	LU	NGU	SSM
Detector	4 L NaI(Tl)	2x4 L NaI(Tl)	2x2 L NaI(Tl)	2x4 L NaI(Tl) 123% HPGe	4x4 L NaI(Tl)	2x4 L NaI(Tl) 120% HPGe
MCA	Radiation Solutions RS-700	Radiation Solutions RS-700	SPARCS mobile survey system	Ortec Digibase Ortec Digidart	Radiation Solutions RSX-5	Ortec Digibase Ortec Digidart
Software	RadAssist	RadAssist	AVID NSCRAD	Gammavision NuggetW	RadAssist	Gammavision NuggetW
Appendix	A1	A2	A3	A4	A5	A6

4.3 “Safe area” measurements along a road with shielded sources

The “safe area” measurements were made along Kraftverksvägen outside the decommissioned Barsebäck Nuclear Power station with the shielded ¹³⁷Cs sources placed according to Fig 11 in locations with code names Sierra and Tango. The source activities, shield thicknesses and distances from the road are given in Tables 3 and 4.



Fig 11. The road Kraftverksvägen passing the source points Sierra and Tango used in the mobile monitoring experiments on Tuesday, October 10 and Thursday, October 12 – map from Google Earth 2023.

Table 3. The Sierra source setup uses a 590 MBq ^{137}Cs point source with three shielding geometries. The U and S geometries are identical but measured by the teams on Tuesday, October 10 (U1, U2, U3) and Thursday, October 12 (S1, S2, S3). Shielding thicknesses refer to distance to detectors in vehicle on road when opposed to the source.

Source geometry	Distance from roadside	Shielding	Shielding including air kg/m ²
U1, S1	20 m	350 mm concrete	833.6
		24 mm wood	12.5
		21 m air	26.1
		Total	872.2
U2, S2	20 m	250 mm concrete	595.4
		24 mm wood	12.5
		21 m air	26.1
		Total	634.0
U3, S3	20 m	150 mm concrete	357.2
		24 mm wood	12.5
		21 m air	26.1
		Total	395.8

Table 4. The Tango source setup uses a 590 MBq ^{137}Cs point source with three shielding geometries. The U and T geometries are identical but measured by the teams on Tuesday, October 10 (U1, U2, U3) and Thursday, October 12 (T1, T2, T3). The trailer wall contains 5 mm fibreglass-reinforced polyester resin plastic (FRP). Shielding thicknesses refer to distance to detectors in vehicle on road when opposed to the source.

Source geometry	Distance from roadside	Shielding	Shielding including air kg/m ²
U1, T1	70 m	150 mm concrete	357.2
		30 mm wood	15.7
		5 mm FRP	88.4
		71 m air	10
Total	471.3		
U2, T2	70 m	100 mm concrete	238.2
		30 mm wood	15.7
		5 mm FRP	88.4
		71 m air	10
Total	352.3		
U3, T3	70 m	50 mm concrete	119.1
		30 mm wood	15.7
		5 mm FRP	10
		71 m air	88.4
Total	233.2		

4.3.1 Mobile measurements, Tuesday October, 10

For each setup, all teams passed the Sierra and Tango sources several times during 45 minutes at 30 km/h. The purpose of the measurements was to collect measuring data of the same type as in the “real-world” search experiment on Wednesday, October 11.

However, the teams did not know at this time that the same geometries would be used in the search experiment conducted on the following day because it would have reduced the realism of the search experiment. They got the information after the “real-world”.

Table 3 - 4 and Appendix B1 give details of the mobile experiments.

4.3.2 Semi-stationary measurements, Thursday October, 12

All teams performed semi-stationary measurements along the road at the Sierra and Tango source setups. The purpose was to collect data to investigate if it is possible to replace semi-stationary measurements with mobile measurements (from the Tuesday experiments), where the vehicle passes the source several times.

Tables 3 - 4 and Appendix B3 give details of the semi-stationary experiments.

4.4. “Real-world” source search experiment

The task was to use mobile gamma spectrometry along three road loops (Bravo, Charlie, Delta) to search for “orphan” ^{137}Cs point sources. The mobile units should behave normally in traffic and maintain traffic speed. Stopping along the road loop while the search was in progress was not permitted because that could cause a traffic hazard. The start and stop should be at the specified points along the road loop. Standing still with the measuring car to perform data analysis and reporting was possible at those points. Fig 12 shows an overview of the road loops.

Appendix B2 provides instructions and the schedule for the source search experiments.



Fig 12. The four road loops (Alpha, Bravo, Charlie, Delta) were defined for the search experiment on Wednesday, October 11. The Alpha loop was not used due to a lack of time – map from Google Earth 2023.

4.4.1 Source search along the road loop Bravo

The road loop Bravo should be measured once in each direction. Sources were not placed in this loop, and the information was not disclosed to the teams during their measurements of the loop. The intention was that teams should get enough measurement data to classify the loop as “clean” from sources above a certain distance and activity after completing the loop in both directions.



Fig 13. The search loop Bravo northeast of Burlöv was used on Wednesday, October 11 – map from Google Earth 2023.

4.4.2 Source search along the road loop Charlie

The ^{137}Cs source in the same shielding geometries as in the Sierra setup (Tuesday, October 10, and Thursday, October 12) was placed 20 m from the roadside near a railway viaduct containing a naturally occurring radiation anomaly. (Fig 14 and 15).

Fig 16 shows part of the shielding construction. Table 5 provides data for the three shielding setups.

Teams were ordered to measure the road loop Charlie twice clockwise for each setup. After completion and analysis, the teams had to report the results to the communication centre, which kept a logbook of the findings.



Fig 14. The search loop Charlie at Lackalänga was used on Wednesday, October 11. The red dot indicates the source location – map from Google Earth 2023.

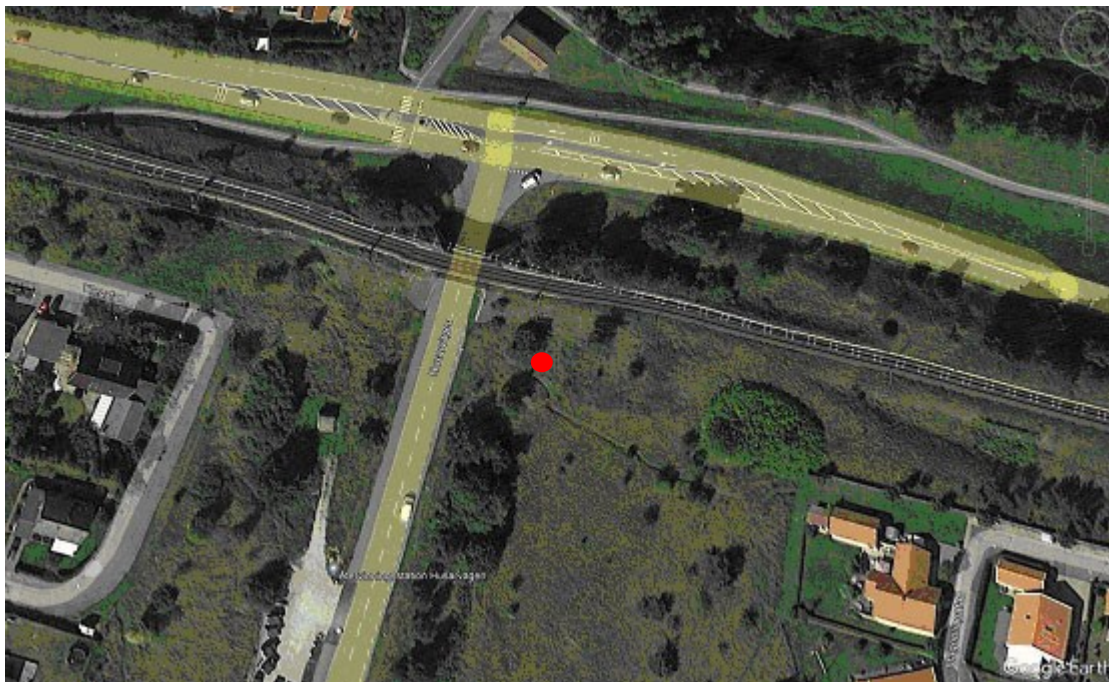


Fig 15. The red dot indicates the location of the shielded ^{137}Cs source at the road loop Charlie in Lackalänga. The distance from the roadside was 20 m – Setup CA1, CA2, CA3, CB1, CB2, CB3 – map from Google Earth 2023.



Fig 16. Example of source geometry shielding. Road loop Charlie, setup CA1 and Sierra, setup U1 and S1. The source position (red arrow) is seen vertically downwards with tree concrete stones thickness as shielding towards the road where the mobile gamma spectrometry cars pass. Another five concrete stones are placed on the other side of the plywood wall (not seen in the picture). The back-reflector with 5 cm bunt clay is visible between the plywood walls at the top of the picture.

Table 5. The road loop Charlie setup using a 590 MBq ¹³⁷Cs point source with three shielding geometries. The CA and CB geometries are identical but measured by the teams at different times of the day. Shielding thicknesses refer to distance to detectors in vehicle on road when opposed to the source.

Source geometry	Distance from roadside	Shielding	Shielding including air kg/m ²
CA1, CB1	20 m	350 mm concrete	833.6
		24 mm wood	12.5
		21 m air	26.1
		Total	872.2
CA2, CB2	20 m	250 mm concrete	595.4
		24 mm wood	12.5
		21 m air	26.1
		Total	634.0
CA3, CB3	20 m	150 mm concrete	357.2
		24 mm wood	12.5
		21 m air	26.1
		Total	395.8

4.4.3 Source search along the road loop Delta

The ^{137}Cs source in the same shielding geometries as in the Sierra setup (Tuesday, October 10 and Thursday, October 12) was placed 35 m from the roadside near a large stone building containing a naturally occurring radiation anomaly. (Figs. 17, 18 and 19). This position was not the original intention. A location had been reconnoitred for placing the source more freely 70 m from the roadside (as in the Tango setup). However, it could not be used that day due to a large pile of potatoes on the site.

Table 6 provides data for the three shielding setups.

The road loop Delta should be measured twice clockwise for each setup. After completion and analysis, the teams had to report the results to the communication centre, which kept a logbook of the findings.



Fig 17. The search loop Delta northeast of Flyinge was used on Wednesday, October 11 – map from Google Earth 2023.



Fig 18. Location for the shielded ^{137}Cs source at the road loop Delta at Kristinetorp. The source distance from the roadside was 35 m – Setup DA1, DA2, DA3, DB1, DB2, DB3 – map from Google Earth 2023.



Fig 19. The shielded ^{137}Cs source was placed in a trailer at the road loop Delta at Kristinetorp. The road stretches along the edge of the forest behind the stone building.

Table 6. The road loop Delta setup using a 590 MBq ^{137}Cs point source with three shielding geometries. The DA* (PM) and DB* (AM) geometries are identical but measured by the teams during different times of the day. The trailer wall consists of 5 mm fibreglass reinforced polyester resin plastic (FRP). Shielding thicknesses refer to distance to detectors in vehicle on road when opposed to the source.

Source geometry	Distance from roadside	Shielding	Shielding including air kg/m^2
DA1, DB1	35 m	150 mm concrete	357.2
		30 mm wood	15.7
		5 mm FRP	10
		36 m air	44.8
		Total	427.7
DA2, DB2	35 m	100 mm concrete	238.2
		30 mm wood	15.7
		5 mm FRP	10
		36 m air	44.8
		Total	308.7
DA3, DB3	35 m	50 mm concrete	119.1
		30 mm wood	15.7
		5 mm FRP	10
		36 m air	44.8
		Total	189.6

5. Results and discussion

A summary of the results from the joint Nordic experiments to search for hidden ^{137}Cs point sources with mobile gamma spectrometry is reported here. Each team's detailed results are given in Appendices A1 - A6.

5.1 “Safe area” measurements along a road with shielded sources

The analysis from part 1 of the experiments, whether mobile measurements alone can give the same or better results for determining distance, shielding and activity of a point source than semi-stationary measurements, requires further analysis using the SODAC and SSC methods. According to the plan, results from the analysis will be reported in the continued NKS REALMORC 2024 project.

5.2 “Real-world” source search experiment

All teams used their propriety software in the search experiment to analyse and identify the placed “orphan” ^{137}Cs sources. The teams manually inspected the measured pulse height distributions for locations where the software indicated “anomalies” or increased count rates in the energy regions of primary and Compton scattered radiation from ^{137}Cs . The detection results are given in Table 7 for loop Charlie and Table 8 for loop Delta, as teams reported it directly to the communication centre after completing each road loop.

The Charlie setup had a 580 MBq ^{137}Cs source placed 20 m from the roadside. When heavily shielded (834 kg/m²), the source was not detected by any team. However, the NGU team got an alarm with the 16 L NaI(Tl) detector from an anomaly at the location of the source.

When medium shielded (594 kg/m²), the Charlie source was detected by all teams with 4 L NaI(Tl)-detectors but not by the team with a 2x2 L NaI(Tl) detector. All teams detected the somewhat shielded (357 kg/m²) Charlie source.

The Delta setup had a 580 MBq ^{137}Cs source placed 35 m from the roadside. With maximum shielding (357 kg/m²), the source was detected by the NGU team with the 16 L NaI(Tl) detector but not by the teams with 4 L NaI(Tl) detectors.

When medium shielded (238 kg/m²) and somewhat shielded (119 kg/m²), the source was detected by all teams with 16 L and 4 L NaI(Tl) detectors. The 2x2 L NaI(Tl) detector team got anomaly alarms for all shielding thicknesses.

It should be noted that detecting the ^{137}Cs sources in the Charlie and Delta road loops was impeded by anomalies of the uranium series nuclides and ^{40}K being nearby. The anomalies increased the count rate in the energy range of primary and scattered radiation from ^{137}Cs . In addition, the railway viaduct in the Charlie loop and the large stone building in the Delta loop shielded the source in a lateral direction. This structure shielding complicated the source detection and utilising the SODAC method to calculate the distance to the source from measurements along the road. These structure problems will be studied more thoroughly in the continued REALMORC 2024 project.

The software’s “anomalies” detection by the Radiation solutions RadAssist and the SPARCS AVID/NSCRAD systems turned out to help indicate possible source locations. However, documentation of how the anomaly detections work is unavailable. Thus, it is not possible to draw any far-reaching conclusions about the effectiveness of the “anomalies” method.

Table 7. Teams results in the Charlie setup presenting the initial reporting from the shielded ¹³⁷Cs point source search in a “real-world” environment using mobile gamma spectrometry and the teams’ proprietary detection software.

Source geometry	Team and detector					
	DEMA 4 L NaI(Tl)	DSA 4 L NaI(Tl)	GR 2x2 L NaI(Tl)	LU 2x4 L NaI(Tl), and 123% HPGe	NGU 4x4 L NaI(Tl)	SSM 2x4 L NaI(Tl), and 120% HPGe
CA1, CB1	not found	not found	not found	not found	alarm ¹	not found
CA2, CB2	found	found	not found	found	found	found
CA3, CB3	found	found	found	found	found	found

1. Software indication of anomaly. Nuclide not identified.

Table 8. Teams results in the Delta setup presenting the initial reporting from the shielded ¹³⁷Cs point source search in a “real-world” environment using mobile gamma spectrometry and the teams’ proprietary detection software.

Source geometry	Team and detector					
	DEMA 4 L NaI(Tl)	DSA 4 L NaI(Tl)	GR 2x2 L NaI(Tl)	LU 2x4 L NaI(Tl), and 123% HPGe	NGU 4x4 L NaI(Tl)	SSM 2x4 L NaI(Tl), and 120% HPGe
DA1, DB1	not found	not found	alarm ¹	not found	found	not found
DA2, DB2	found	found	alarm ¹	found	found	found
DA3, DB3	found	found	alarm ¹	found	found	found

1. Software indication of anomaly. Nuclide not identified.

Table 9. Average detection outcome for the 4 L NaI(Tl) detectors in the search experiment, locating shielded ¹³⁷Cs point sources, compared to theoretically calculated maximum detection distances when using an alarm level for the primary photon count rate. The detection probability is 95%, and the false positives are at most one per hour. The vehicle speed is assumed to be 40 km/h at the C** source geometries and 50 km/h at the D** geometries.

Source geometry	Source distance m	Max detection distance / m	Should be detected	Was detected
CA1, CB1	22	3	No	No
CA2, CB2	22	11	No	Yes
CA3, CB3	22	29	Yes	Yes
DA1, DB1	32	27	No	No
DA2, DB2	32	42	Yes	Yes
DA3, DB3	32	64	Yes	Yes

The NKS project AUTOMORC developed a model for calculating maximum detection distances in mobile search for gamma-ray sources (Räaf et al., 2019; Finck et al., 2022). The model is governed by a probability of detecting the primary photon fluence from a gamma-ray source and a maximum acceptable false positive indications per hour. The maximum detection distances for the six different combinations of distance and shielding in the REALMORC search experiment (source geometries from C*1 to D*3) were calculated for the teams' 4 L NaI(Tl) detectors, assuming a vehicle speed of 50 km/h. Table 9 shows the result of the calculated maximum detection distances.

The calculated maximum detection distances predict that the shielded ^{137}Cs sources would be detected in three cases (C*3, D*2, and D*3) out of six. It was detected in all cases where the source was predicted to be detected. However, the source was detected in an additional case, C*2, where the source distance was at 22 m and the predicted maximum detection distance was 11 m. Thus, the actual outcome of detecting the shielded sources was somewhat better than predicted.

Sources shielded by thick layers of building material produce substantial amounts of Compton scattered photons, which register in the pulse height distribution below the full energy peak (Räaf et al., 2020). Due to its low resolution, a NaI(Tl) detector registers part of the Compton photons in the region of the full energy peak, increasing the ROI P count rate and triggering an alarm. The "Compton-boosted" count rate in ROI P tends to increase the distance at which shielded sources could be detected compared to unshielded, presuming that the shielded and unshielded sources have the same primary fluence at the detector.

A second reason the C*2 source was detected when not predicted from the alarm level on ROI P is that the teams used manual observations of the changes in the recorded pulse height distributions (gamma spectra) to identify minor increased count rates in the region of the primary radiation from ^{137}Cs . Manual observation can make detection more sensitive but also more laborious. Most teams' software for detection also "alerted" the operator when a recorded pulse height distribution deviated from the expected background, which happens when many Compton scattered photons are registered. The anomaly alert helped the teams to focus on "suspect" locations and examine the pulse height distributions there more thoroughly.

6. Conclusion

The report contains a theoretical part and an experimental part. The theoretical part describes how frequency analysis methods can be used in mobile gamma spectrometry to locate hidden gamma-ray sources that are difficult to detect. The experimental part reports the outcome of a joint Nordic experiment to search for hidden and shielded ^{137}Cs point sources with mobile gamma spectrometry in a “real-world” environment.

6.1 Suggested frequency analysis methods to identify lost gamma-ray sources by mobile gamma spectrometry

The report has shown two methods of analysing measurement data from mobile gamma spectrometry to improve the possibilities of identifying lost gamma-ray sources. The methods rely on analysing standard deviations in collected measurement data rather than just observing the “raw” measurement data. The standard deviation approach has the advantage of suppressing the slowly varying signals from the natural background from uranium, thorium and potassium and highlighting fast-varying signals from local radiation sources.

The method of calculating the standard deviation indication quotient (SDIQ) shows whether a collection of spectrometric measurement data contains signals from local radiation sources that the measuring vehicle has passed.

Calculating standard deviation units (SDU) shows where local radiation sources may be along the measuring vehicle's path. The SDU indicates both primary and scattered radiation simultaneously and can detect if the contributions are in phase, which strengthens an indication of a local radiation source.

Frequency analysis performed on SDU data reduces the statistical background noise in the measurement data by filtering the data. Choosing a suitable filter can emphasise signals from radiation sources within given distance ranges. The method can potentially extend the detection distances by utilising more of the structure of the recorded measurement data than relying solely on an alarm level for the number of counts per channel or ROI.

The conclusions are based on studies of the methods for a limited measurement database and 4 L NaI(Tl) detectors. It is essential to investigate the ability and effectiveness of the methods in well-controlled experiments and “real-world” surroundings.

6.2 The search experiments

Six Nordic mobile gamma spectrometric search teams took part in the joint “real-world” search experiments to locate six ^{137}Cs point sources geometries behind walls of standard building material having mass shield thicknesses from 145 to 846 kg/m².

The outcome of the search experiments for locating shielded ^{137}Cs point sources was slightly better than predicted by theoretical calculations of maximum detection distances. The reason is probably that Compton scattered photon registrations in a NaI(Tl) detector contribute to the count rate in the region of the full energy peak, thereby increasing the detection distance somewhat. Software giving indications of

“anomalies” where the recorded pulse height distribution differs from an expected natural radiation background can help an operator inspect measurement data more thoroughly to find the anomaly’s cause.

All participating teams found the search experiments exciting and rewarding. Some teams could send measurement data to their home laboratory as a reach-back function. This procedure allows the car crew to concentrate on handling the car and the measuring equipment, and the home laboratory can put expertise into analysing measurement data.

The standard data formats (MGS.CSV), specially developed for the REALMORC activity, enable the exchange of measurement data between all Nordic mobile teams and facilitate the joint use of analysis software developed within the NKS *MORC* projects. It also means that Nordic reach-back laboratories can help each other analyse mobile measurement data.

Teams have pointed out that the calibrations, measurements and methods developed for orphan source search in the NKS projects SHIELDMORC, COMBMORC, and REALMORC are helpful for emergency preparedness and strengthen the ability to carry out mobile gamma spectrometric search of orphan sources should a real threat situation occur.

References

Antanas Bukartas, Robert Finck, Jonas Wallin, Christopher L. Rääf. A Bayesian method to localize lost gamma sources, *Applied Radiation and Isotopes*, 145 pp 142-147. March 2019. <https://doi.org/10.1016/j.apradiso.2018.11.008>, 2019.

Bukartas A, Wallin J, Finck R, Rääf C, Bayesian algorithm to estimate position and activity of an orphan gamma source utilizing multiple detectors in a mobile gamma spectrometry system. *PloS ONE* 16(1):e0245440. <https://doi.org/10.1371/journal.pone.0245440>, 2021

Bukartas A, Wallin J, Finck R, Rääf C, Accuracy of a Bayesian technique to estimate position and activity of orphan gamma-ray sources by mobile gamma spectrometry: Influence of imprecisions in positioning systems and computational approximations. *PLoS ONE* 17(6): e0268556. <https://doi.org/10.1371/journal.pone.0268556>, June 2022.

Robert Finck, Jan Johansson, B. Åke Persson, Christer Samuelsson, Karl Östlund.. Close Reality in Radiological Emergency Exercises, in *Proceedings of the 12th Congress of the International Radiation Protection Association (IRPA) in Buenos Aires, on October 19 –24, 2008*.

R. Finck, T. Geber-Bergstrand, J. Jarneborn, G. Jónsson, M. Jönsson, S. Juul Krogh, S. Karlsson, J. Nilsson, M. Persson, P. Reppenhagen Grim, C.L. Rääf, M. Sickel, P. Smolander, R. Watson, K. Östlund, Mobile search of material out of regulatory control (MORC) – Detection limits assessed by field experiments, *Nordic Nuclear Safety Research Report NKS-421*, ISBN 978-87-7893-510-6, March 2019.

Finck, R., Bukartas, A., Jönsson, M., Rääf, C., Maximum detection distances for gamma emitting point sources in mobile gamma spectrometry, *Applied Radiation and Isotopes*, doi: <https://doi.org/10.1016/j.apradiso.2022.1101>, 2022.

Peder Karl-Johan Kock; Robert R Finck; Jonas M Nilsson; Karl Östlund; Christer Samuelsson. A Deviation Display Method for Visualising Data in Mobile Gamma-ray Spectrometry, *Applied Radiation and Isotopes*, Volume 68, Issue 9, pp 1832-1838, September 2010.

Christopher L. Rääf (chair), Robert R. Finck (co-chair) Antanas Bukartas, Gísli Jónsson, Sune Juul Krogh, Simon Karlsson, Morten Sickel, Petri Smolander, Jonas Wallin, Robin Watson, AUTOMORC – Improvement of automatic methods for identification of radioactive material out of regulatory control (MORC) by mobile gamma spectrometric search experiments. Report 2017. *Nordic Nuclear Safety Research Report NKS 422*, March 2019.

Christopher L. Rääf (chair), Robert R. Finck (co-chair), Vikas C. Baranwal, Antanas Bukartas, Marie-Andrée Dumais, Kjartan Guðnason, Yvonne Hinrichsen, Gísli Jónsson, Mattias Jönsson, Peder Kock, Sune Juul Krogh, Simon Karlsson, Frode Ofstad, Jan Steinar Rønning, Petri Smolander, Kasra Tazmani, Mikael Westin, SHIELDMORC– Detection distances and methods to locate orphan gamma radiation sources in shielded building geometries by mobile gamma spectrometry, *Nordic Nuclear Safety Research, Report NKS-433*, March 2020.

Christopher L. Rääf, Robert R. Finck, Vikas C. Baranwal, Jonas Boson, Antanas Bukartas, Marie-Andrée Dumais, Kjartan Guðnason, Marjan Ilkov, Gísli Jónsson, Mattias Jönsson, Simon Karlsson, Marie Lundgaard Davidsdóttir, Frode Ofstad, Jan Steinar Rønning, Petri Smolander, Mikael Westin, Detection of orphan gamma radiation sources in shielded building geometries by mobile gamma spectrometry. A method of using Compton scattered radiation

to estimate the shielding mass thickness of common building material, Nordic Nuclear Safety Research Report NKS-448, June 2021.

Christopher L. Rääf (chair), Robert R. Finck (co-chair), Einar Ameen, Vikas C. Baranwal, Marco Brønner, Antanas Bukartas, Jon Drefvelin, Johannes Eriksson, Kjartan Guðnason, Gísli Jónsson, Mattias Jönsson, Simon Karlsson, Peder Kock, Marie Lundgaard Davidsdóttir, Bredo Møller, Petri Smolander, Mikael Westin, COMBMORC - Combined analysis of primary and scattered components in mobile gamma spectrometric data for detection of materials out of regulatory control, NKS-B COMBMORC Report 2021, NKS-474, ISBN 978-87-7893-569-4, June 21, 2023a.

Christopher L. Rääf (chair), Robert R. Finck (co-chair), Vikas C. Baranwal, Marius-Catalin Dinca, Jon Drefvelin, Charlotte Alfast Espensen, Kjartan Guðnason, Per Otto Hetland, Gísli Jónsson, Mattias Jönsson, Marie Lundgaard Davidsdóttir, Bredo Møller, Frode Ofstad, Jan Gert Olsen, Petri Smolander, COMBMORC - Combined analysis of primary and scattered components in mobile gamma spectrometric data for detection of materials out of regulatory control, NKS-B COMBMORC Report 2022, NKS-476, ISBN 978-87-7893-571-7, August 11, 2023b.

UNSCEAR, Sources and Effects of Ionizing Radiation, United Nations Scientific Committee on the Effects of Atomic Radiation, Report UNSCEAR 2008, Volume II, Annex C, Radiation Exposures in Accidents, pp 9-13, United Nations, New York. 2011.

Acknowledgement

The authors thank Barsebäck Kraft AB for the access to the zones for certain parts of the experimental measurements.

The experiments made by Lund University were carried out with measuring equipment financed by the former Swedish Radiation Protection Authority (SSI) and the Swedish Radiation Safety Authority (SSM).

NKS conveys its gratitude to all organizations and persons who by means of financial support or contributions in kind have made the work presented in this report possible.

Disclaimer

The views expressed in this document remain the responsibility of the authors and do not necessarily reflect those of NKS. In particular, neither NKS nor any other organisation or body supporting NKS activities can be held responsible for the material presented in this report.

Appendix A1

Results from team DEMA, Danish Emergency Management Agency–nuclear division, Denmark

A1.1 Measuring equipment

The DEMA mobile spectrometry unit is a converted VW Multivan operated by one driver, an optional co-driver and up to two operators (Fig 1). The car is equipped with a Radiation Solutions RSI RS-700 system with two detectors connected, an RSX 4 litre NaI(Tl) and an RSX 3"x3" NaI(Tl) crystal. Detectors are contained in a rooftop box and connected to RadAssist software on interior PC with mapping and radionuclide identification capability.



Fig 1. The DEMA mobile spectrometry unit.

Table 1. The ROI setup for DEMA during REALMORC 2023 experiment. The intervals for energy and corresponding channel are based on the findings during the SHIELDMORC 2020 experiment.

ROI	Energy node (keV)	Energy interval (keV)	Channel interval	Number of channels
A	74	75-240	25-80	55
B	242	243-408	81-136	55
C	410	441-576	137-192	55
PL	578	579-660	193-220	27
PC	662	663	221	1
PR		666-747	222-249	27

A1.2 Software

Radiation Solutions RSI RS-700 system is operated using the proprietary software RadAssist, provided by the vendor.

The software has quite sophisticated options in order to set and invoke alarms. This can be done using measures of the standard deviation compared to the background, and measures of an anomaly factor.

During the REALMORC experiment, we chose to rely primarily on visual inspection of the waterfall diagram during acquisition in order to detect the sources.

This was done for two reasons:

- Our experience is that when the surrounding background radiation varies, sources have to be quite distinct in order to be detected through the set alarm values.
- The scope of the project was not primarily to test the RSI software, but the software developed by Lund University.

A1.3 Results

The results obtained by DEMA are presented with maps and examples of waterfall diagrams below.

For the first road loop, Bravo, we erroneously thought to identify a source. This is likely an effect caused by local changes in background radiation. When investigated again, it is obvious that it cannot be Cs-137, since the increase in radiation is also seen above 660 keV (Fig 2).

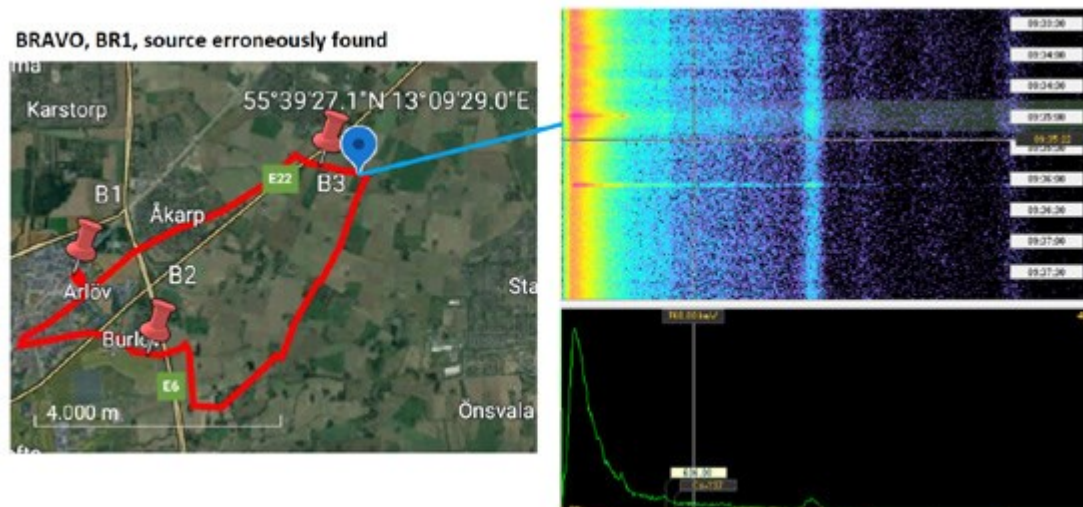


Fig 2. Map of Bravo loop with source coordinate and corresponding waterfall diagram. False detection as no source was present.

For the road loops, Charlie and Delta, we did not identify any sources during the first drive, but during the second (Fig 3) and third (Fig 4). The source signal was most prominent during the third drive for both Charlie and Delta, causing isotope alarms with nuclide identification Cs-137 using standard alarm settings.

The RSI system is currently not operated nor calibrated at a level where we can set a quantitative estimate of the distance at which an unshielded Cs-137 radiation source is likely not to be found.

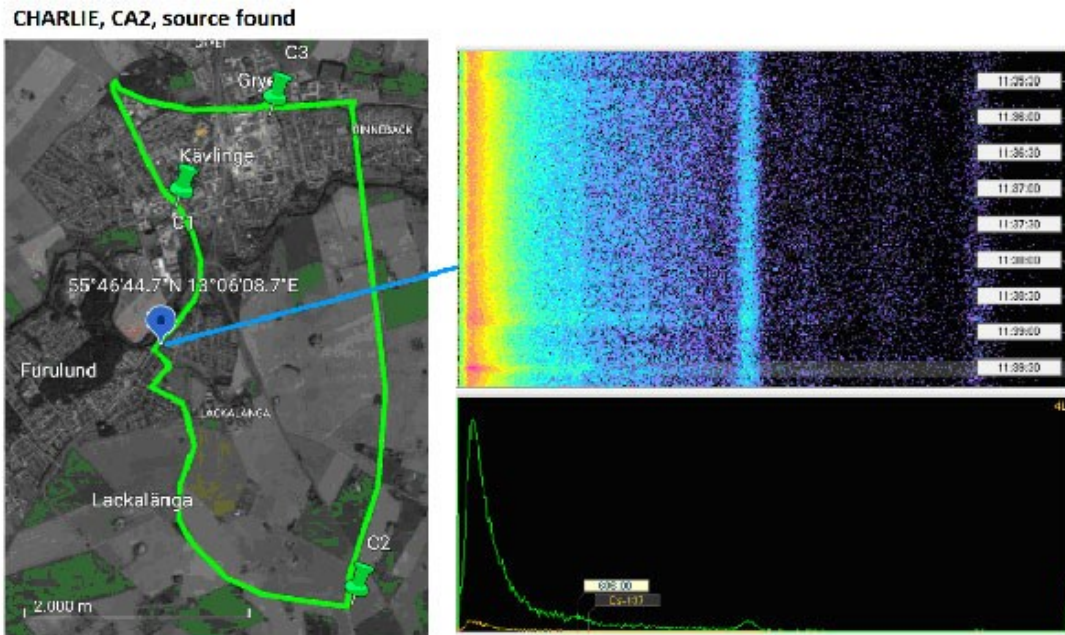


Fig 3. Map of Charlie loop with source coordinate and corresponding waterfall diagram.

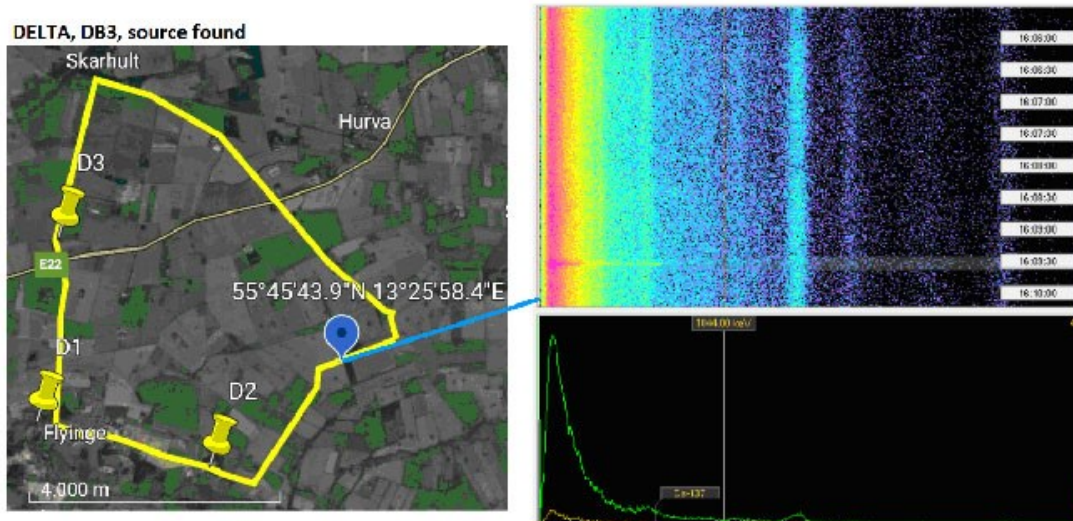


Fig 4. Map of Delta loop with source coordinate and corresponding waterfall diagram.

A1.4 Conclusion

Following the aim of the REALMORC experiment the DEMA mobile spectrometry unit was tested in a real life setting, in public areas, following local traffic speed limits and regulations. As DEMA participated with two persons, one driving the vehicle and one operating the equipment, it was clear that thorough analysis of data was not possible during the drive. It was possible to identify and detect sources with the measurement equipment, but it is not within scope or capability currently to identify clean areas.

In case of deployment of DEMAs equipment for source searching in a real setting, the options for live streaming of data should be invoked, allowing a home base support to assess and analyse the data from remote, allowing the driver and operator to focus on the operation of the car and the system.

Appendix A2

Results from team Norway – Norwegian Radiation and Nuclear Safety Authority (DSA).

A2.1 Measuring equipment

For the experiment, a modified 2008 VW Caravelle with shelf-mounted detectors inside the car was used. The equipment consists of two 4-liter (10cmx10cmx40cm) NaI-detectors, mounted on each side inside the car. The system is also set up with a 3-inch NaI-detector mounted in front of the left 4-liter detector. This detector can perform measurements in highly contaminated areas where 4-liters might get saturated. The setup also has a neutron detector between the two 4-liter detectors in the center of the car, and thus function as “shielding” between the two side mounted detectors. All equipment is of the self from RSI.



Car used for carborne measurements – all equipment mounted in the back of the car.

The following channel settings was used for the ROIs:

ROI_A_Chan_Left = 26

ROI_A_Chan_Right = 80

ROI_B_Chan_Left = 82

ROI_B_Chan_Right = 136

ROI_C_Chan_Left = 138

ROI_C_Chan_Right = 192

ROI_PL_Chan_Left = 194

ROI_PL_Chan_Right = 220

ROI_PR_Chan_Left = 222

ROI_PR_Chan_Right = 248

ROI_P_Chan_Left = 194

ROI_P_Chan_Right = 248

A2.2 Software

The measurements were done using the RS-700 spectrometer connected to a PC running Radassist v 6.2.32.0. During all the measurements, the acquisition time was set to 1 second. The vehicle speed was manually held as close as possible to 50 km/h for all the measurements.

During all the measurements, Radassist's anomaly detection was used for the alarming. The alarm level was set to 5 standard deviations. As this considers the changes in the shape of the spectrum, no ROIs were used.

When an alarm was triggered, Radassist does an analysis of a spectrum integrated over the last three seconds and tries to identify peaks from the integrated spectrum.

A2.3 Results

Normal traffic rules apply – no stopping allowed.

Loop Bravo. BR2.

No source found. Clean area statement: Max detection distance at 50 km/h for 100 MBq unshielded Cs-137 source is 50 meters. Slightly elevated dose rate under railway underpass at 55.6592 13.1447. NORM.

Loop Bravo. BR1.

No source found. Clean area statement: Max detection distance at 50 km/h for 100 MBq unshielded Cs-137 source is 50 meters.

Loop Delta. DA1.

No source found. Clean area statement: Max detection distance at 50 km/h for 100 MBq unshielded Cs-137 source is 50 meters.

Loop Delta. DA2.

Cs-137 source on right side of road at 55.7624 13.4336.

Loop Delta. DA3.

Cs-137 source on right side of road at 55.7624 13.4336.

Loop Charlie. CB1.

No source found. Clean area statement: Max detection distance at 50 km/h for 100 MBq unshielded Cs-137 source is 50 meters.

Loop Charlie. CB2.

Cs-137 source at 55.7782 13.1022. Might be close to railway underpass. Difficult to decide which side of the road.

Loop Charlie. CB3.

Cs-137 source on right side of road at 55.7782 13.1022. Suspicious people observed in a car close by the railway underpass.

A2.4 Conclusion

The search exercise was a nice break from the endless trips back and forth in front of Barsebäck NPP.

The search was divided into three different loops with different lengths: Bravo, Delta and Charlie. We did not see any sources in the Bravo loop, but in both Delta loop and Charlie loop we were able to detect quite clear signals from Cs-137 at the 2nd and 3rd round. We had no detection for the 1st round for both Delta and Charlie. In these cases, we reported a clean area statement.

We could at several locations observe elevated signals from tunnels, buildings and nearby rocks, and it can be difficult to separate these from shielded real sources when we are not able to stop for more careful measurements. However, keeping an extra eye on the spectrum and the alarm settings we were able to differ them from real case sources.

All in all, the exercise was very useful – also from the technical aspect as all instruments and software worked as planned. We also had real-time reach-back to our emergency centre at Østerås in Oslo as a part of the exercise.

Appendix A3

Results from team GR, the Icelandic Radiation Safety Authority, Iceland

This report summarizes the results obtained by GR, the Icelandic Radiation Safety Authority, during the REALMORC experiment taking place at Barsebäck, Sweden 10-12 October 2023. The experiment included mobile (carborne) and semi stationary gamma-ray searching of Cs-137 sources.

A3.1 Measuring equipment

The Icelandic team used a SPARCS mobile survey system. It comprises two, 2 litre NaI(Tl) detectors connected to an acquisition unit (ATU). The ATU is connected to a laptop computer on which the software AVID is employed for data acquisition and analysis. The detector was placed in the back seat of a hired station wagon near the right door. This would be a typical setup, in case of a search effort for a lost or stolen radiation source on Icelandic soil.

Results from previous experiments (SHIELDMORC 2020; COMBMORC 2021-2022) performed within the framework of this NKS series have been used in the measurements performed in the present experiment. The experiments series has investigated the possibility of using detection of primary and Compton-scattered photons in a Gamma spectrometer to assess the thickness of a shield between the radiation source and the detector, as well as the distance to and the activity of the source. Stationary and mobile detection have been studied under controlled conditions. Relevant data derived from previous measurements and employed in the present experiment are shown below.

In Table 1, the channel settings for the A, B, C and P ROI's are shown.

Table 1. The ROI setup for IRSA.

ROI	Energy node (keV)	Energy interval (keV)	Channel interval	Number of channels
	74			
A		79-238	32-84	53
	242			
B		247-405	87-139	53
	410			
C		415-573	142-194	53
	578			
PL		582-659	197-222	26
PC	662	662	223	1
PR		665-741	224-249	26

Calibration coefficients for two different models, an exponential model and a polynomial model, employed to describe the shield mass thickness from gamma-spectrometric count rate ratios in the respective ROI's shown in table 1 were determined experimentally within the COMBMORC project. The coefficients for the GR team that were previously determined for the exponential model, given on the form $a e^{b z^p}$, are shown in table 2a. The coefficients for the GR team that were previously determined for the five degree polynomial model are shown in table 2b.

Table 2a. GR calibration coefficients a and b for the exponential model, $a e^{b z^p}$.

ROI Ratio	a	b
ROI A/PR	4.28	0.00516
ROI B/PR	2.16	0.00448
ROI C/PR	1.38	0.00355
ROI PL/PR	1.21	0.00169
ROI A/P	1.89	0.00401
ROI B/P	0.953	0.00333
ROI C/P	0.612	0.00210

Table 2b. GR calibration coefficients $a_1 - a_5$ for the five degree polynomial model

ROI Ratio	a_5	a_4	a_3	a_2	a_1	a_0
ROI A/PR	2.465	-32.96	139.4	-162.9	37.26	0
ROI B/PR	2.747	-18.94	-3.988	227.6	-172.9	0
ROI C/PR	34.82	-251.5	569.6	-365.7	173.1	0
ROI PL/PR	3729	-15280	23050	-15750	5438	-654.9
ROI A/P	9.104	-72.58	148.0	51.77	-63.92	0
ROI B/P	1.168	44.20	-266.5	403.3	194.6	0
ROI C/P	572.5	-1021	-161.9	636.2	439.4	153.1

A3.2 Software

AVID is a technical software platform used for acquisition and analysis of radiological data and provides a common interface for connecting to a variety of radiological sensors. It also allows for remote monitoring of telemetry streams in real time and includes modules for visualization and analysis of incoming or uploaded radiological data. The software employs two different types of alarming algorithms, one count rate algorithm employed for gamma and neutron anomaly detections and one algorithm based on the spectral shape rather than the amplitude. For the former, the computation is simply a subtraction of the background from the signal divided by the standard deviation of the background, and default threshold values of 3 and 4 are employed for neutron (November) and gamma (Golf) radiation, respectively. These values were not changed during the REALMORC exercise. For the spectral shape algorithm (NSCRAD), which is based on the observation that the spectral shape of the background radiation is more stable than its amplitude, a set of windows are created over the spectrum and the count rate is predicted in one window by the trending count rate in another and a spectral ratio is calculated. A threshold value is set for this ratio and the default value of 12 was used and not changed during the exercise.

A3.3 Results

Cs-137 radiation sources with various shielding, different so-called setups, were placed at unknown locations along three different routes on October 11 2023: Bravo, Charlie and Delta. Below, the results from each route are presented.

A3.3.1 Road loop Bravo measurements

The road loop Bravo, displayed in Figure 1, was the first loop investigated by the GR team by driving the loop counterclockwise starting at the location B1 followed by a second clockwise loop ending at the same location.



Figure 1. Road loop Bravo.

No radiation sources were detected by the GR team along either of the two loops. It was afterwards revealed that no sources were placed along the Bravo loop.

A3.3.2 Road loop Delta measurements

The Delta loop, see Figure 2, was investigated by driving twice clockwise at three different setups (denoted DA1, DA2 and DA3) starting and stopping at the point D2 each time. The findings for the three setups are shown in table 3. The identified location of the radiation source (Cs-137) is indicated with a red circle in Figure 2.

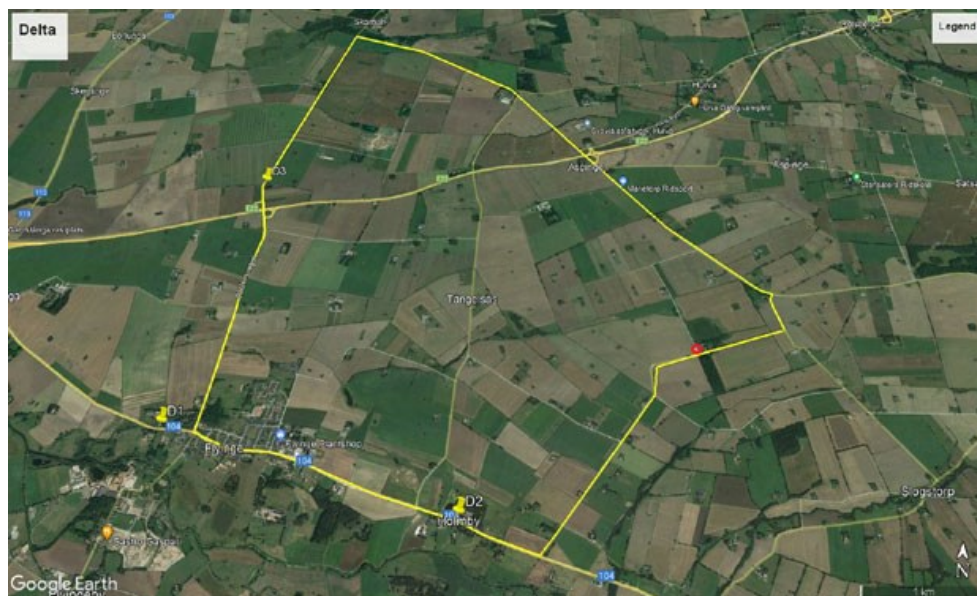


Figure 2. The Delta loop is illustrated with yellow lines. The red circle indicates the identified location of the source, see coordinates in Table 3.

Table 3. Results for the respective setups in the Delta loop investigation. If the AVID software has shown a detection alarm for neutrons (November), gamma (Golf) or spectral shape (NSCRAD), the GR team assessed the resulting spectrum and the if the assessment is positive, the source is deemed to have been identified.

Setup	Source identified	Alarm	Location of source
DA1	Yes	NSCRAD	55.76234, 13.43343
DA2	Yes	NSCRAD/GOLF	55.76234, 13.43343
DA3	Yes	NSCRAD	55.76234, 13.43343

A3.3.3 Road loop Charlie measurements

The Charlie loop, see Figure 3, was investigated by driving twice clockwise at three different setups (denoted CB1, CB2 and CB3) starting and stopping at the point C2 each time. The findings for the three setups are shown in table 4. The identified location of the radiation source (Cs-137) is indicated with a red circle in Figure 2.



Figure 3. The Charlie loop is illustrated with green lines. The red circle indicates the identified location of the source, see coordinates in Table 4.

Table 4. Results for the respective setups in the Charlie loop investigation. If the AVID software has shown a detection alarm for neutrons (November), gamma (Golf) or spectral shape (NSCRAD), the GR team assessed the resulting spectrum and the if the assessment is positive, the source is deemed to have been identified.

Setup	Source identified	Alarm	Location of source
CB1	No	No	-
CB2	No	No	-
CB3	Yes	NSCRAD	55.77842, 13.10198

A3.3.4 Results discussion

After the exercise, the different setups were revealed, see table 5.

Table 5. Sources and shielding employed in the different investigated setups.

Setup	Source	Activity (MBq)	Shielding (cm concrete)	Distance to road (m)
BR1	No	-	-	-
BR2	No	-	-	-
DA1	Cs-137	600	15	35
DA2	Cs-137	600	10	35
DA3	Cs-137	600	5	35
CB1	Cs-137	600	35	20
CB2	Cs-137	600	25	20
CB3	Cs-137	600	15	20

It is noted that during the Bravo loop investigation no radiation source was employed, and the experiment for that loop was performed merely to yield sufficient background data. As can be seen in Table 4, the software detection alarm thresholds were not exceeded during the first two setups in the Charlie loop. In these cases, a radiation source was present, but the thickness of the concrete shielding was greatest in these respective setups, CB1 and CB2, see Table 5. The distance to the road, and hence to the detector, was however shorter in the Charlie loop setups than in the Delta loop setups, 20 meters compared to 35. It should however be stated that, based on previous measurements within this NKS experiment framework where unshielded and shielded radiation sources have been measured at both stationary and mobile conditions, the GR detector should be able to detect an unshielded source similar to that used in the present experiment, i.e. a 600 MBq Cs-137 source, at a distance of 215 m while moving at a speed of 50 km/h.

A3.4 Conclusion

The present experiment included mobile detection at quasi-real conditions where carborne surveys along predefined routes were employed with the aim to detect Cs-137 sources with various shielding at various distances from the road. The measurement equipment of the GR team, constituted by 2x2 litre NaI(Tl) detectors, managed to detect sources shielded with concrete up to a thickness of 15 cm. The distance to the sources varied, but the GR equipment should be able to detect an unshielded source with the activity used in the present experiment up to a distance of 215 m, i.e. considerably larger than the different distances employed here. Acquired data will be employed to in further work with the algorithms derived within this NKS research framework to develop useful tools to be used in mobile searches of lost radiation sources.

Appendix A4

Results from the team LU, Lund University, Medical Radiation Physics, Sweden

The measuring equipment, calibration and measurement results from the REALMORC 2023 search experiment on Wednesday, October 11, 2023, are presented here.

A4.1 Measuring equipment

A4.1.1 Vehicle and detectors

The team from Lund University (LU) used a monitoring car and equipment owned by the Swedish Radiation Safety Authority (SSM) under a contract for use in research and emergency preparedness. The car was a Chevrolet Silverado with a freight compartment in the back where the gamma detectors were mounted (Fig 1). Reading of the detectors was done from the passenger compartment.

Two 4-litre NaI(Tl) detectors were placed directly under the rooftop, about 1.8 m above ground, on the right side in the freight compartment. The detectors were mounted one behind the other with their short (front) sides in the direction of travel. The detectors' most sensitive (largest) surface areas were towards the roadsides. (Fig 2 and 3). An Ortec Digibase multi-channel analyser was used for the data collection. The conversion gain for the NaI(Tl)-detectors was 256 channels covering the energy range 0 - 2990 keV.

A 123% HPGe detector was placed at the back of the freight compartment about 1.5 m above ground with its sensitive volume directed backwards. (Fig 3). An Ortec Digidart multi-channel analyser was used for the data collection. The conversion gain was 2048 channels covering 0 - 2990 keV energy range.



Fig 1. The mobile gamma spectrometry car used by team LU from Lund University. The detectors were mounted in the cargo compartment in the back of the car.



Fig 2. Sketch of the freight compartment with gamma detectors. Two 4 litre NaI(Tl) detectors are mounted on the upper right side of the compartment (blue). The 123% HPGe detector is mounted in the middle-back of the compartment with its sensitive volume facing backwards. The 3"x3" NaI(Tl) detector (light blue) at the bottom of the compartment was not used in the experiment.

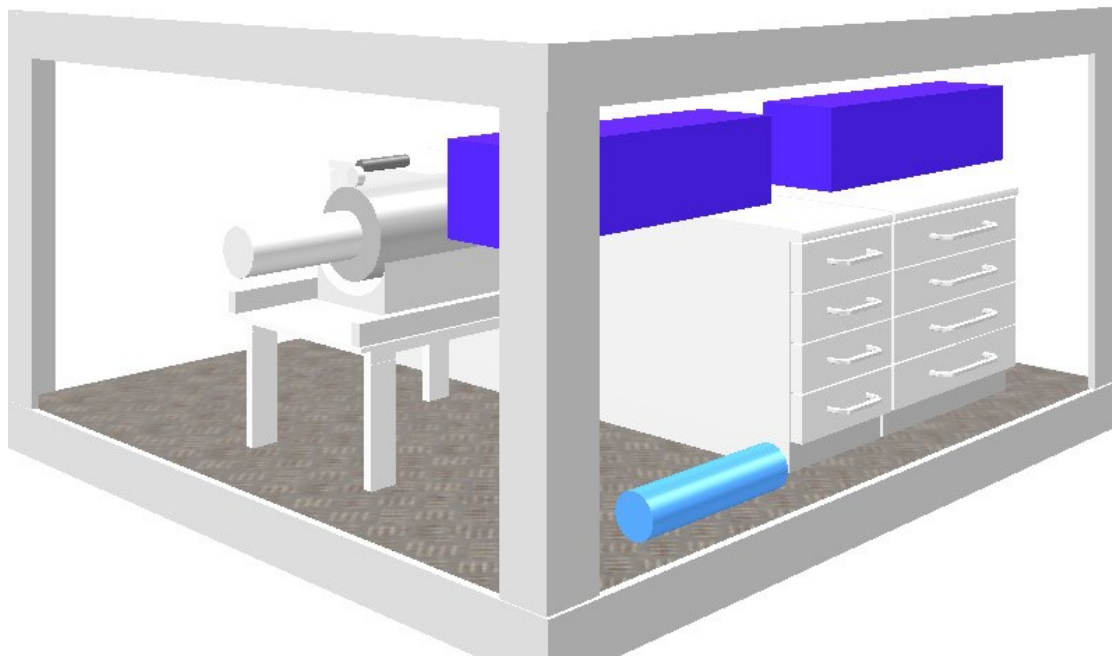


Fig 3. The gamma spectrometry freight compartment is seen obliquely from the rear right side with the two 4 litre NaI(Tl) detectors (blue) and the 123% HPGe detector (grey).

A4.1.2 The region of interest (ROI) setting

The energy calibration and ROI settings for the detectors are given for the 4-litre NaI(Tl) detectors in Table 1 and for the 123% HPGe detector in Table 2.

Table 1. The setting of regions of interest (ROI) for the two 4 litre NaI(Tl) spectrometers in the REALMORC 2023 search experiment (Wednesday, October 11), using 256 channels and the energy calibration $E = 11.6866K$, where E is the photon energy in keV and K is the channel number.

Region of interest	Energy interval (keV)	Channel interval	Number of channels
ROI A	58.4 - 222.0	5 - 19	15
ROI B	233.7 - 397.3	20 - 34	15
ROI C	409.0 - 572.6	35 - 49	15
ROI P	584.3 - 747.9	50 - 64	15
ROI PL	584.3 - 654.4	50 - 56	7
ROI PR	677.8 - 747.9	58 - 64	7

Table 2. The setting of regions of interest (ROI) for the 123% HPGe spectrometer in the REALMORC 2023 search experiment (Wednesday, October 11), using 2048 channels and the energy calibration $E = 1.2729 + 1.46269K - 1.78714E-07K^2$, where E is the photon energy in keV and K is the channel number.

Region of interest	Energy interval (keV)	Channel interval	Number of channels
ROI A	74.4 - 241.1	50 - 164	115
ROI B	242.6 - 409.3	165 - 279	115
ROI C	410.8 - 577.5	280 - 394	115
ROI P	579.0 - 745.7	395 - 509	115
ROI PL	579.0 - 660.9	395 - 451	57
ROI PR	663.8 - 745.7	453 - 509	57

A4.2 Software

The analyzing software used during the search experiments was NuggetW, developed by SSM. NuggetW can display time series of region of interest (ROI) measurement data and “waterfall” diagrams. It has a versatile ability to set alarm levels and display results. The usual acquisition time during mobile measurements was 1 s for all detectors.

For semi-stationary measurements made over several minutes at each location, Ortec’s software Gammavision and Maestro were used for data collection and analysis. The conversion gain for the 4 litre NaI(Tl) detectors was 1024 channels, and for the 123% HPGe detector, it was 2048 channels. Data from the semi-stationary measurements are not reported here. It will be subject to further analysis in 2024.

A4.3 Results

The LU team measured along the Charlie and Delta road loops according to the schedule defined for all teams. There was no time for the LU team to measure the loop Bravo (where no sources were placed), because LU resources were needed to set up the sources at the road loops Charlie and Delta.

All analysis of measurement results along the Charlie and Delta road loops was made by visual inspection. When a Cs-137 source was identified, its coordinates were reported to the communication centre.

A4.3.1 Road loop Charlie

Road loop Charlie had one 580 MBq Cs-137 source at road coordinates 13.10232 E, 55.77827 N (RT90 1330414, 6186554). The source was placed on the right side of the driving direction 20 m from the roadside. Three different shield thicknesses were used (CA1: 35 cm concrete, CA2: 25 cm concrete, CA3: 15 cm concrete, and in addition, 2.4 cm wood in all cases). The road loop was driven at an average traffic speed (40 - 70 km/h) clockwise twice for each shield thickness. The speed was 30 - 40 km/h when passing the source location.

The source was not detected in the CA1 setup. An indication of the source was noted in the CA2 setup by manual observation of the pulse height distributions from the 4-litre NaI(Tl) detectors. In the CA3 setup, the full energy peak at 662 keV from Cs-137 was detected with the NaI(Tl) detectors when passing the source.

Variations in the natural radiation background were detected along the road loop. A natural anomaly existed near the location of the source, making it more difficult to detect the source. The ROI count rate variations along a part of the road passing the source are shown for the three shielding setups for the 123% HPGe detector (Fig 4 - 6) and for the rear 4-litre NaI(Tl) detector (Fig 7 - 9).

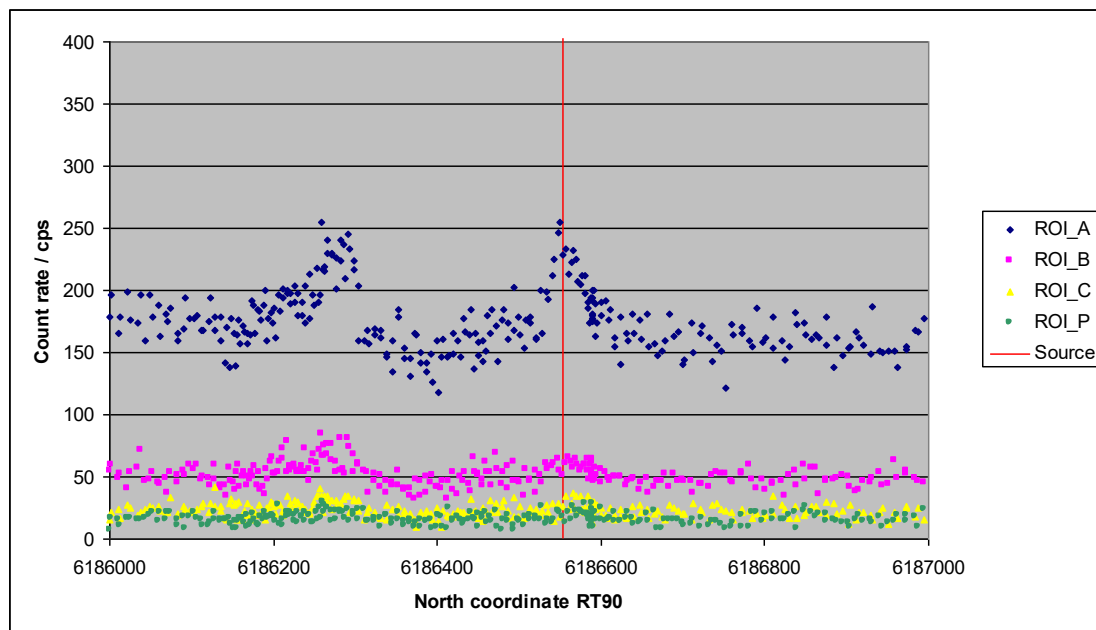


Fig 4. CA1 setup, HPGe detector. Count rates in ROI A, B, C, and P obtained by the 123% HPGe detector when driving along part of the road loop Charlie passing the 580 MBq Cs-137 source with shield mass thickness 872 kg/m^2 including the air space between the source and the detector. Count rate variations are due to natural anomalies. The source was not detected.

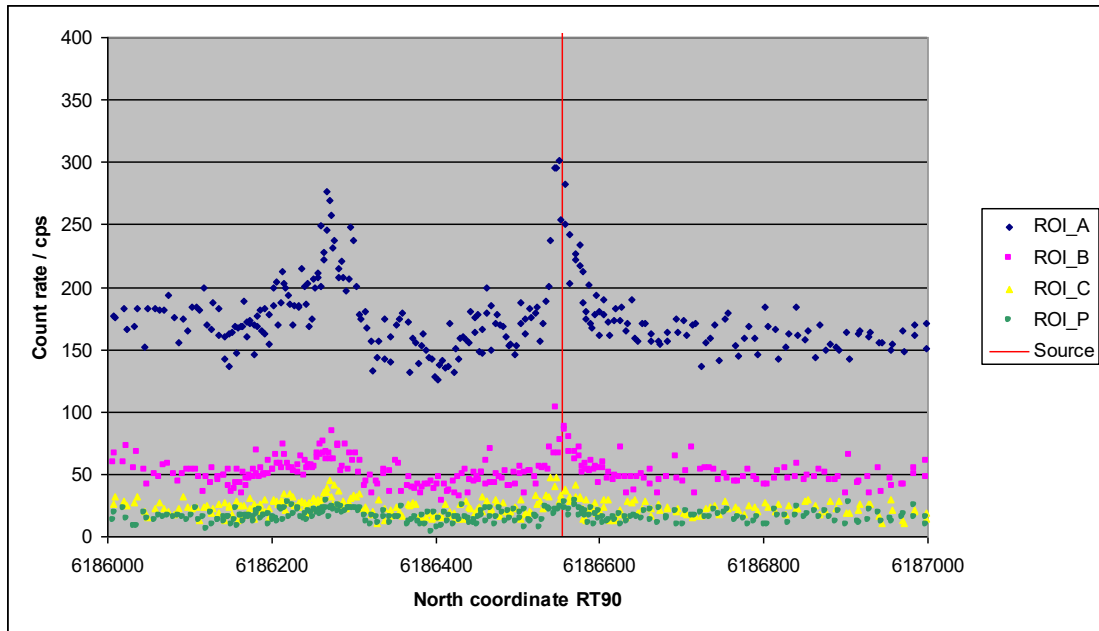


Fig 5. CA2 setup, HPGe detector. Count rates in ROI A, B, C, and P obtained by the 123% HPGe detector when driving along part of the road loop Charlie passing the 580 MBq Cs-137 source with shield mass thickness 634 kg/m² including the air space between the source and the detector. Count rate variations are due to natural anomalies and some scattered photon fluence from the source near its location. The source was not detected from primary radiation.

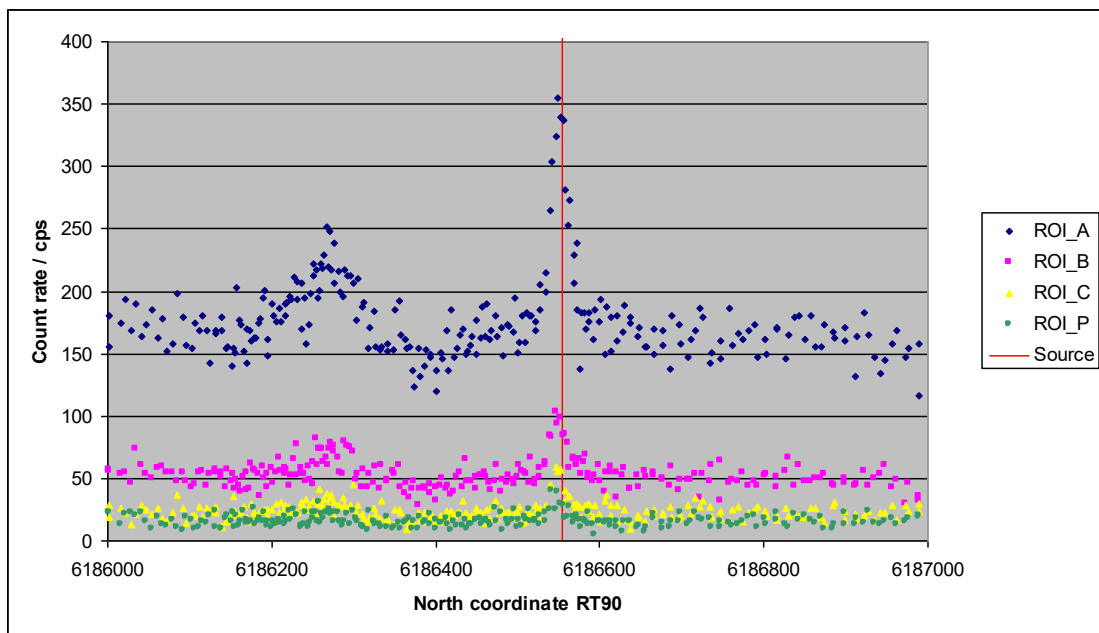


Fig 6. CA3 setup, HPGe detector. Count rates in ROI A, B, C, and P obtained by the 123% HPGe detector when driving along part of the road loop Charlie passing the 580 MBq Cs-137 source with shield mass thickness 396 kg/m² including the air space between the source and the detector. Count rate variations are due to natural anomalies and scattered photon fluence from the source near its location. The source was detected by its primary radiation.

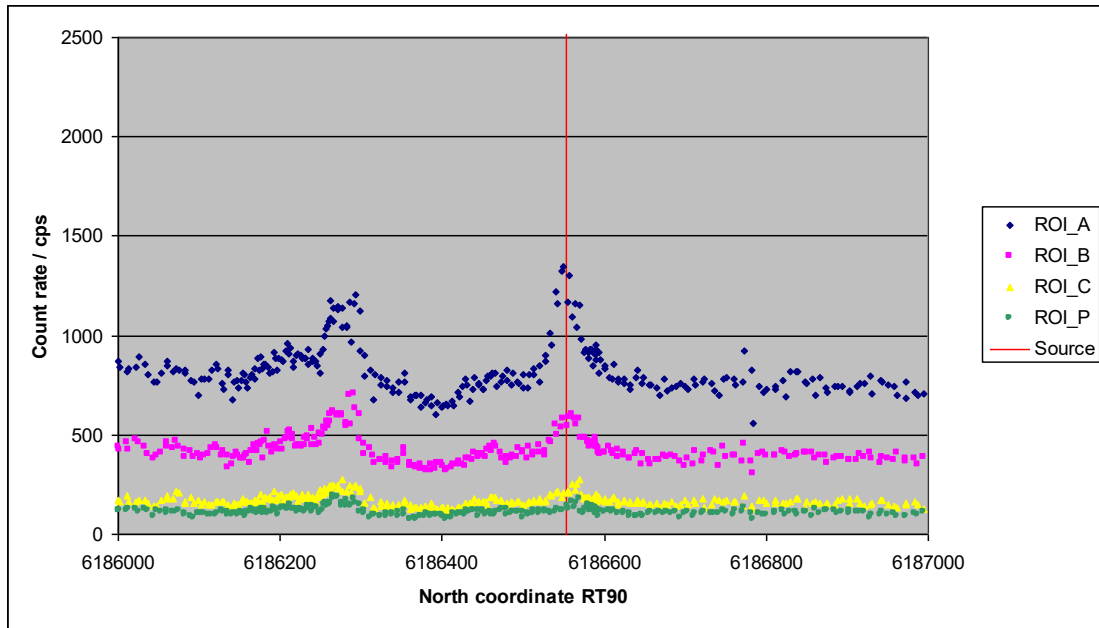


Fig 7. CA1 setup, NaI(Tl) detector Count rates in ROI A, B, C, and P obtained by the rear 4 litre NaI(Tl) detector when driving along part of the road loop Charlie passing the 580 MBq Cs-137 source with shield mass thickness 872 kg/m² including the air space between the source and the detector. Count rate variations are due to natural anomalies. The source was not detected.

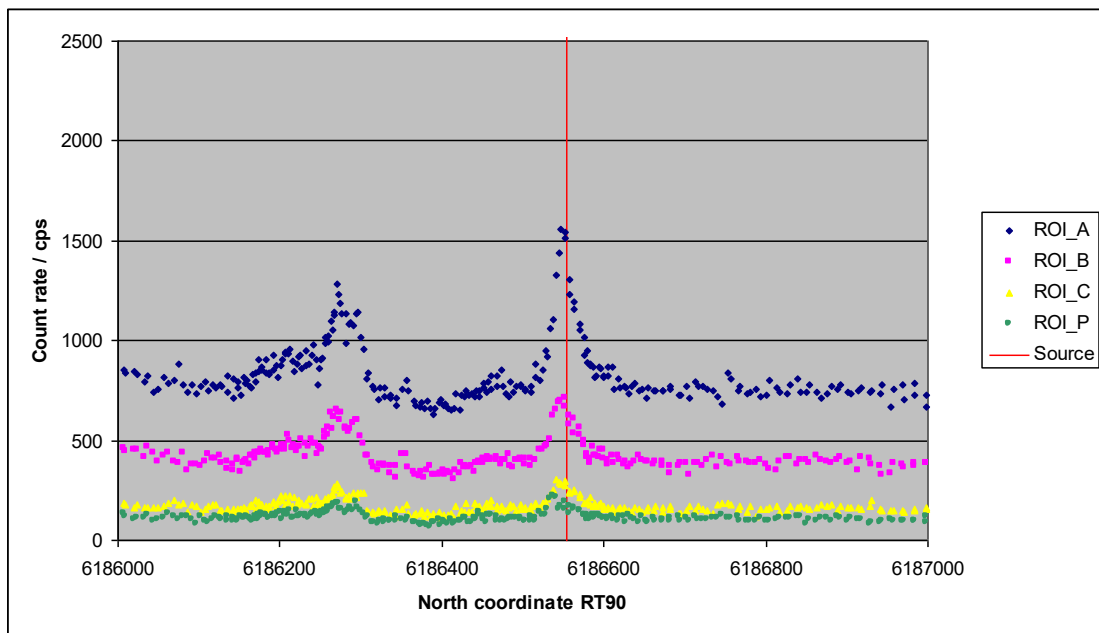


Fig 8. CA2 setup, NaI(Tl) detector. Count rates in ROI A, B, C, and P obtained by the 123% HPGe detector when driving along part of the road loop Charlie passing the 580 MBq Cs-137 source with shield mass thickness 634 kg/m² including the air space between the source and the detector. Count rate variations are due to natural anomalies and primary and scattered photon fluence from the source near its location. The source was detected by its primary radiation.

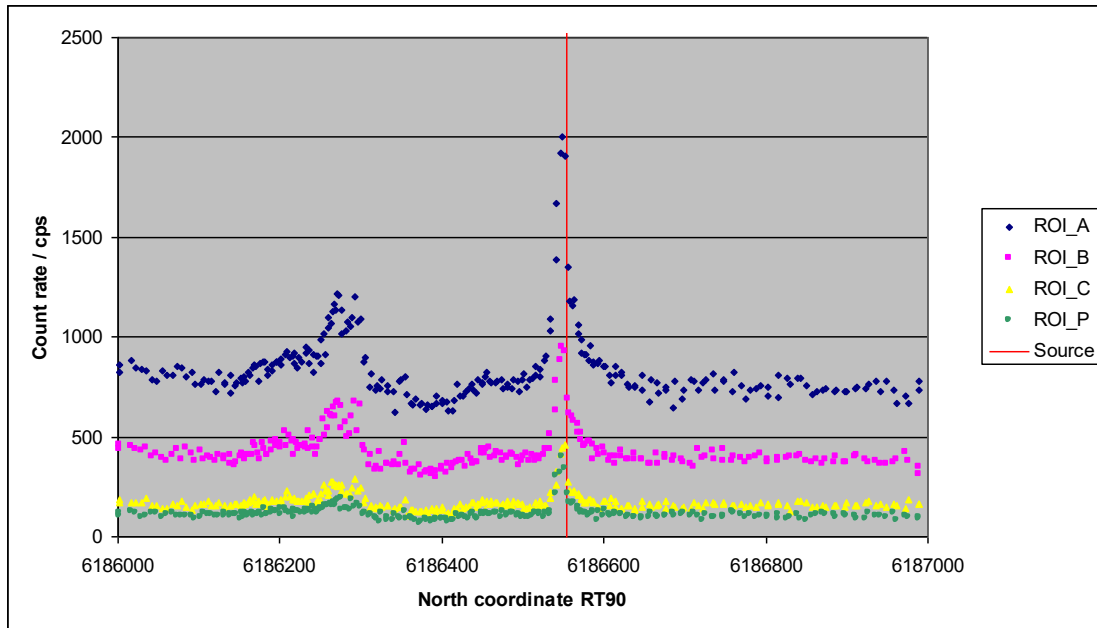


Fig 9. CA3 setup, NaI(Tl) detector. Count rates in ROI A, B, C, and P obtained by the 123% HPGe detector when driving along part of the road loop Charlie passing the 580 MBq Cs-137 source with shield mass thickness 396 kg/m^2 including the air space between the source and the detector. Count rate variations are due to natural anomalies and primary and scattered photon fluence from the source near its location. The source was detected by its primary radiation.

A4.3.2 Road loop Delta

Road loop Delta had one 580 MBq Cs-137 source at road coordinates 13.43389 E, 55.76240 N (RT90 1351152, 6184025). The source was placed on the right side of the driving direction, 35 m from the roadside, close to a building with stonewalls. Three different shield thicknesses were used (DB1: 15 cm concrete, DB2: 10 cm concrete, DB3: 5 cm concrete, and 3 cm wood in all cases). The road loop was driven at an average traffic speed (40 - 70 km/h) clockwise twice for each shield thickness. The speed was 40 - 50 km/h when passing the source location.

The source was not detected in the DB1 setup. An indication of the source was noted in the DB2 setup by manual observation of the pulse height distributions from the 4-litre NaI(Tl) detectors. In the DB3 setup, the full energy peak at 662 keV from Cs-137 was detected with the NaI(Tl) detectors when passing the source.

Variations in the natural radiation background were detected along the road loop. A large building with stonewalls created a natural anomaly near the location of the source, making it more difficult to detect the source. The building also shielded the source, making it hard to use the SODAC routine to determine the source distance. The ROI count rate variations along a part of the road passing the source are shown for the three shielding setups for the 123% HPGe detector (Fig 10 - 12) and for the rear 4-litre NaI(Tl) detector (Fig 13 - 15).

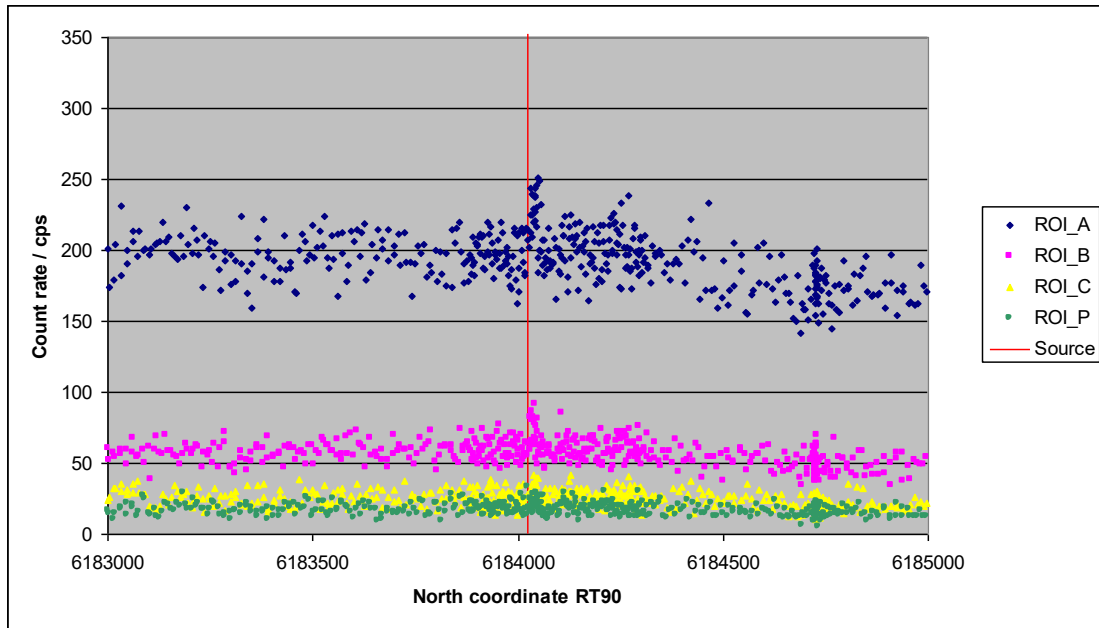


Fig 10. DB1 setup, HPGe detector. Count rates in ROI A, B, C, and P obtained by the 123% HPGe detector when driving along part of the road loop Delta passing the 580 MBq Cs-137 source with shield mass thickness 418 kg/m² including the air space between the source and the detector. Count rate variations are due to natural anomalies. The source was not detected

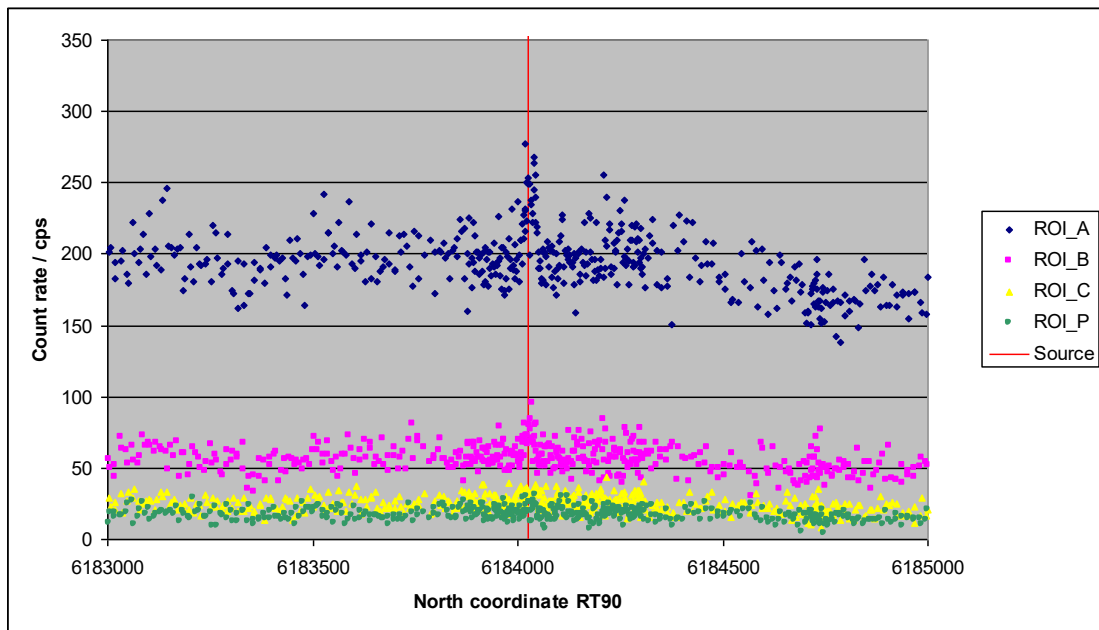


Fig 11. DB2 setup, HPGe detector. Count rates in ROI A, B, C, and P obtained by the 123% HPGe detector when driving along part of the road loop Delta passing the 580 MBq Cs-137 source with shield mass thickness 299 kg/m² including the air space between the source and the detector. Count rate variations are due to natural anomalies and some scattered photon fluence from the source near its location. The source was not detected from primary radiation registered by the HPGe detector.

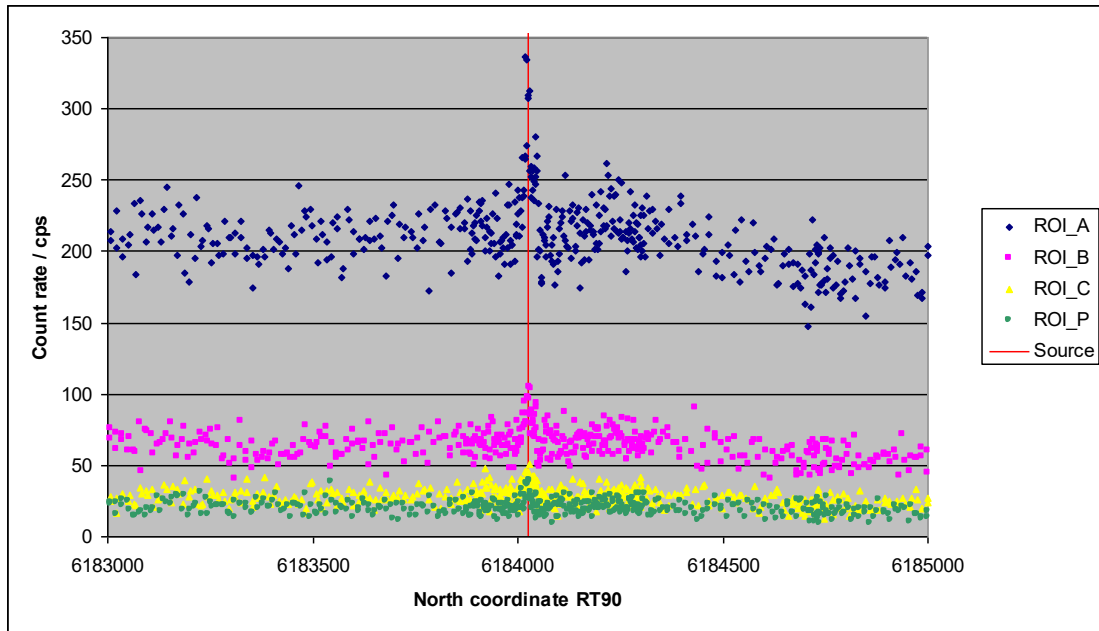


Fig 12. DB3 setup, HPGe detector. Count rates in ROI A, B, C, and P obtained by the 123% HPGe detector when driving along part of the road loop Delta passing the 580 MBq Cs-137 source with shield mass thickness 180 kg/m² including the air space between the source and the detector. Count rate variations are due to natural anomalies and primary and scattered photon fluence from the source near its location. The source was on the edge of being detected by manual analysis of from primary radiation registered by the HPGe detector.

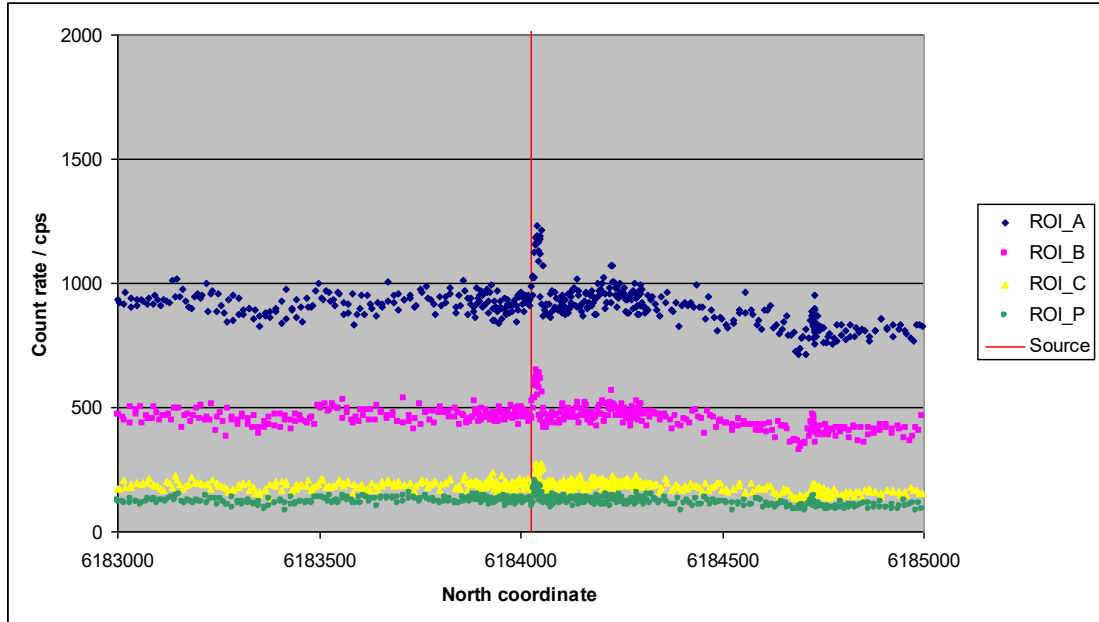


Fig 13. DB1 setup, NaI(Tl) detector. Count rates in ROI A, B, C, and P obtained by the rear 4 litre NaI(Tl) detector when driving along part of the road loop Charlie passing the 580 MBq Cs-137 source with shield mass thickness 418 kg/m² including the air space between the source and the detector. Count rate variations are due to natural anomalies. The source was not detected.

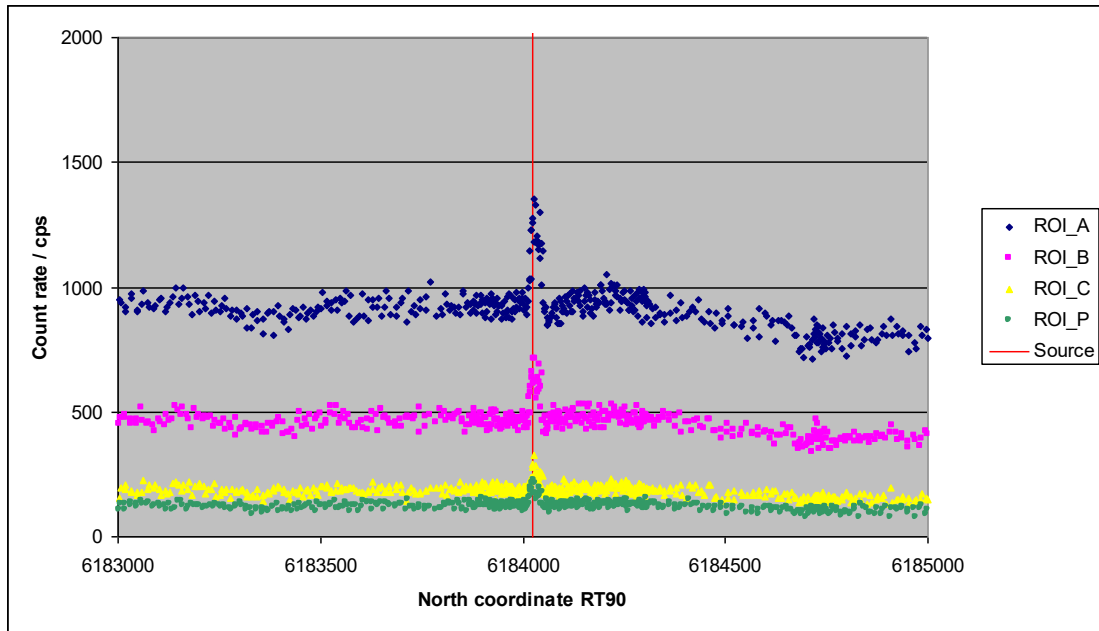


Fig 14. DB2 setup, NaI(Tl) detector. Count rates in ROI A, B, C, and P obtained by the 123% HPGe detector when driving along part of the road loop Delta passing the 580 MBq Cs-137 source with shield mass thickness 299 kg/m² including the air space between the source and the detector. Count rate variations are due to natural anomalies and primary and scattered photon fluence from the source near its location. The source was detected by its primary radiation.

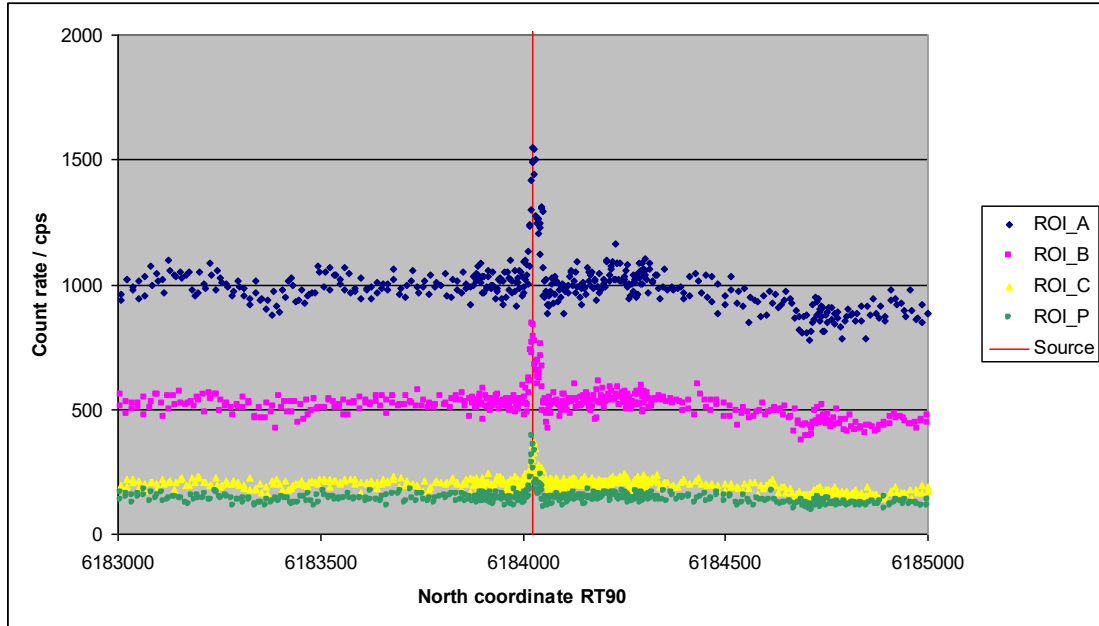


Fig 15. DB3 setup, NaI(Tl) detector. Count rates in ROI A, B, C, and P obtained by the 123% HPGe detector when driving along part of the road loop Delta passing the 580 MBq Cs-137 source with shield mass thickness 178 kg/m² including the air space between the source and the detector. Count rate variations are due to natural anomalies and primary and scattered photon fluence from the source near its location. The source was detected by its primary radiation.

A4.4 Conclusion

The Cs-137 sources in the search experiment were located near natural anomalies. It increased the difficulty of identifying the sources. All analysis was done manually, which requires skilled personnel. In the least shielded geometries, an automatic alarm for the count rate in the full energy peak of Cs-137 would have worked to identify the source. These geometries also gave a clear result for the registration of the scattered radiation from the source. Combining primary and scattered radiation in different ROIs may be developed as a method to increase the sensitivity to identify lost radiation sources. Continued analysis of gamma spectrometric data is required to verify whether it is possible to use such a method.

Appendix A5

Results from team NGU, Geological Survey of Norway, Norway

A5.1 Measuring equipment

NGU measuring system is an RSX-5 spectrometer (Radiation Solutions, Canada) consisting of five 4 L NaI crystals. The spectrometer was mounted vertically close behind the passenger seat inside a Toyota HiAce van owned by NGU (Figure 1). It was oriented with the four "downward" crystal detectors facing right and one "upward" crystal detector facing the opposite side. As the upward detector is centered to the downward detectors, it partly shields the downward detectors in the opposite direction and is completely shielded by the downward detectors. In the analysis below, the downward signal is the sum of the four detectors with an active volume of 16 L, while the upward signal is the left detector with an active volume of 4 L. The signals from all the crystals are processed in an onboard spectrometer and exported via TCP/IP to a laptop in the front cabin of the vehicle, using RadAssist v6.2.68.0 software (RSI, 2022).



Figure 1. RSX-5 spectrometer was installed vertically in the rear cabin with four crystal detectors (referred as "downward") measuring signals from the right side of the vehicle and one crystal detector ("upward") for the left side.

The system measures spectral energies between 0 to 3 MeV within 1024 channels each covering 3 keV at a sample rate of 1 Hz. The system measured continuously along the road while the car followed the traffic code.

A5.2 Software

RadAssist v6.2.68.0 software (RSI, 2022) used for the spectral data acquisition detects and identifies nuclides. The built-in anomaly parameters are set to five times of standard deviations. An automatic spectral analysis is performed when counts within the isotope windows are higher or equal to three times of standard deviation. The alarm parameters were calculated from a background measurement in Barsebäck.

Table 1. ROI setup for the NGU recording system (using MGS channel convention)

ROI	Energy node (keV)	Energy interval (keV)	Channel interval	Number of channels
	74			
A		77 - 239	27 – 81	55
	242			
B		245 - 407	83 - 137	55
	410			
C		413 - 575	139 - 193	55
	578			
PL		581 - 659	195 - 221	27
PC	662	662	222	1
PR		665 - 743	223 - 249	27
	746			

A5.3 Results

A5.3.1 Road loop Bravo measurements

During both Bravo loop BR1 and BR2, no obvious high values for the Central Cs peak or any ratios are detected by the instrument (Figure 2). It is easily seen when the data are mapped with a similar colour scale as the one used for Charlie and Delta described below. The waterfall chart in RadAssist showed higher counts at several locations without triggering an alarm. These higher counts were likely due to higher natural background at those locations.

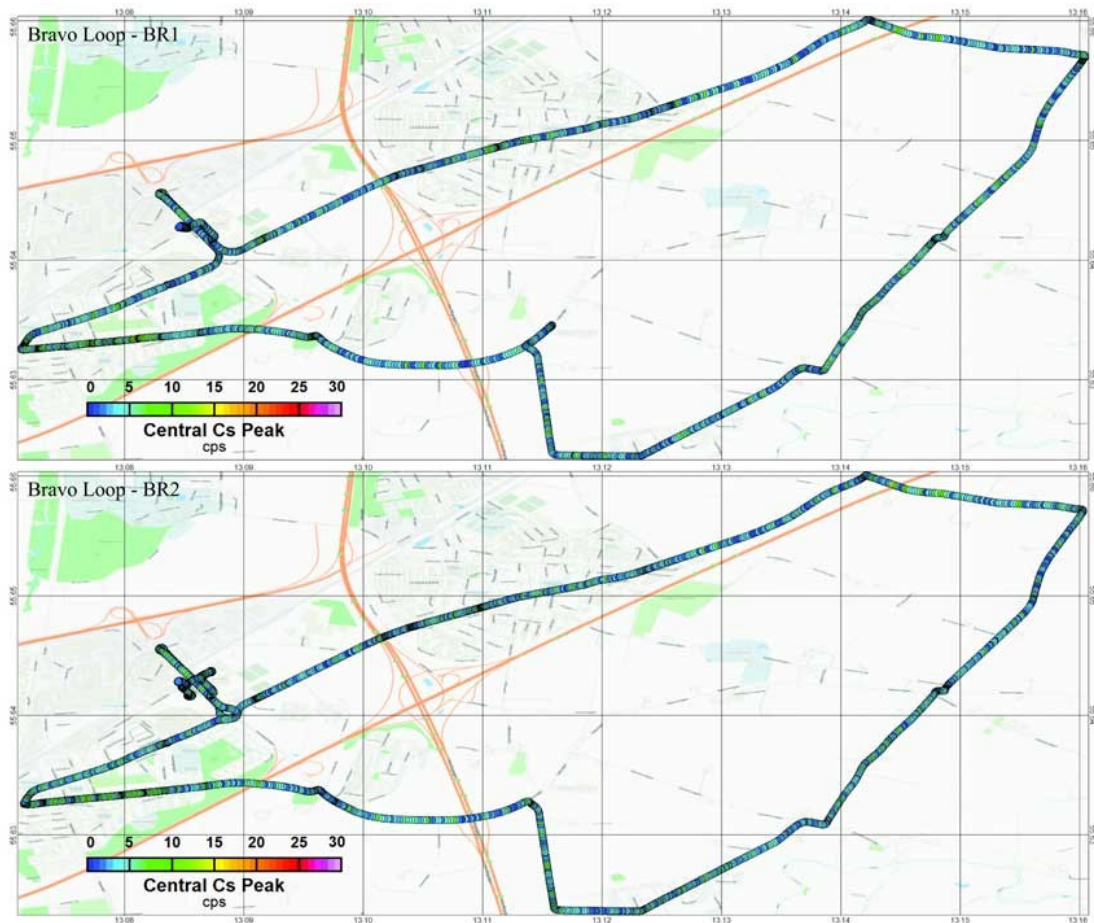


Figure 2. Loop BR1 and BR2 ROI PC for detector 1: no strong Cs signature is detected.

A5.3.2 Road loop Charlie measurements

During the first loop CA1 (35 cm concrete shielding), high Cs peaks were detected away from the location of the source to be searched at GPS position 55.7903786°N, 13.1041498°E (red x on Figure 3, and green line on Figure 4). This reading is likely caused by the building materials of the road at that specific location. The different ratios calculated are not particularly elevated at that location. The built-in alarm system detected high radiations without any specific radioelements at that location as reported to the CC. However, the highest ratio values for detector 1 are located at the true location of the source 55.7782326°N, 13.1023531°E (green circle, Figure 3 and purple line, Figure 4) whilst no Cs peak is directly detected.

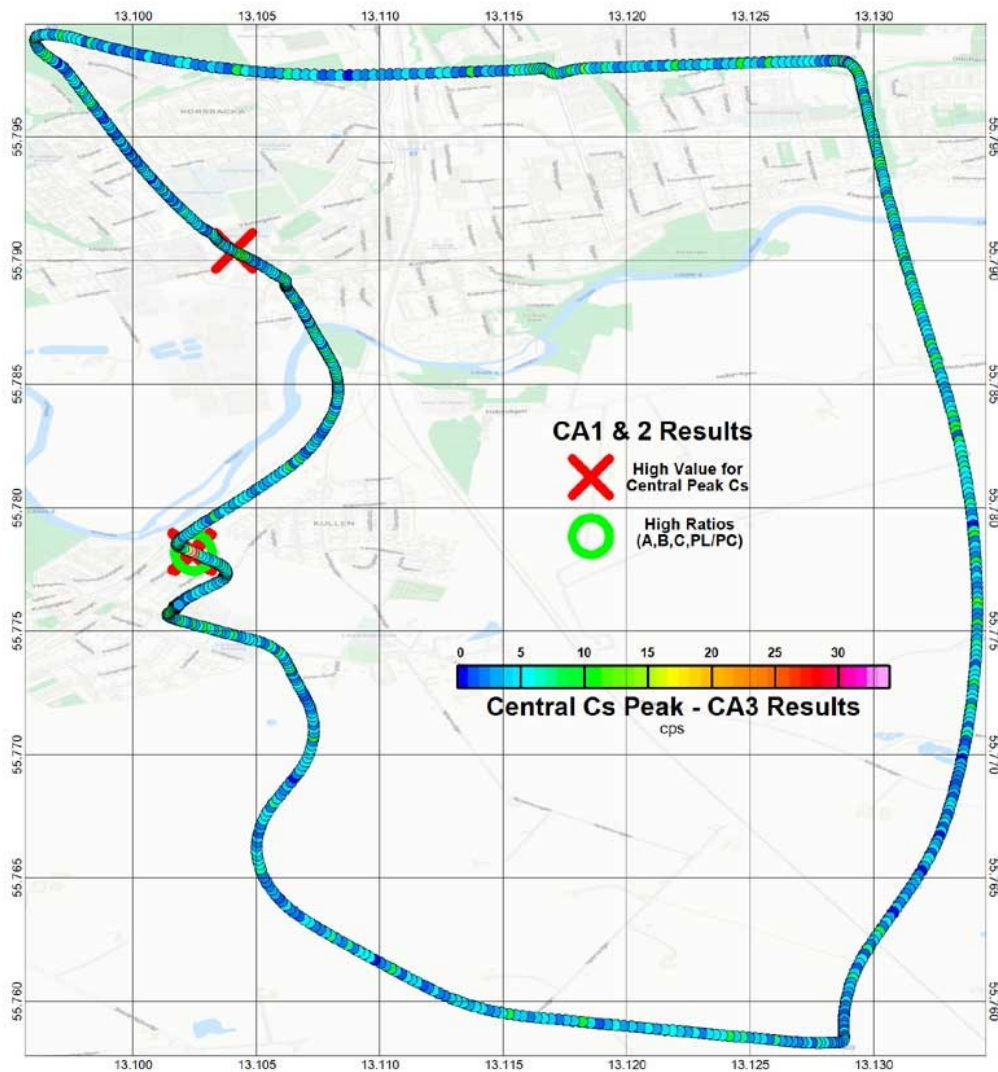


Figure 3. Loop CA3 ROI PC for detector 1 with 15 cm shielding: the source is easily located with the central peak of Cs data. High measurements for the Central Cs peak are recorded at two locations for CA1 and CA2 loops likely due to the road fabric.

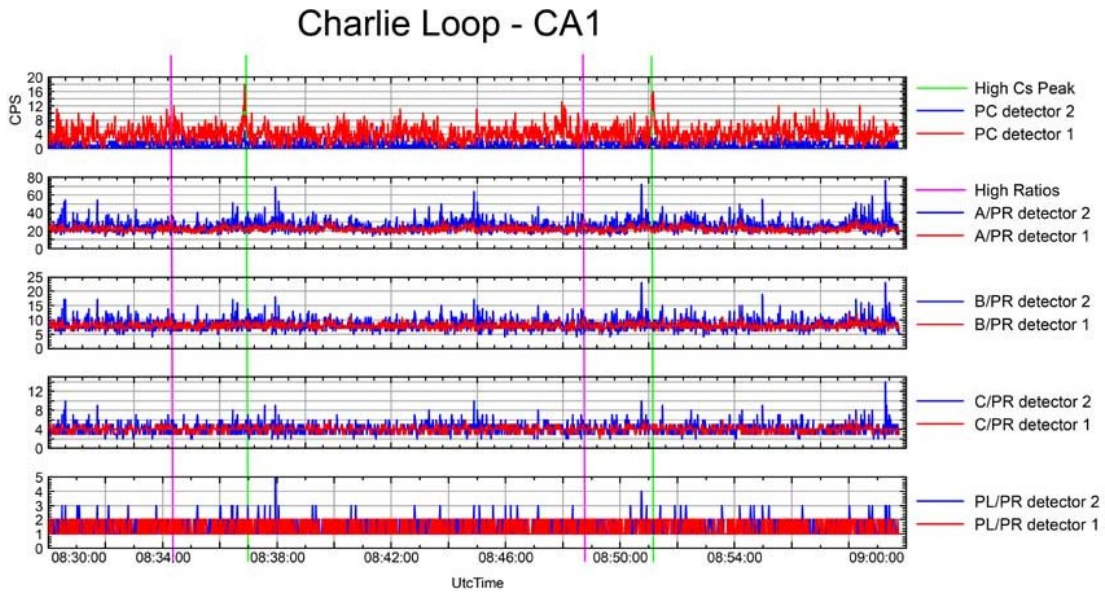


Figure 4. Plots of the Cs measurements in counts per second (cps) and its ratios for the Charlie Loop CA1 where the highest Cs peak refers to an anomaly of the road and the highest ratio values to the location of the source.

During the second loop CA2 (25 cm concrete shielding), the highest Cs peak measurements are related to an anomaly of road as explained earlier (Figure 3). However, another high Cs peak is found at the source location during the first pass (Figures 3 & 5). The highest values for the ratio of detector 1 are located at the source location. During the final loop CA3 (15 cm concrete shielding), a very clear measurement of high Cs is located at the position of the source. The signal is high above the background level of the area and exceeds by three or four times the higher signal from the anomaly on the road located in CA1 and CA2 (Figure 6). The ratio values are not particularly higher at that location. Moreover, RadAssist alarm system detected and identified the source as Cs-137 during the last loop.

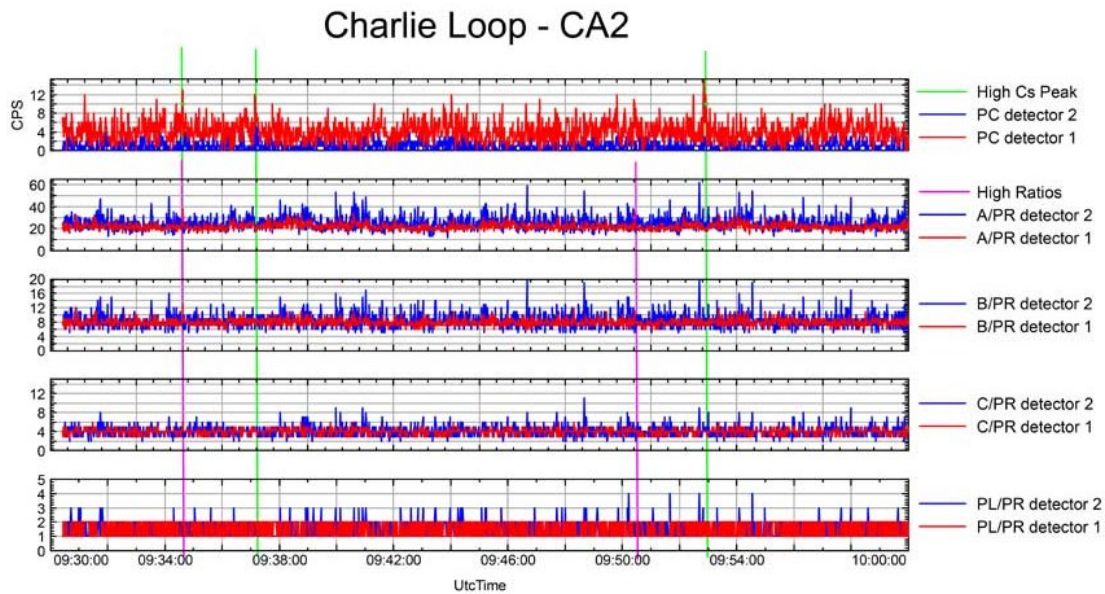


Figure 5. Plots of the Cs measurements in counts per second (cps) and ratio for the Charlie Loop CA2 where the highest Cs peak refers to an anomaly of the road and the location of the source on the first pass. The highest ratio values for detector 1 locate the source.

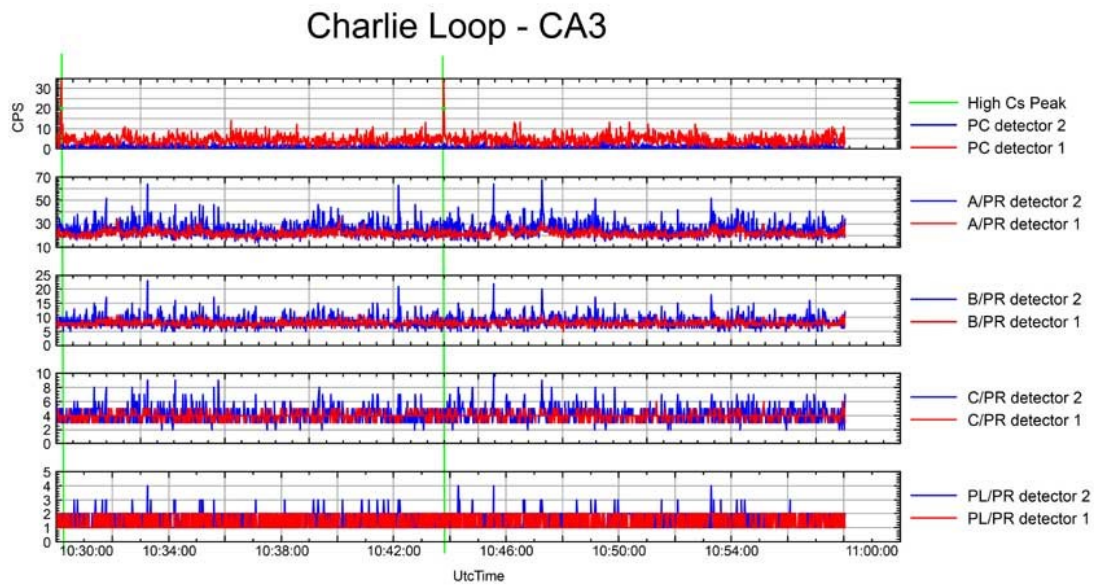


Figure 6. Plots of the Cs measurements in counts per second (cps) and ratio for the Charlie Loop CA3 where the highest Cs peak refers to the location of the source. Note the starting point of loop CA3 is different than the loops CA1 and CA2 due to logistic reasons.

A5.3.3 Road loop Delta measurements

During the first loop DB1 (15 cm concrete shielding), several potential areas are detected in real time from the RSI built-in system and post-processing does not establish a clear source location (Figure 7). The RadAssist alarm system detected the source and identified it as Cs-137. Although some false alarms were triggered near the church. During the second loop DB2 (10 cm concrete shielding), the central peak of Cs is identified at the source location (Figures 8 & 9). The signal is elevated for Cs during the first pass; however, it is much sharper and high above the background during the second pass. The ratios show an indication of the source location when the Cs peak is unclear while there is no indication from the ratios on the second when the Cs peak is very clear. There is 5 s delay between the highest Cs peak (PC) signal and the highest ratios signal, equivalent to about 3 m offset. The weather changing during that loop, from rain and windy to overcast with no precipitation, could have affected the signature of the source. During the last loop DB3 (5 cm concrete shielding), a clear sharp signal is seen at the source location (Figures 9 & 10) but with no indication in the ratio values.

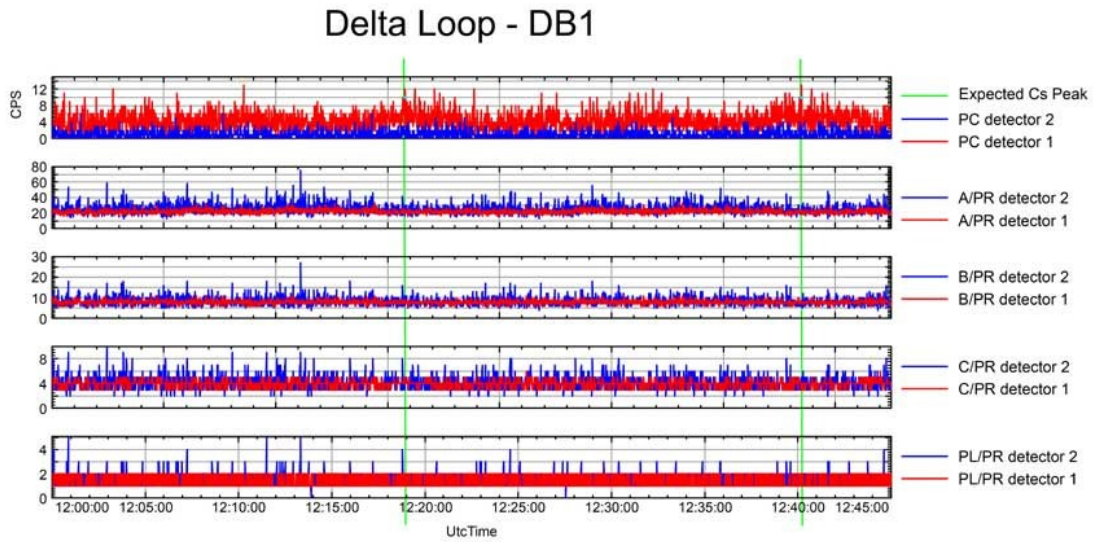


Figure 7. Plots of the Cs measurements in counts per second (cps) and ratio for the Delta Loop DB1 where the source is not located with the central CS peak signature or ratios.

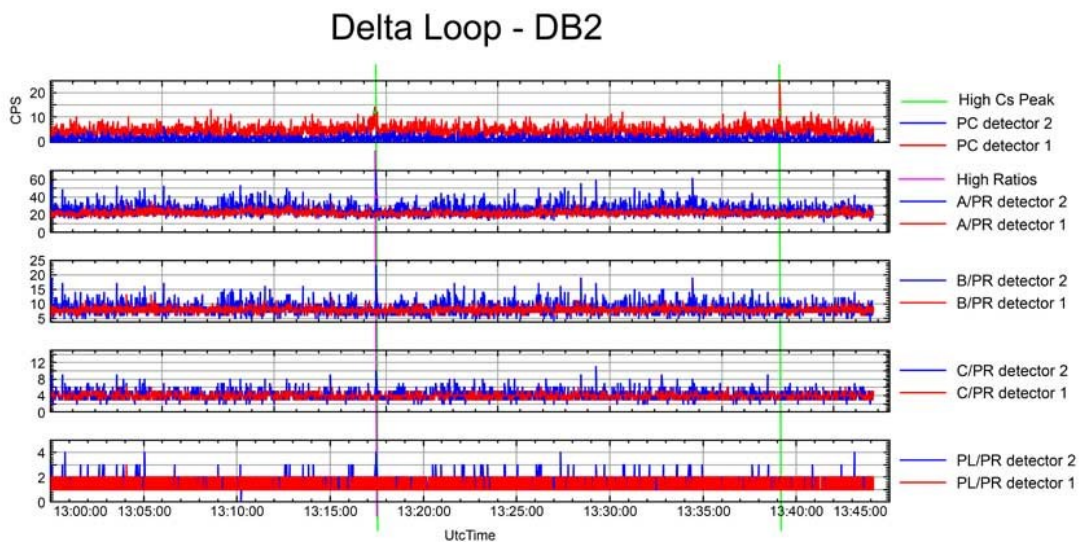


Figure 8. Plots of the Cs measurements in counts per second (cps) and ratio for the Delta Loop DB2 where the source is located with the central CS peak signature and the high ratios during the first pass. A small delay equivalent to 3 m on the ground is noted between the highest Cs peak intensity and the highest ratio values.



Figure 9. Loop DB3 Delta ROI PC for detector 1 at 5 cm shielding: the source is easily located with the central peak of Cs data.

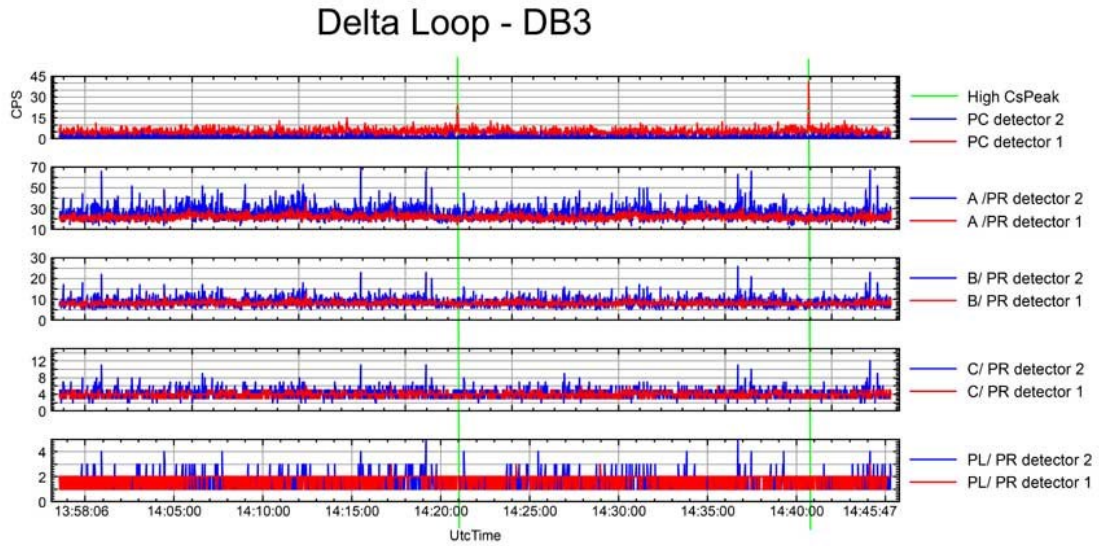


Figure 10. Plots of the Cs measurements in counts per second (cps) and ratio for the Delta Loop DB3 where the source is located with the central CS peak signature.

A5.4 Conclusion

When the source is least shielded, the Cs peak (ROI PC) identifies well the location of the source. However, in the case of significant shielding, the ratios of the different ROIs pinpoint the location of the source and the presence of shielding. In a real scenario, it is important to consider both possibilities of high Cs peak and high ratios values independently.

The built-in alarm system from RadAssist was able to identify the presence of the source as Cs-137 when it was least shielded. When the source was more shielded, the system recognized the presence of “unknown” isotopes and triggered an alarm.

The effect of the radiation of the source is very local. The signal fade quickly within less than 10-20 seconds while passing the source, which is equivalent to about 10 m. For example, the high ratios in loop DB2 are found 3 m further than the highest Cs peak in loop DB3 where the source is expected.

A5.5 Reference

RSI, 2022: RadAssist User Manual RS-700 Series, Revision 3.11, RadAssist Software Version 6.2.43.0, Radiation solutions, Ontario, Canada

Appendix A6

Results from team SSM, Swedish Radiation Safety Authority, Sweden

These are the results from mobile gamma ray searching of Cs-137 sources on Wednesday October 11, 2023, during the exercise REALMORC.

A6.1 Measuring equipment

The SSM team used the standard Swedish Chevrolet Silverado-setup, with two 4 liter NaI(Tl)-spectrometers and one 120% HPGe-detector. The system use Ortec Digibase MCA:s for the NaI(Tl)-detectors and Ortec Digidart MCA for the HPGe-detector.

The NaI(Tl)-detectors were both positioned on the right side in the van-cabinet at a height of about 180 cm above ground. The 4×4×16” crystals are horizontally aligned one after the other in the direction of the vehicle. The spectroscopic resolution for the NaI(Tl)-detectors is 256 channels.

The 120% HPGe-detector is placed in the middle of the van-cabinet at a height of about 150 cm above ground, with the symmetry axis of the crystal coincident with the direction of the vehicle and the end cap facing opposite to the direction of the vehicle. The spectroscopic resolution for the HPGe-detector is 2048 channels.

Table for channel settings for ROI A, B, C, and P				
ROI	Win lo (keV)	Win hi (keV)	Win lo (chn)	Win hi (chn)
NaI_A	86	230	10	32
NaI_B	254	398	24	36
NaI_C	422	566	39	51
NaI_P	590	734	53	66
HPGe_A	75.35	241.8	52	166
HPGe_B	243.26	409.73	167	280
HPGe_C	411.19	577.68	281	395
HPGe_P	653.63	669.69	447	458

Coefficients for the energy calibration equation				
deg	0:th	1:st	2:nd	CH
HPGe	0	1.46075	0	2048
NaI	-29.376	11.57153	0.00149347	256

A6.2 Software

Software	Description
Gammavision	The software is used for energy calibration, initial setup and energy stabilization of the detectors. Stabilization is obtained over the K-40 peak.
NuggetW	The software was developed at SSM and is used for visualization and analysis of mobile gamma spectrometry data. It has several possibilities to use radiation alarms, individual alarms can be set for every variable calculated.

A6.3 Results

No alarm-functions were used by SSM during the measurements in Realmorc 2023, but these can be applied in post-analysis. During driving visual inspection was continuously conducted, mainly in the background subtracted waterfall plot and in the strip charts with time series of the variables that had been set up. The variables set up was mainly ROI:s over the Cs-137 window (the P ROI) for 1, 3 and 5 second measurements as well as an ASS (area specific stripping) variable developed during the Momorc experiment, for 1 and 3 seconds.

A6.3.1 Road loop Bravo measurements

Road loop Bravo was measured two times, starting in position B1, first counter clockwise and then clockwise, one lap per loop. No artificial sources were detected in any of the laps. The detection limit at a certain distance for an unshielded Cs-137-source was supposed to be calculated, but this has not been successful.

A6.3.2 Road loop Charlie measurements

Road loop Charlie was measured clockwise, two laps per loop, in three different setups. In the first setup no source could be detected. In the second setup a Cs-137 source was detected in position 55.778277, 13.102506. In the third setup the full energy peak from Cs-137 was clearly visible in this position.

A6.3.3 Road loop Delta measurements

Road loop Delta was also measured clockwise, two laps per loop, in three different setups. A Cs-137 source was seen in position 55.762456, 13.433409, in all three setups, with signal increasing in every setup.

A6.4 Conclusion

It was interesting to perform this type of source search exercise along three different loops with varying background radiation. To be able to estimate source activity and distance to a source it is necessary to use SODAC and SSC, but this was not performed during these measurements.

Appendix B1
**Instructions and time schedules for teams during the Tuesday,
October 10, mobile data monitoring experiments.**

The purpose of the Tuesday measurements was to investigate whether it would possible to use a number of mobile measurements past a shielded Cs-137 source using the ROI method to determine the distance, shielding and activity of the source instead of semi-stationary measurement as applied in the COMBMORC 2022 experiments. Semi-stationary measurements for comparison were made on Thursday, October 12 according to the schedule in Appendix D.

Evaluation of the results is planned to be conducted in a REALMORC 2024 activity.

REALMORC experiments Tuesday, October 10

Tuesday's mobile measurements along Kraftverksvägen pass two shielded sources; Sierra and Tango (see map). Speed 30 km/h. The purpose of the measurements is to investigate whether it is possible to replace semi-stationary measurements with mobile ones where the vehicle passes the source several times.

Comparison will be made against semi-stationary measurements that we do on Thursday.

The timetable for the measurements can be found below. Make as many rounds along the southern part of Kraftverksvägen past Sierra and Tango as you can in the allotted time. In the pause between setups, the shielding thickness for the sources will be changed, but the distance to the sources remains the same.

Tuesday Time Schedule

Setup	Time	Speed	Activity
	11:00-12:00		Meeting with review of the REALMORC experiments
	12:00-13:00		Lunch and teams own preparations
BG	13:00-13:45	30 km/h	Mobile measurements along Kraftverksvägen. One data file per instrument File name: TTTT_BG_DDDD
	13:45-14:00		Pause
U1	14:00-14:45	30 km/h	Mobile measurements along Kraftverksvägen. One data file per instrument File name: TTTT_U1_DDDD
	14:45-15:15		Coffe break
U2	15:15-16:00	30 km/h	Mobile measurements along Kraftverksvägen. One data file per instrument File name: TTTT_U2_DDDD
	16:00-16:15		Pause
U3	16:15-17:00	30 km/h	Mobile measurements along Kraftverksvägen. One data file per instrument File name: TTTT_U3_DDDD
	17:00-17:45		Evening meal. Summing up for the day. Instructions for Wednesday

TTTT is the team (DEMA, DSA, NGU, GR, SSM, LU)

DDDD is the detector, for example 4LNAI or 4LNAI_R för a right detector and 4LNAI_L for a left detector.

For GR, Iceland, if the two 2 L NaI(Tl) detectors produce separate gamma spectra, mark the detectors 2LNAI1 and 2LNAI2

Appendix B2**Instructions and time schedules for teams during the Wednesday, October 11, search experiments.**

The one-page instruction contains rules and format for reporting is given followed by the teams' individual time schedules for the Wednesday, October 11 search experiments.

Measurements along the road loop Alpha was not applied in this experiment, due to lack of time.

REALMORC experiments Wednesday, October 11

REALMORC experiment Rules

In this experiment it is important to follow the time schedule. Each setup (source activity, distance, and shielding) only applies for the specified setup time.

The task is to use mobile gamma spectrometry along road loops (Alpha, Bravo, Charlie, Delta) to search for Cs-137 point sources. The vehicle must maintain normal traffic speed. It is not permitted to stop along the road loop while the search is in progress (traffic hazard).

Start and stop must be at the specified point along the road loop. At that point it should be possible to stand still with your car for a while.

Measurement/driving along the road loop must be started at the appointed time according to the schedule, which is a full or half hour. The road loops Charlie and Delta should be driven/measured twice in succession for each setup. Do not stop after the first lap, but drive a second lap directly. Then stop at the specified start/stop point, evaluate the measurement and report to CC.

The road loops Alpha and Bravo should be driven only once in the specified direction, and then reporting.

Do not start measurement/driving along a road loop too early. Wait for the start time (full or half hour)

If you cannot follow the time schedule, the following applies:

- If you are less than 5 minutes late to start, start anyway
- If you are more than 5 minutes late to start but not 10 minutes, start but measure the road loop only once.
- If you are more than 10 minutes late to start, do not start, wait for the appointed time for the next setup or drive to the next road loop if it is on turn according to the time schedule.

Reporting during the day

After driving/measuring each setup, stop at the start/stop point, analyse your data (if you have time) and call CC on your mobile phone.

Report the following:

1. Team
2. Road loop (Alpha, Bravo, Charlie, Delta)
3. Road loop start/stop point (where you are at the moment)
4. Setup code
5. Source found or source not found
 - If source found
 - 5a. longitude (decimal degrees, 5 decimals)
 - 5b. latitude (decimal degrees, 5 decimals)

Mission for team DEMA

Time	Setup code	Mission for team DEMA
08:00		Meeting at "Grevinnan". Pick up food for the whole day. Last minute briefing
08:30-09:00		Drive to Bravo start/stop point B1
09:00-09:30	BR1	Measure loop Bravo clockwise once. Stop at B1. Report to CC
09:30-10:00	BR2	Measure loop Bravo counterclockwise once. Stop at B1. Report to CC
10:00-10:30		Drive to Charlie start/stop point C3
10:30-11:30	CA1	Measure loop Charlie clockwise twice. Stop at C3. Report to CC
11:30-12:30	CA2	Measure loop Charlie clockwise twice. Stop at C3. Report to CC
12:30-13:30	CA3	Measure loop Charlie clockwise twice. Stop at C3. Report to CC
13:30-14:00		Drive to Delta start/stop point D3
14:00-15:00	DB1	Measure loop Delta clockwise twice. Stop at D3. Report to CC
15:00-16:00	DB2	Measure loop Delta clockwise twice. Stop at D3. Report to CC
16:00-17:00	DB3	Measure loop Delta clockwise twice. Stop at D3. Report to CC
17:00-17:30		Drive to "Grevinnan"
17:30-19:30		Meeting, summing experiences. Evening meal

Produce one measurement file in format MGS.CSV for each setup.

File name: TTTT_SSS_DDDD

TTTT is the team (DEMA, DSA, NGU, GR, SSM, LU)

SSS is the setup code given above

DDDD is the detector

Put the files on the USB-stick

Mission for team DSA

Time	Setup code	Mission for team DSA
08:00		Meeting at "Grevinnan". Pick up food for the whole day. Last minute briefing
08:30-09:00		Drive to Bravo start/stop point B1
09:00-09:30	BR2	Measure loop Bravo counterclockwise clockwise once. Stop at B1. Report to CC
09:30-10:00	BR1	Measure loop Bravo clockwise once. Stop at B1. Report to CC
10:00-10:30		Drive to Delta start/stop point D1
10:30-11:30	DA1	Measure loop Delta clockwise twice. Stop at D1. Report to CC
11:30-12:30	DA2	Measure loop Delta clockwise twice. Stop at D1. Report to CC
12:30-13:30	DA3	Measure loop Delta clockwise twice. Stop at D1. Report to CC
13:30-14:00		Drive to Charlie start/stop point C1
14:00-15:00	CB1	Measure loop Charlie clockwise twice. Stop at C1. Report to CC
15:00-16:00	CB2	Measure loop Charlie clockwise twice. Stop at C1. Report to CC
16:00-17:00	CB3	Measure loop Charlie clockwise twice. Stop at C1. Report to CC
17:00-17:30		Drive to "Grevinnan"
17:30-19:30		Meeting, summing experiences. Evening meal

Produce one measurement file in format MGS.CSV for each setup.

File name: TTTT_SSS_DDDD

TTTT is the team (DEMA, DSA, NGU, GR, SSM, LU)

SSS is the setup code given above

DDDD is the detector

Put the files on the USB-stick

Mission for team GR

Time	Setup code	Mission for team GR
08:00		Meeting at "Grevinnan". Pick up food for the whole day. Last minute briefing
08:30-09:00		Drive to Bravo start/stop point B1
09:00-09:30	BR2	Measure loop Bravo counterclockwise clockwise once. Stop at B1. Report to CC
09:30-10:00	BR1	Measure loop Bravo clockwise once. Stop at B1. Report to CC
10:00-10:30		Drive to Delta start/stop point D2
10:30-11:30	DA1	Measure loop Delta clockwise twice. Stop at D2. Report to CC
11:30-12:30	DA2	Measure loop Delta clockwise twice. Stop at D2. Report to CC
12:30-13:30	DA3	Measure loop Delta clockwise twice. Stop at D2. Report to CC
13:30-14:00		Drive to Charlie start/stop point C2
14:00-15:00	CB1	Measure loop Charlie clockwise twice. Stop at C2. Report to CC
15:00-16:00	CB2	Measure loop Charlie clockwise twice. Stop at C2. Report to CC
16:00-17:00	CB3	Measure loop Charlie clockwise twice. Stop at C2. Report to CC
17:00-17:30		Drive to "Grevinnan"
17:30-19:30		Meeting, summing experiences. Evening meal

Produce one measurement file in format MGS.CSV for each setup.

File name: TTTT_SSS_DDDD

TTTT is the team (DEMA, DSA, NGU, GR, SSM, LU)

SSS is the setup code given above

DDDD is the detector

Put the files on the USB-stick

Mission for team LU

Time	Setup code	Mission for team LU
08:00		Meeting at "Grevinnan". Pick up food for the whole day. Last minute briefing
08:30-09:00		Drive to Charlie source location. Help setting up the trailer and the source
09:00-09:30		
09:30-10:00		
10:00-10:30		Drive to Charlie start/stop point C1
10:30-11:30	CA1	Measure loop Charlie clockwise twice. Stop at C1. Report to CC
11:30-12:30	CA2	Measure loop Charlie clockwise twice. Stop at C1. Report to CC
12:30-13:30	CA3	Measure loop Charlie clockwise twice. Stop at C1. Report to CC
13:30-14:00		Drive to Delta start/stop point D1
14:00-15:00	DB1	Measure loop Delta clockwise twice. Stop at D1. Report to CC
15:00-16:00	DB2	Measure loop Delta clockwise twice. Stop at D1. Report to CC
16:00-17:00	DB3	Measure loop Delta clockwise twice. Stop at D1. Report to CC
17:00-17:30		Drive to "Grevinnan"
17:30-19:30		Meeting, summing experiences. Evening meal

Produce one measurement file in format MGS.CSV for each setup.

File name: TTTT_SSS_DDDD

TTTT is the team (DEMA, DSA, NGU, GR, SSM, LU)

SSS is the setup code given above

DDDD is the detector

Put the files on the USB-stick

Mission for team NGU

Time	Setup code	Mission for team NGU
08:00		Meeting at "Grevinnan". Pick up food for the whole day. Last minute briefing
08:30-09:00		Drive to Bravo start/stop point B1
09:00-09:30	BR1	Measure loop Bravo clockwise once. Stop at B1. Report to CC
09:30-10:00	BR2	Measure loop Bravo counterclockwise once. Stop at B1. Report to CC
10:00-10:30		Drive to Charlie start/stop point C2
10:30-11:30	CA1	Measure loop Charlie clockwise twice. Stop at C2. Report to CC
11:30-12:30	CA2	Measure loop Charlie clockwise twice. Stop at C2. Report to CC
12:30-13:30	CA3	Measure loop Charlie clockwise twice. Stop at C2. Report to CC
13:30-14:00		Drive to Delta start/stop point D3
14:00-15:00	DB1	Measure loop Delta clockwise twice. Stop at D2. Report to CC
15:00-16:00	DB2	Measure loop Delta clockwise twice. Stop at D2. Report to CC
16:00-17:00	DB3	Measure loop Delta clockwise twice. Stop at D2. Report to CC
17:00-17:30		Drive to "Grevinnan"
17:30-19:30		Meeting, summing experiences. Evening meal

Produce one measurement file in format MGS.CSV for each setup.

File name: TTTT_SSS_DDDD

TTTT is the team (DEMA, DSA, NGU, GR, SSM, LU)

SSS is the setup code given above

DDDD is the detector

Put the files on the USB-stick

Mission for team SSM

Time	Setup code	Mission for team SSM
08:00		Meeting at "Grevinnan". Pick up food for the whole day. Last minute briefing
08:30-09:00		Drive to Bravo start/stop point B1
09:00-09:30	BR2	Measure loop Bravo counterclockwise clockwise once. Stop at B1. Report to CC
09:30-10:00	BR1	Measure loop Bravo clockwise once. Stop at B1. Report to CC
10:00-10:30		Drive to Delta start/stop point D3
10:30-11:30	DA1	Measure loop Delta clockwise twice. Stop at D3. Report to CC
11:30-12:30	DA2	Measure loop Delta clockwise twice. Stop at D3. Report to CC
12:30-13:30	DA3	Measure loop Delta clockwise twice. Stop at D3. Report to CC
13:30-14:00		Drive to Charlie start/stop point C3
14:00-15:00	CB1	Measure loop Charlie clockwise twice. Stop at C3. Report to CC
15:00-16:00	CB2	Measure loop Charlie clockwise twice. Stop at C3. Report to CC
16:00-17:00	CB3	Measure loop Charlie clockwise twice. Stop at C3. Report to CC
17:00-17:30		Drive to "Grevinnan"
17:30-19:30		Meeting, summing experiences. Evening meal

Produce one measurement file in format MGS.CSV for each setup.

File name: TTTT_SSS_DDDD

TTTT is the team (DEMA, DSA, NGU, GR, SSM, LU)

SSS is the setup code given above

DDDD is the detector

Put the files on the USB-stick

Appendix B3**Instructions and time schedules for teams during the Thursday, October 12, semi-stationary monitoring experiments.**

The purpose of the Thursday measurements was to perform semi-stationary measurements for the same source setups as on the Tuesday experiments to investigate whether it would possible to use a number of mobile measurements past a shielded Cs-137 source using the ROI method to determine the distance, shielding and activity of the source instead of semi-stationary measurement.

Evaluation of the results is planned to be conducted in a REALMORC 2024 activity.

REALMORC experiments Thursday, October 12

Thursday's measurements should be made semi-stationary at road locations at Kraftverksvägen at two shielded sources; Sierra and Tango (see map). All measurements should be done standing still for five minutes at a distance-marked location. The purpose of the measurements is to investigate whether it is possible to replace semi-stationary measurements with mobile ones where the vehicle passes the source several times.

Comparison will be made against the mobile measurements that we did on Tuesday.

The timetable for the measurements can be found below. Do as many five minutes measurements at Sierra and Tango as you can in the allotted time (3 - 5 at each source location). In the pause between setups, the shielding thickness for the sources will be changed, but the distance to the sources remains the same.

Thursday Time Schedule

Setup	Time	Speed	Activity
	08:30-08:45		Morning meeting
	08:45-09:00		Pause, own preparations
S1,T1	09:00-10:00	0 km/h	Semi stationary measurements at points along Kraftverksvägen where distances are marked along the road at Sierra and Tango. One data file per measurement point and instrument File names: TTTT_S1_DDDD-xx (at Sierra) TTTT_T1_DDDD-xx (at Tango)
	10:00-10:15		Coffe break
S2,T2	10:15-11:00	0 km/h	Semi stationary measurements at points along Kraftverksvägen where distances are marked along the road at Sierra and Tango. File names: TTTT_S2_DDDD-xx (at Sierra) TTTT_T2_DDDD-xx (at Tango)
	11:00-11:15		Pause
S3,T3	11:15-12:00	0 km/h	Semi stationary measurements at points along Kraftverksvägen where distances are marked along the road at Sierra and Tango. File names: TTTT_S1_DDDD-xx (at Sierra) TTTT_T1_DDDD-xx (at Tango)
	12:00-13:00		Lunch. Summing up.

-xx is the distance along the road before reaching the origo, which is the road crossing where the source is located.

+xx is the distance along the road after the origo

Appendix C

Recommended ROI regions for gamma spectrometers and teams

Here are the settings of regions-of-interest, ROIs, recommended to be used by participating teams in the REALMORC 2023 experiments. The settings were originally developed and defined in the NKS SHIELDMORC 2019-2020 and COMB-MORC 2021-2022 activities.

C1. Generic ROI

Generic ROI is meant to guide how the different ROIs should be chosen for gamma spectrometers with different conversion gains so that the respective energy intervals cover roughly the same width.

Table C1 provides examples of ROI selections for different conversion gains and energy width per channel.

Table C1. Suggested ROIs with energy interval limits given in keV for detecting primary and scattered photons measured by a gamma spectrometer having 1024, 512 or 256 channels corresponding to channel widths of 3, 6 or 12 keV/channel. The peak area ROI is suitable for a NaI(Tl) spectrometer and is divided into three sub-components: left peak area (PL), centre channel (PC) and right peak area (PR), which together constitute the full energy peak area (P).

ROI	Energy node (keV)	Compton scattered degree	3 keV/ch (keV)	ROI width chs	6 keV/ch (keV)	ROI width chs	12 keV/ch (keV)	ROI width ch
	74							
A			77-239	55	80-236	27	86-230	13
	242	110						
B			245-407	55	248-404	27	254-398	13
	410	58						
C			413-575	55	416-572	27	422-566	13
	578	27						
PL			581-659	27	584-656	13	590-650	6
PC			662	1	662	1	662	1
PR			665-743	27	668-740	13	674-734	6
P			581-743	55	584-740	27	590-734	13

C2. DEMA

Table C2. The ROI setup for the DEMA shielding experiment in SHIELDMORC 2020 and COMBMORC 2021-22

ROI	Energy node (keV)	Energy interval (keV)	Channel interval	Number of channels
	74			
A		75 - 240	25 - 80	55
	242			
B		243 - 408	81 - 136	55
	410			
C		441 - 576	137 - 192	55
	578			
PL		579 - 660	193 - 220	27
PC	662	663	221	1
PR		666 - 747	222 - 249	27

C3. DSA

Table C3. The ROI setup for the DSA 4-litre NaI(Tl) detectors during REALMORC 2023.

ROI	Energy node (keV)	Energy interval (keV)	Channel interval	Number of channels
A			26 - 80	55
B			82 - 136	55
C			138 - 192	55
PL			194 - 220	27
PR			222 - 248	27
P			194 - 248	55

C4. IRSA/GR

Table C4. The ROI setup for the IRSA/GR shielding experiment in SHIELDMORC 2020 and COMBMORC 2021-22.

ROI	Energy node (keV)	Energy interval (keV)	Channel interval	Number of channels
	74			
A		79 - 238	32 - 84	53
	242			
B		247 - 405	87 - 139	53
	410			
C		415 - 573	142 - 194	53
	578			
PL		582 - 659	197 - 222	26
PC	662	662	223	1
PR		665 - 741	224 - 249	26

C5. LU, Lund University

Table C5-1. ROI application for the Lund University 4 litre NaI(Tl) spectrometer system (Ortec Digibase) using a conversion gain of 1024 channels and setting the energy calibration for Cs-137, 661.66 keV in channel 231 and for K-40, 1460.66 keV in channel 500.

ROI	Compton scattered degree	Channel numbers	Photon energy keV	Number of channels
Node		32	74.1	1
ROI A		33-88	77.0-239.1.0	56
Node	110	89	242.1	1
ROI B		90-145	245.0-407.4	56
Node	58	146	410.3	1
ROI C		147-202	413.3-575.8	56
Node	27	203	578.8	1
ROI PL		204-230	581.8-658.7	27
ROI PC	0	231	661.7	1
ROI PR		232-258	664.6-741.6	27
Node		259	744.6	1

Table C5-2. ROI application for the Lund University 3"x3" NaI(Tl) spectrometer system (Ortec Digibase) using a conversion gain of 1024 channels and setting the energy calibration for Cs-137, 661.66 keV in channel 231 and for K-40, 1460.86 keV in channel 500.

ROI	Compton scattered degree	Channel numbers	Photon energy keV	Number of channels
Node		36	75.9	1
ROI A		37-91	78.9-240.4	55
Node	110	92	243.4	1
ROI B		93-147	246.4-407.7	55
Node	58	148	410.7	1
ROI C		149-203	413.7-575.0	55
Node	27	204	578.0	1
ROI PL		205-231	581.0-658.6	27
ROI PC	0	232	661.7	1
ROI PR		233-259	664.6-742.2	27
Node		260	745.2	1

Table C5-3. ROI application for the Lund University DetectiveX HPGe spectrometer system

using a conversion gain of 16383 channels and setting the energy calibration for Cs-137 661.66 keV in channel 3615.87, K-40 1460.86 keV in channel 7979.71, and Tl-208 2614.53 keV in channel 14278.57. (A, B, C, D (PLNaI), P - variant).

ROI	Compton scattered degree	Channel numbers	Photon energy keV	Number of channels
Node		412	74.92	1
ROI A		413-1330	75.11-243.04	918
Node	109.2	1331	243.22	1
ROI B		1332-2249	243.40-411.34	918
Node	57.96	2250	411.52	1
ROI C		2251-3168	411.70-579.64	918
Node	27.0	3169	579.82	1
ROI D (PLNaI)		3170-3598	580.00-658.38	429
Node	4.89	3599	658.57	1
ROI PL		3600-3615	658.75-661.50	16
ROI PC		3616	661.68	1
ROI PR		3617-3633	661.86-664.61	16
ROI P		3600-3632	658.75-664.61	33
Node		3633	664.79	1

C6. NGU

Table C6. The ROI setup for the NGU shielding experiment in SHIELDMORC 2020 and COMBMORC 2021-22

ROI	Energy node (keV)	Energy interval (keV)	Channel interval	Number of channels
	74			
A		77 - 239	26 - 80	55
	242			
B		245 - 407	82 - 136	55
	410			
C		413 - 575	138 - 192	55
	578			
PL		581 - 659	194 - 220	27
PC	662	662	221	1
PR		665 - 743	222 - 248	27
	746			

C7. SSM

Table C7-1. The ROI setup for the SSM shielding experiment in SHIELDMORC 2020

using a 4 liter NaI(Tl) detector (L).

ROI	Energy node (keV)	Energy interval (keV) \pm 1.5 keV	Channel interval	Number of channels
	74		34	
A		78 – 238	35 - 90	56
	242		91	
B		244 – 408	92 - 148	57
	410		149	
C		414 – 576	150 - 205	56
	578		206	
PL		582 – 659	207 - 233	27
PC	662	662	234	1
PR		665 – 742	235 - 261	27
	745			

Table C7-2. The ROI setup for the SSM shielding experiment in SHIELDMORC 2020 using a 4 liter NaI(Tl) detector (R).

ROI	Energy node (keV)	Energy interval (keV) \pm 1.5 keV	Channel interval	Number of channels
	74		34	
A		76 – 240	35 - 91	57
	242		92	
B		246 – 407	93 - 148	56
	410		149	
C		413 – 575	150 - 205	56
	578		206	
PL		581 – 658	207 - 233	27
PC	662	661	234	1
PR		664 – 741	235 - 261	27
	745			

Table C7-3. The ROI setup for the SSM shielding experiment in SHIELDMORC 2020 using a 120% HPGe detector.

ROI	Energy node (keV)	Energy interval (keV) \pm 1.5 keV	Channel interval	Number of channels
	74.1		204	
A		74.5 – 241.8	205 - 663	459
	242.2		664	1
B		242.6 – 409.5	665 - 1122	458
	409.9		1123	1
C		410.2 – 577.6	1124 – 1582	459
	577.9		1583	1
P		653.5 -669.6	1790 - 1834	45

Appendix D1

Conversion of measured gamma spectra to MGS.CSV files

To be able to analyze registered mobile pulse height distributions (gamma spectra) in REALMORC, the data in the measurement system's format needs to be converted to a standard format, here called MGS.CSV (Mobile Gamma Spectrum, Comma Separated Values)

The **ConvertNblToMgsFile** executable module converts SSM's and LU's native formats from Nugget *.NBL, *.NBL.NaI and *.NBL.HPGe formats to *MGS.CSV formats

The **ConvertRsiToMgsFile** executable module converts Radiation Solutions CSV files to *MGS.CSV format

The executable modules only work in Windows.

For the conversion to work, the original measurement data file name must have contiguous characters. Spaces and national characters (äåöø) must not be in the file name.

The measurement data file and the conversion program (the executable module) must be in the same directory.

Double-click on the conversion program file. Enter the measurement data file name. The conversion then takes place automatically. The new file gets the name of the measurement data file plus the extension MGS.CSV

Longitude and latitude are converted to the Rikets nät grid 2.5 gon V, which is a flat coordinate system. It works for coordinates in Skåne, but not for other locations.

Produce one measurement data file for each setup or search mission and speed.

Put the MGS.CSV files on the USB stick

Appendix D2

Conversion of measured MGS.CSV to ROI.CSV files

To be able to calculate the distance, shielding and activity of a Cs-137 point source, gamma spectra must be converted to ROI files according to the previous definition in SHIELDMORC and COMBMORC using ROI A, B, C, and P

The **ConvertMgsToRoiFile** executable module does the conversion from MGS.CSV format to ROI.CSV format

The channel numbers for the ROI borders must be given in the file SETTING_ROI.NML

The *MGS.CSV file, the conversion program (the executable module), and the SETTING_ROI.NML file must be in the same directory.

Double-click on the conversion program file. Enter the *MGS.CSV file name. The conversion then takes place automatically. The new file gets the name of the measurement data file plus the extension ROI.CSV

The ROI.CSV file can be imported to Excel by double-clicking on the file (provided that the ‘,’ the ‘comma’ is not redefined by Windows as decimal separator)

Produce one ROI.CSV data file for each setup or search mission and speed.

Put the ROI.CSV files on the USB stick

Title	Development and testing methods to locate lost gamma-ray sources in ordinary environs by mobile gamma spectrometry, NKS-B REALMORC Report 2023
Author(s)	Christopher L. Rääf ¹ (chair), Robert R. Finck ¹ (co-chair), Christian Bernhardsson ¹ (organizer), Vikas Chand Baranwal ⁴ , Marius-Catalin Dinca ¹ , Jon Drefvelin ⁵ , Marie-Andrée Dumais ⁴ , Per Otto Hetland ⁵ , Gísli Jónsson ³ , Naya Sophie Rye Jørgensen ² , Simon Karlsson ⁶ , Marie Lundgaard Davidsdóttir ² , Bredo Møller ⁵ , Charlotta Nilsson ¹ , Frode Ofstad ⁴ , Josefine Palmcrantz ⁶ , Henrik Öberg ³
Affiliation(s)	¹ Medical Radiation Physics, ITM, Lund University, Sweden ² Danish Emergency Management Agency; Denmark ³ Geislavarnir ríkisins, Iceland ⁴ Geological Survey of Norway, Norway ⁵ Norwegian Radiation and Nuclear Safety Authority Norway ⁶ Swedish Radiation Safety Authority, Sweden
ISBN	978-87-7893-579-3
Date	February 2024
Project	NKS-B / REALMORC, AFT/B(23)3
No. of pages	96
No. of tables	41
No. of illustrations	52
No. of references	13
Abstract max. 2000 characters	The REALMORC 2023 report describes the Excel applications Source Distance and Activity Calculator (SODAC) and Source Shielding Calculator (SSC) to determine distance, shielding and activity of identified Cs-137 sources in lost source searching using mobile gamma-ray spectrometry. The report furthermore outlines a frequency analysis routine intended to enhance the advancement of detecting lost gamma-ray sources. The development proceeds towards detecting sources that may produce weak signals in a mobile gamma spectromete due to their distance and shielding. Standard deviations of the pulse height distribution (gamma spectrum) are utilised to indicate the presence of a radiation source instead of using fixed alarm levels for the count rate. REALMORC 2023 includes joint field experiments in mobile gamma spectrometric search of

shielded Cs-137 point sources in actual environmental conditions. Six Nordic teams participated, and the report documents their results from the search experiment using the teams' proprietary analysis software to detect orphan sources.

Key words

Mobile gamma spectrometry, orphan sources, source search, shielding, MORC, radiation accidents, Compton scattering